JAERI-M
90-080

EVALUATION REPORT ON SCTF CORE-III TEST S3-20

(INVESTIGATION OF WATER BREAK-THROUGH AND CORE COOLING BEHAVIORS UNDER INTERMITTENT ECC WATER DELIVERY TO UPPER PLENUM DURING REFLOOD PHASE IN PWRS WITH COMBINED-INJECTION TYPE ECCS)

May 1990

Tsutomu OKUBO, Tadashi IGUCHI, Takamichi IWAMURA
Hajime AKIMOTO, Akira OHNUKI, Yutaka ABE
Isao SAKAKI*, Hiromichi ADACHI and Yoshio MURAO

日本原子力研究所
Japan Atomic Energy Research Institute

JAERI-Mレポートは，日本原子力研究所が不定期に公刊している研究報告書です。
入手の問合わせは，日本原子力研究所技術情報部情報資料課（〒319－11茨城県那珂郡東海村）あて，お申しこしください。なお，このほかに財団法人原子力弘済会資料センター（〒319-11茨城県那珂郡東海村日本原子力研究所内）で複写による実費頒布をおこなっております。

JAERI-M reports are issued irregularly.
Inquiries about availability of the reports should be addressed to Information Division, Department of Technical Information, Japan Atomic Energy Research Institute, Tokai-mura, Naka-gun, Ibaraki-ken 319-11, Japan.

編集兼発行　日本原子力研究所
印　　刷　日立高速印刷株式会社

Evaluation Report on SCTF Core-III Test S3-20 (Investigation of Water Break-through and Core Cooling Behaviors under Intermittent ECC Water Delivery to Upper Plenum during Reflood Phase in PWRs with Combined-injection Type ECCS)

Tsutomu OKUBO, Tadashi IGUCHI, Takamichi IWAMURA
Hajime AKIMOTO, Akira OHNUKI, Yutaka ABE
Isao SAKAKI*, Hiromichi ADACHI and Yoshio MURAO

Department of Reactor Engineering
Tokai Research Establishment
Japan Atomic Energy Research Institute
Tókai-mura, Naka-gun, Ibaraki-ken

(Received April 12, 1990)

During the reflood phase of the loss-of-coolant accident (LOCA) in a Pressurized Water Reactor (PWR) with the combined-injection type Emergency Core Cooling System (ECCS), the ECC water injected into the hot legs is considered to be deliverd to the upper plenum. Although this water delivery is expected to be steady, there are some information which show that the ECC water delivery to the upper plenum is not steady but intermettent due to steam condensation in the hot legs. One of them is recent test results from the Upper Plenum Test Facility (UPTF) in West Germany. Another is calculational results with TRAC codes in the USA.

Based on these information, a test (Test S3-20) was conducted with the Slab Core Test Facility (SCTF) Core-III in order to investigate the water break-through and core cooling behaviors under the intermittent ECC water delivery to the upper plenum during the reflood phase. In this test, the subcooled ECC water was injected intermittently just above the upper core support plate above Bundles 7 and 8 of the core. The average injection

---

* Toshiba, Ltd.

rate was set to be the same as that in SCTF Test S3-13, which was conducted under an Evaluation Model condition with continuous ECC water injection.

Analyzing the test data together with those of Test S3-13, the following has been found:

(1) The break-through occurred intermittently immediately corresponding to the intermittent ECC water injection. When the break-through occurred, there observed two different thermo-hydrodynamic behaviors between the break-through region and the non-break-through region.

(2) During the periods when the ECC water injection was nearly zero, the core water head decreased and this resulted in degradation of the core cooling in those periods. The reason of the decrease in the core water head is considered to be the increase in the intact loop differential pressure due to the decrease in the steam condensation in the upper plenum.

(3) Although the core cooling behavior was oscillatory, it has been found to be nearly identical to that for the continuous injection case.

Keywords: Reactor Safety, PWR, LOCA, Combined-injection Type ECCS, Reflood Experiments, Break-through, Core Cooling, Heat Transfer, Two-phase Flow, SCTF

JAERI－M 90－080

ＳＣＴＦ第３次炉心試験Ｓ３－20評価報告書
（複合注水型ＥＣＣＳ付ＰＷＲの再冠水時における上部プレナムへのＥＣＣ水の間欠的流入下でのブレークスルー及び炉心冷却挙動の検討）

日本原子力研究所東海研究所原子炉工学部
大久保　努・井口　　正・岩村　公道・秋本　　肇
大貫　　晃・阿部　　豊・榊　　勲*・安達　公道
村尾　良夫

（1990年４月12日受理）

複合注水型緊急炉心冷却系（ＥＣＣＳ）を備えた加圧水型原子炉（ＰＷＲ）における冷却材喪失事故（ＬＯＣＡ）時の再冠水過程では，ホットレグに注入されたＥＣＣ水は上部プレナムに供給されると考えられている。この供給は安定的に行われると期待されるが，ホットレグ内での蒸気の凝縮により，安定的では無く間欠的に行れるとの情報もある。その１つが，西ドイツの上部プレナム試験装置（ＵＰＴＦ）による最近の実験結果であり，また他にも，米国におけるＴＲＡＣコードによる計算結果もそれを示している。

これらの情報に基づいて，平板炉心試験装置（ＳＣＴＦ）第３次炉心を用いて試験（試験Ｓ３－20）を実施して，再冠水時の上部プレナムへのＥＣＣ水の供給が間欠的な場合に於けるブレークスルー及び炉心冷却挙動を検討した。本試験では，サブクールのＥＣＣ水を炉心のバンドル７及び８の上方の上部炉心板直上に間欠的に供給した。注水流量の平均値は，評価モデル（ＥＭ）条件下で連続的なＥＣＣ注水により実施した平板炉心試験Ｓ３－13と同一に設定した。

本試験のデータを試験Ｓ３－13のデータも含めて検討して，以下の事柄が明らかとなった。

(1) ブレークスルーは間欠的に発生し，間欠的に行なわれたＥＣＣ水の注入に即座に呼応して発生した。ブレークスルーの発生している期間には，ブレークスルー領域と非ブレークスルー領域で異なった二つの熱水力学的挙動が見られた。

(2) ＥＣＣ注水流量がほぼ零の期間には，炉心の水頭が減少し，この期間の炉心冷却を悪化させた。炉心水頭の減少の原因は，上部プレナムでの蒸気の凝縮の減少による健全ループ差圧の増加にあると考えられる。

(3) 炉心の冷却挙動は，振動的ではあったが連続的な注水を行なった場合とほぼ同じであることが明らかになった。

東海研究所：〒319-11　茨城県那珂郡東海村白方字白根2-4
＊　（株）東芝

Contents

目　　次

List of Tables

List of Figures

Fig. 3.14 Comparison of rod surface temperature at nine axial elevations in Bundle 2 between Tests S3-20 and S3-13

1. Introduction

The Slab Core Test Facility (SCTF) test program is a part of the large scale reflood test program[1] together with the Cylindrical Core Test Facility (CCTF) test program, which are performed by Japan Atomic Energy Research Institute (JAERI) under a contract with Atomic Energy Bureau of Science and Technology Agency of Japan. The SCTF test program is also one of the research activities based on the trilateral agreement among JAERI, the United States Nuclear Regulatory Commission (USNRC) and the Federal Minister for Research and Technology (BMFT) of the Federal Republic of Germany (FRG).

There are three test series (Core-I, -II and -III) in the SCTF test program. The SCTF Core-I[2] and Core-II[3] test series have been already performed mainly to investigate the two-dimensional thermal hydraulic behavior in the core during the reflood phase of a loss-of-coolant accident (LOCA) of a Westinghouse type (US/J type) pressurized water reactor (PWR). On the other hand, one of the major objectives of the SCTF Core-III[4] test series is to investigate the effectiveness of the combined-injection type emergency core cooling system (ECCS) in a German type PWR (GPWR). In addition, simulation tests for a US/J type PWR were also conducted with the SCTF Core-III for further investigation of the core two-dimensional thermo-hydrodynamic behavior.

The reflood phenomena for PWRs with combined-injection type ECCS have been investigated mainly in FRG, since PWRs of such type are manufactured only there. One of the main characteristics of them is the heterogeneous core thermo-hydrodynamic behavior. However, the test facilities used for the investigation are rather small for the investigation of it. Then it is necessary to investigate it further with a facility having a fully radius core. Therefore, the tests to study the reflood phenomena for PWRs with the combined-injection type ECCS have been performed with the SCTF, because it has a full radius core.

According to the previous information, the ECC water injected into the hot legs is considered to be delivered stably to the upper plenum during reflood phase of a GPWR large-break LOCA. However, some information show the delivery is not continuous but intermittent. One of them is the recent test results[5] from the Upper Plenum Test Facility (UPTF) in FRG, and another is calculational results[6] with TRAC codes in the USA.

Based on these information, one test was performed in order to investigate the break-through and core cooling behaviors during the reflood phase of a GPWR under an evaluation model (EM) condition with the intermittent ECC water delivery to the upper plenum. This test is named Test S3-20 (Run 724). The average ECC water injection rate was set to be the same as that in SCTF Test S3-13[7], which was conducted also under the EM condition. This report describes the major results of the present test and discussion on them, also utilizing the data from Test S3-13.

A brief information on the test is presented in the following:

(1) Test name

GPWR simulation integral EM test

where, GPWR : German type PWR with combined-injection type ECCS

EM : Evaluation model

(2) Test number

S3-20 (Run 724)

where, S : SCTF

3 : Core-III

20 : Sequential number of main test

(3) Objectives of test

i) To investigate the break-through phenomena during the reflood phase in a GPWR under the intermittent ECC water delivery to the upper plenum

ii) To investigate the core cooling behavior during the reflood phase in a GPWR under the intermittent ECC water delivery to the upper plenum

(4) Type of test

Refill and reflood integral test simulating a GPWR under an EM condition

2. Test Description

2.1 Test Facility[4]

The SCTF was originally designed to study two-dimensional effects on thermal hydraulics during the reflood phase in the PWR core with full length radius[2],[3]. A flow diagram of the SCTF is shown in Fig. 2.1. The SCTF is simulating a 200% cold-leg-large-break with a simplified primary system and can be operated at the system pressure less than 0.6 MPa. It consists of a pressure vessel, a combined intact loop, a broken loop at the pressure vessel side, and a broken loop at the steam-water separator side.

Figure 2.2 shows a vertical cross section of the pressure vessel. The pressure vessel includes a simulated core, an upper plenum with its internals, a lower plenum, a core baffle region and a downcomer. The configurations of the upper plenum structure and the end box simulate those of a 1,300 MWe class GPWR as practically as possible. The core and the upper plenum are enveloped by honeycomb thermal insulators with wall plates to minimize the wall thermal effects.

The core is full-height, full-radius and one-bundle width one. The core flow area scaling ratio is 1/21.4 to a typical 1,000 MWe class US/J PWR. 1,888 electrical heater rods are installed in the core to simulate fuel rods. Dimensions of a heater rod is 10.7 mm in diameter and 3,613 mm in heated length, simulating those of PWRs. The maximum available power supplied to the core is 10 MW.

The heater rods are assembled in a 16 x 16 square array bundle being positioned with grid spacers. Eight bundles are installed in a row in the core, as shown in Fig. 2.2. In the SCTF, the leftmost bundle in the figure is named Bundle 1 and orderly to the right direction the bundles are named Bundle 2, 3, ..., 8. Since the downcomer and the hot leg are connected to the Bundle 8 side, the Bundle 1 and 8 sides are corresponding to the central and the peripheral sides of PWRs, respectively.

The ECC water can be injected into the lower plenum, the cold leg and the upper plenum in the SCTF. Since the SCTF has no injection port in the hot leg, the hot leg injection of the ECC water in PWRs with the combined-injection type ECCS was substituted by the upper plenum injection. The ECC water can be injected into the upper plenum from both the top and the side (just above the upper core support plate (UCSP)) walls.

Description of the SCTF Core-III is presented more in detail in Appendix A.

2.2 Test Conditions and Sequence

The test conditions were selected to simulate the refill and reflood phenomena under the EM conditions for a GPWR 200% cold-leg-large-break LOCA. The bases for the test conditions are summarized in Sec. 2.3. Table 2.1 shows the planned and the measured test conditions.

Figure 2.3 shows the conceptual initial set-up of the facility for Test S3-20. The ECC water was injected from an injection port located just above the UCSP (named side injection port UCSP1) and at the cold leg. The port UCSP1 is located above Bundles 7 and 8 of the core. Although the ECC water injection into the upper plenum was intermittent, the average value was set to be the same as that for SCTF Test S3-13[7], which is an integral test conducted under an EM condition.

Orifice diameters for the steam-water separator side broken cold leg, the intact cold leg and the pump simulator are 75.1, 164.5 and 173.7 mm, respectively. No orifice is inserted in the pressure vessel side broken cold leg. The water in steam-water separator was drained to the containment tank II to keep the maximum water level in the steam-water separator at 1.1 m. The differences in the test conditions between Tests S3-20 and S3-13 were the upper plenum injection rate (intermittent *vs.* continuous) and the loop flow resistance of the broken cold leg (with a orifice of 63.4 mm diameter in Test S3-13).

Figure 2.4 shows the sequence of Test S3-20. In this figure, the time when the maximum clad temperature reached 700 ^{o}C is defined as 0 s. The pressure in the containment tank II was kept constant at 0.3 MPa by controlling discharge rate of the steam through the below valve to the atmosphere after 0 s. The ECC water was injected both into the cold leg and the upper plenum after 0 s. The ECC water injection rate into the upper plenum was oscillatory as show in Fig. 2.4. The water temperature for this was set to be 35 ^{o}C. The injection rate from the cold leg was decreased monotonously. The temperature of the water was also 35 ^{o}C. The core power was initially set at 7.5 MW and was decreased to simulate the decay as shown in Fig. 2.4.

2.3 Bases for Test Conditions

Bases for test conditions are summarized in Table 2.2. A brief explanation is as follows:

(1) Pressure

According to a TRAC calculation, pressure in the pressure vessel is about 0.3 MPa during the reflood period. Pressure in the containment tank II was initially set at 0.3 MPa and was intended to be kept constant during the reflood phase. However, the initial pressure in the primary system was set at 0.6 MPa and decreased to 0.3 MPa after 0 s by opening the blowdown valves (*i.e.* V1 and V2 in Fig. 2.3) in order to simulate the end of the blowdown and refill phases.

(2) Core power

Core power for the present test was determined by the following equation:

$$P_{SCTF} = P_{o\ GPWR} \times S_F \times (\text{Old ANS} \times 1.03 + \text{Act.})$$

(t s after scram)

where, $P_{o\ GPWR} = 3{,}765$ MW

$$S_F = \text{Scaling ratio} = \frac{\text{SCTF core volume}}{\text{GPWR core volume}} = \frac{0.8931}{21.5} = \frac{1}{24.07}$$

$t = 25$ s

As a result,

$$P_{SCTF} = 7.5 \text{ MW}$$

(3) Power profile

Radial power ratio in the present test at given radius F(r) was determined to simulate that in a GPWR. Namely,

$$F(r)_{SCTF} = k \cdot F(r)_{GPWR}$$

where, $F(r)_{SCTF}$ is based on the slab geometry, while $F(r)_{GPWR}$ is based on the sector or circular geometry. The constant k was determined to achieve

$$(F(r)_{SCTF})_{Average} = 1.0$$

(4) Initial clad temperature

Initial clad temperature was determined to simulate the stored energy in rods at the pressure of 0.6 MPa. The referred data base is the test result of PKL-IIB-2 performed in FRG.

(5) Mode of ECC injection

Since the present test is an integral test to investigate the effects of the intermittent ECC water delivery to the upper plenum on the water break-through and the core cooling behaviors, the ECC water was injected at the cold leg and on the UCSP of the upper plenum instead of the hot leg. The injection location on the UCSP was corresponding location above Bundles 7 and 8.

Selection base for the ECC water injection mode is the same as in Test S3-13 and summarized in Table 2.2. This is one of the EM conditions and based on the following situation proposed by FRG:

(i) ECC water injected into the broken cold leg is not effective
(ii) One LPCI pump is not working
(iii) One Acc in the hot leg is under repair
(iv) One valve in the hot leg injection line is closed as an assumption of the single failure.

(6) ECC injection rate and temperature

According to the mode of the ECC injection presented above, the injection rates are determined as:

3 Acc + 2.6 LPCI (cold leg)
2 Acc + 1.4 LPCI (upper plenum)

2.4 Measured Boundary Conditions

The major measured test conditions are listed in Table 2.1. Table 2.3 shows the chronology of events occurred during the test. Figure 2.5 through 2.10 show the measured boundary conditions of the test.

There observed no significant differences between the planned and the measured except for the pressure in the upper plenum. The pressure was controlled at 0.3 MPa by venting the excessive steam. However, the control was not accurate enough to keep the pressure at 0.3 MPa because of oscillatory steam generation and condensation due to the intermittent subcooled

ECC water injection, so that the pressure decreased oscillatory, as shown in Fig. 2.5.

Table 2.1 Conditions for Test S3-20

Item	Planned	Measured
Pressure (MPa)		
Containment tank	0.3	0.28 ~ 0.37
Pressure vessel	0.6 → 0.3	0.6 → 0.28 ~ 0.44
Power		
Initial power (MW)	7.5	7.45
Decay curve	ANS × 1.03 + Act.	ANS × 1.03 + Act.
Time after scram (s)	25	25
Radial profile	1.04:1.08:1.08:1.04 :1.04:1.04:0.97:0.71	1.04:1.08:1.08:1.04 :1.04:1.04:0.97:0.71
Peak clad temperature at ECC water injection initiation (K)	973	1001
ECC water injection location	UCSP1 and cold leg	UCSP1 and cold leg
UCSP injection		
Injection rate (kg/s)	As specified	See Fig. 2.6
Water temperature (K)	308	309
Cold leg injection		
Injection rate (kg/s)	As specitied	See Fig. 2.7
Water temperature (K)	308	310

Table 2.2 Summary of bases of test conditions

Pressure		
in PV	0.6 MPa → 0.3 MPa	Blowdown from 0.6 MPa
in CT II	0.3 MPa	TRAC calculation
Power		
Initial power	7.5 MW	Scaled value (following Eq.)
Decay curve	P_0 × (Old ANS × 1.03 + Act.)	Similar to GPWR-EM
Timing at 0.6 MPa	25 s after scram	
	$P_{SCTF} = P_{0\ GPWR} \times S_F \times$ (Old ANS × 1.03 + Act.) after t sec	
	$P_{0\ GPWR}$ = 3765 MW	
	S_F = 0.8931/21.5 = 1/24.07	
	t = 25	
Power profile	1.04:1.08:1.08:1.04 :1.04:1.04:0.97:0.71	Preserved GPWR power profile against radius
Clad temperature		
Initial PCT (0.6 MPa, GPWR profile)	700°C	• Preserved GPWR initial stored energy • Referred to PKL-IIB-2 result
ECC mode		
CL	3Acc + 2.6 LPCI	• ECC into broken cold leg is not considered • One HL valve is on single failure • One LPCI pump and one hot leg Acc are under repair
HL	2Acc + 1.4 LPCI	

Table 2.3 Chronology of events for Test S3-20

Item	Time (s)
Core power "ON"	0
Core power decay initiation	109.0
UCSP injection initiation	109.0
Cold leg injection initiation	109.0
BOCREC	128.5
Whole core quench	270.5

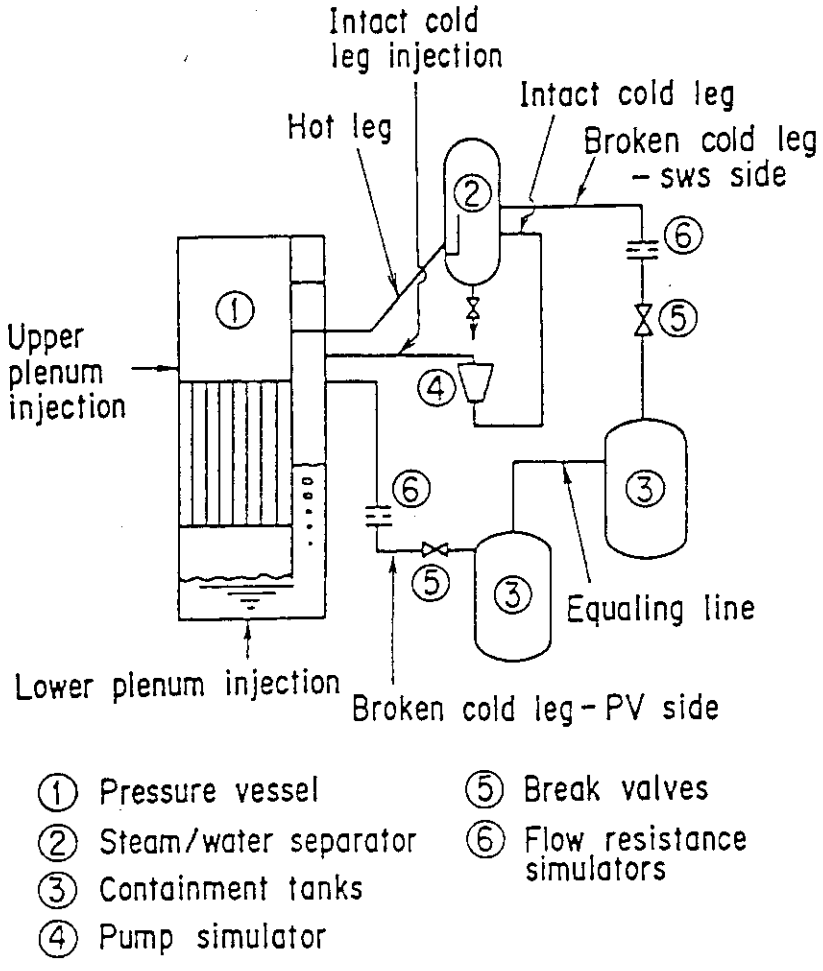

Fig. 2.1 Flow diagram of SCTF

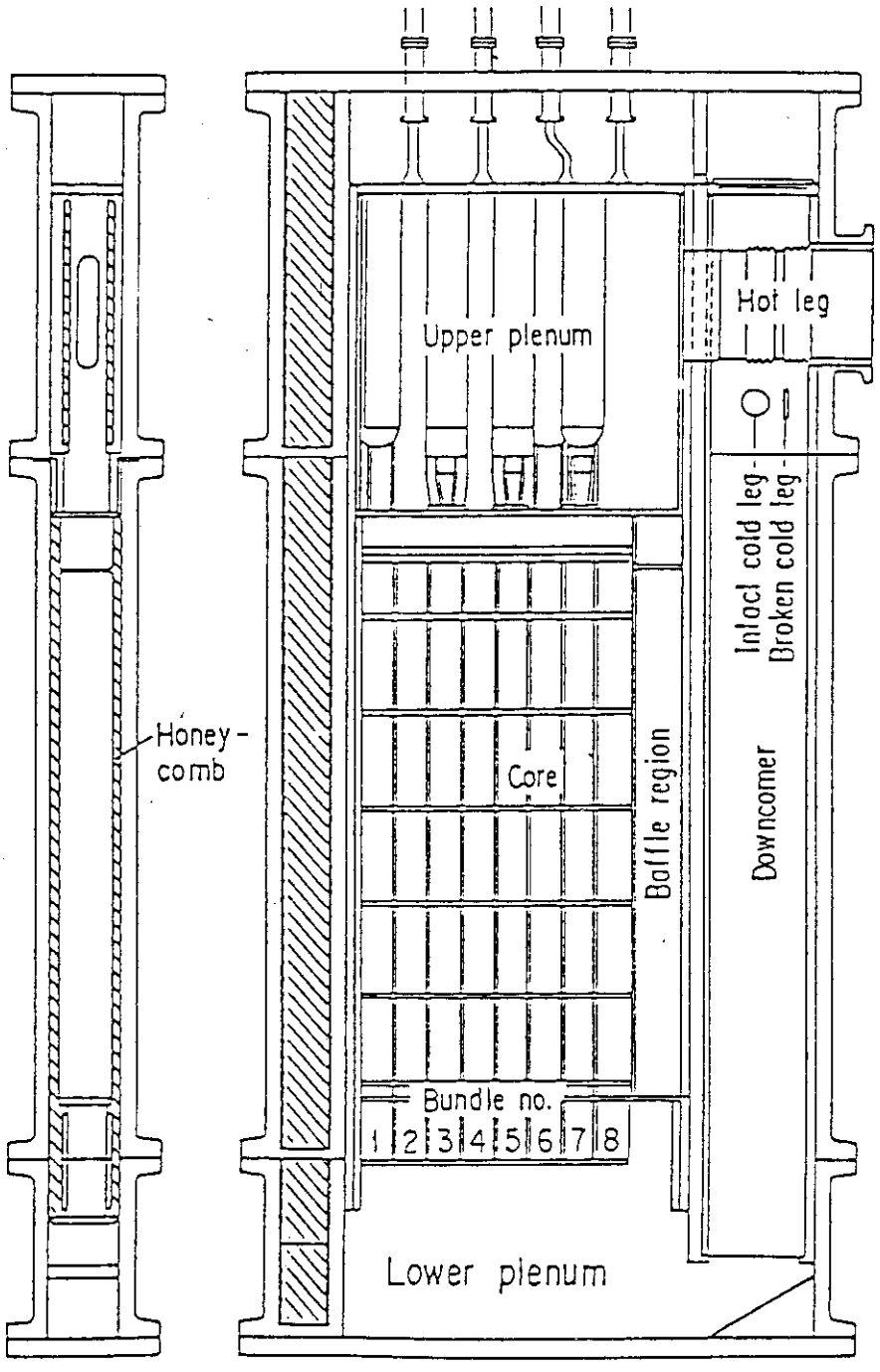

Fig. 2.2 Vertical cross section of pressure vessel

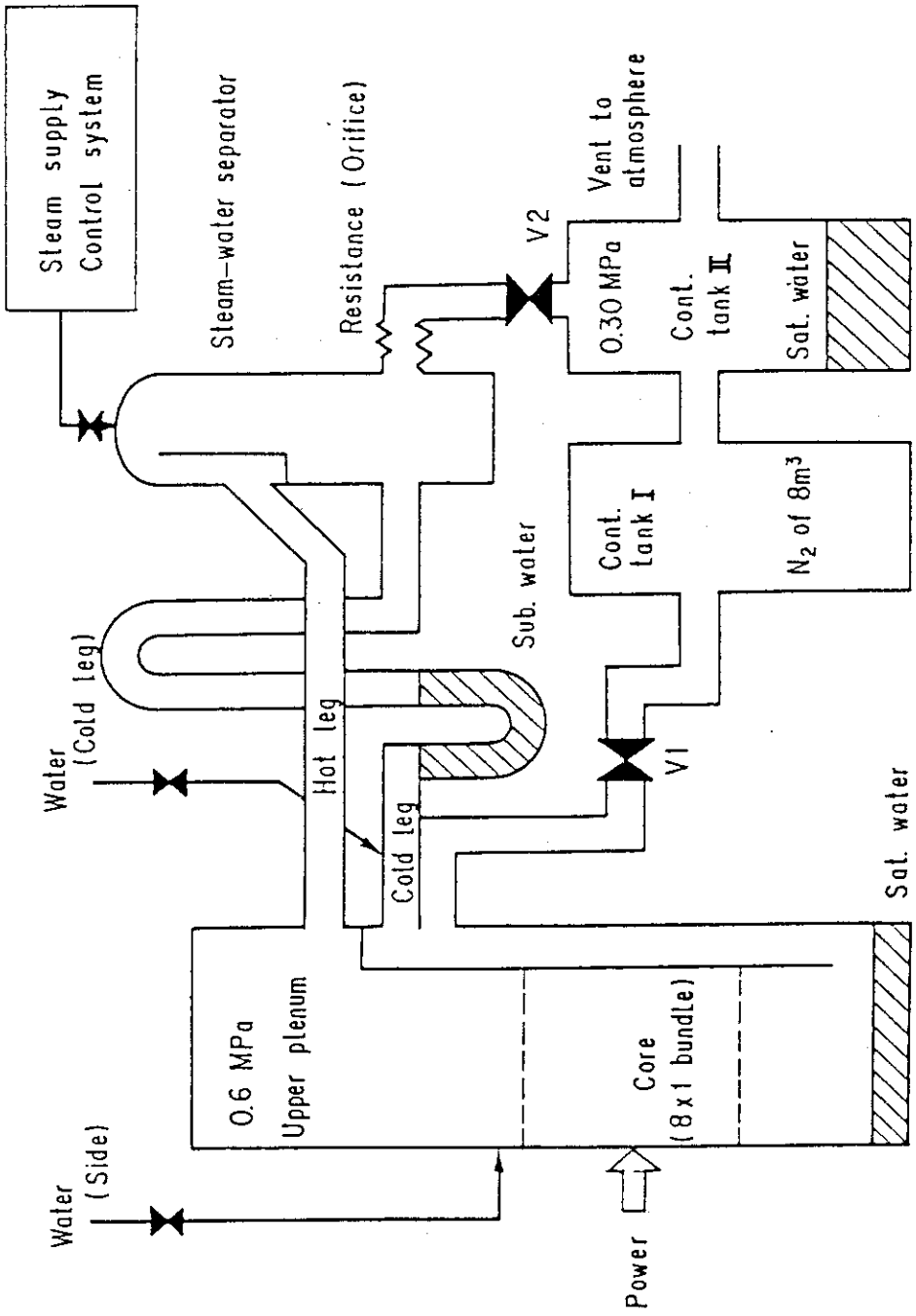

Fig. 2.3 Initial set-up of Test S3-20

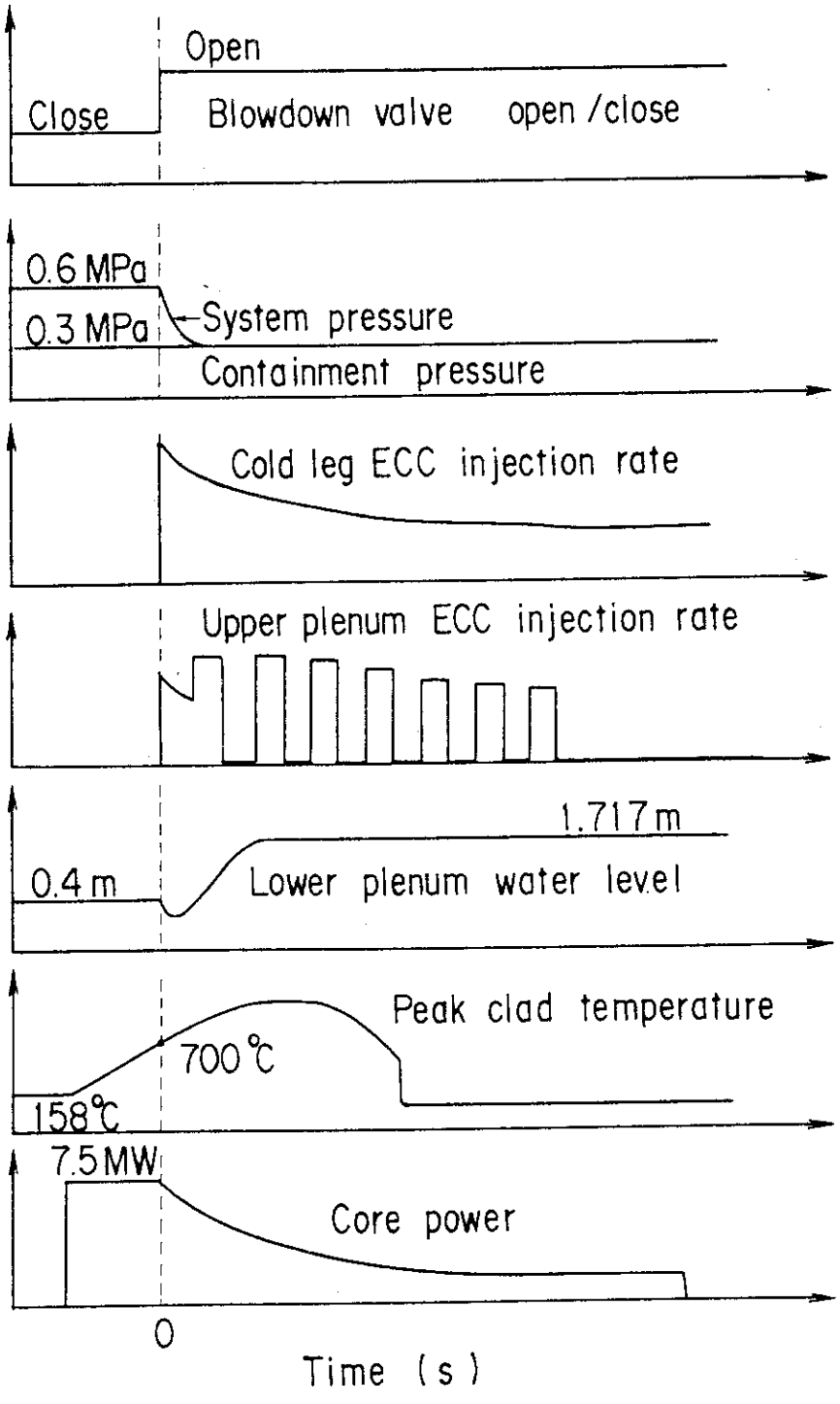

Fig. 2.4 Sequence for Test S3-20

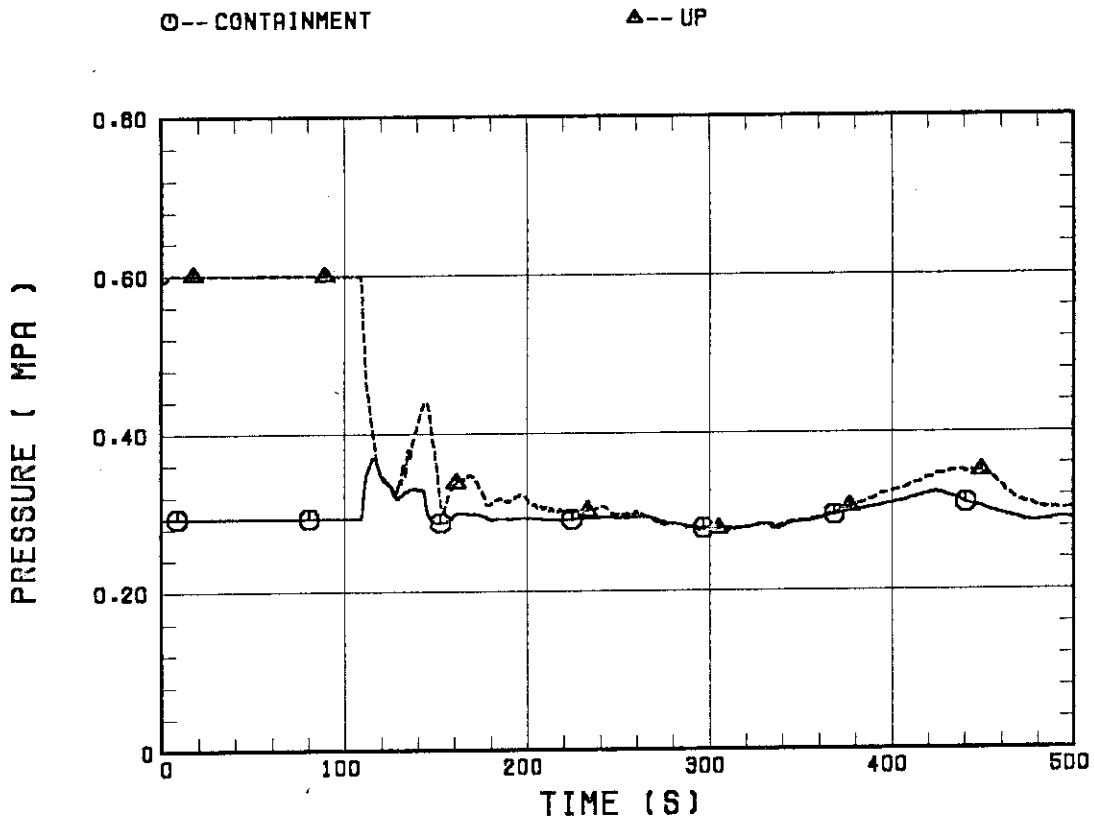

Fig. 2.5 Pressures of containment tank II and upper plenum

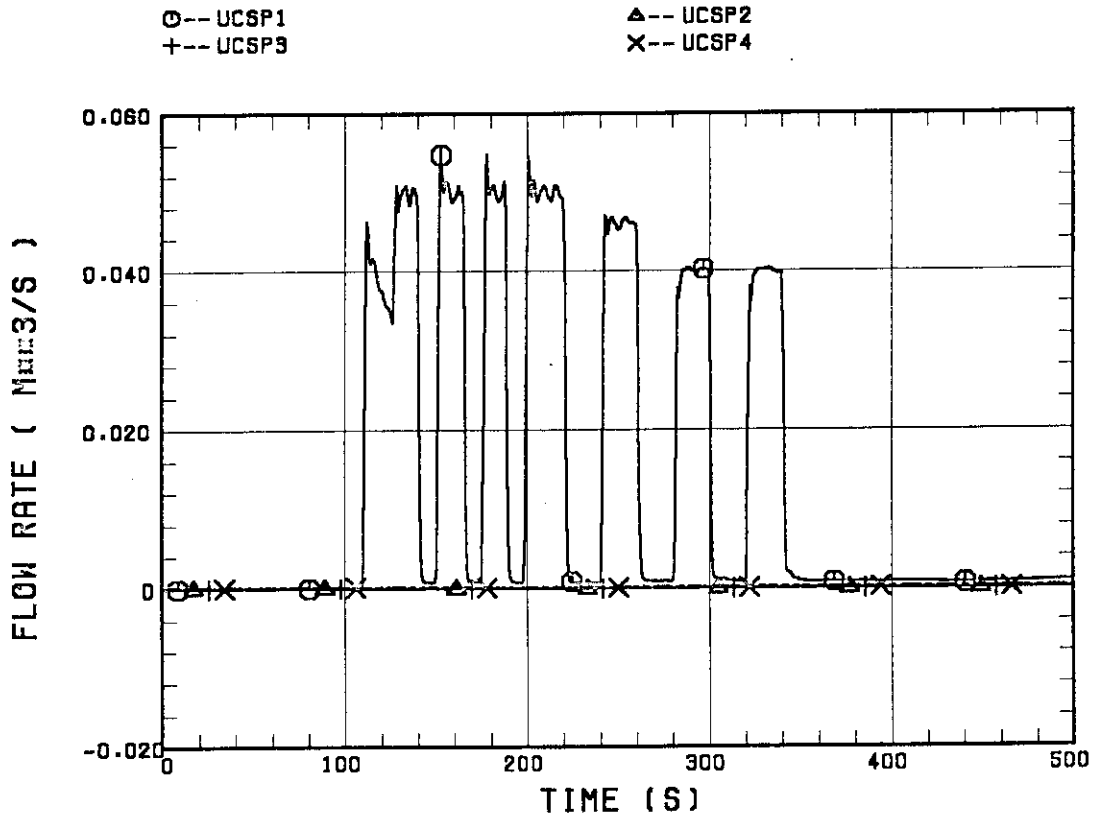

Fig. 2.6 ECC injection rate into upper plenum

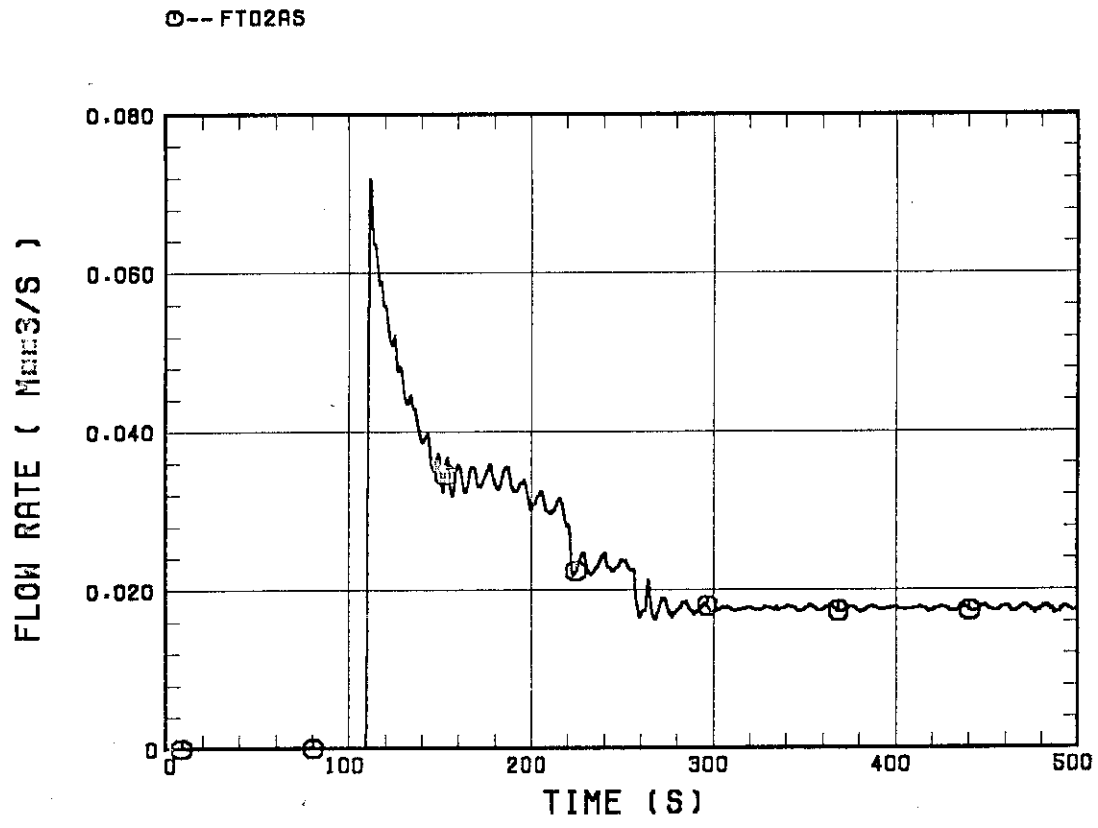

Fig. 2.7 ECC injection rate into cold leg

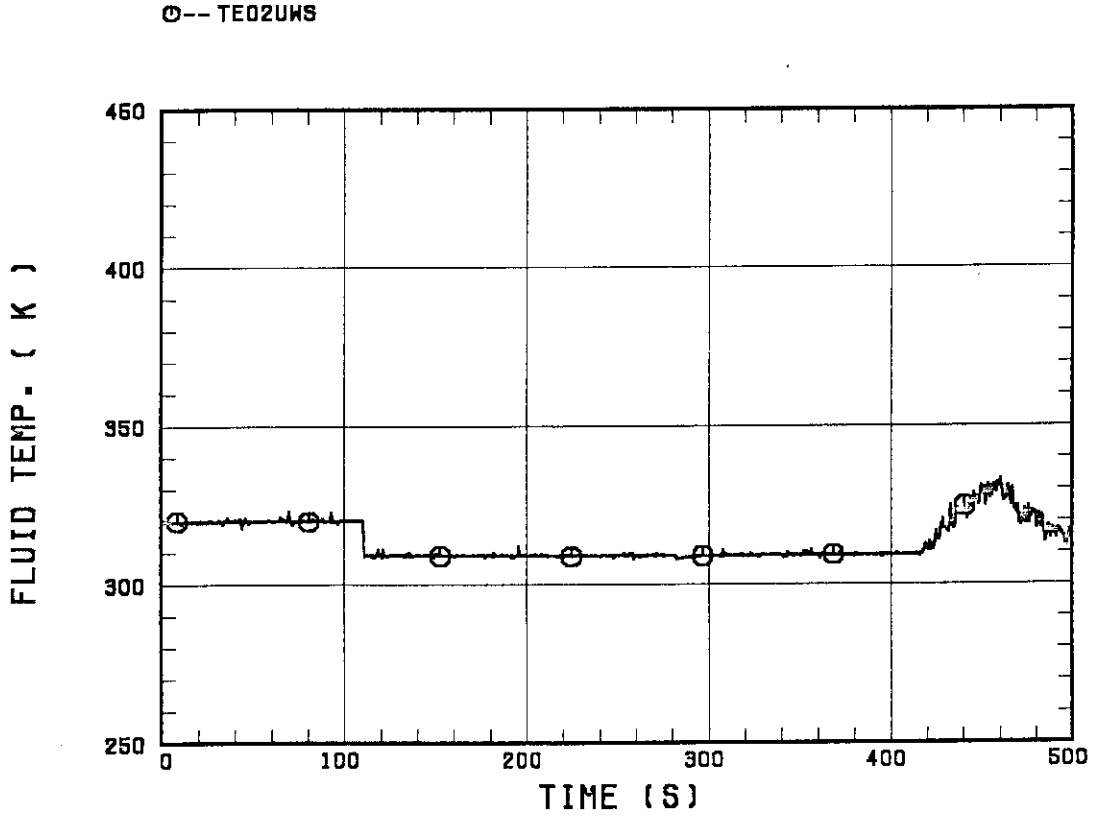

Fig. 2.8 Water temperature of upper plenum injection

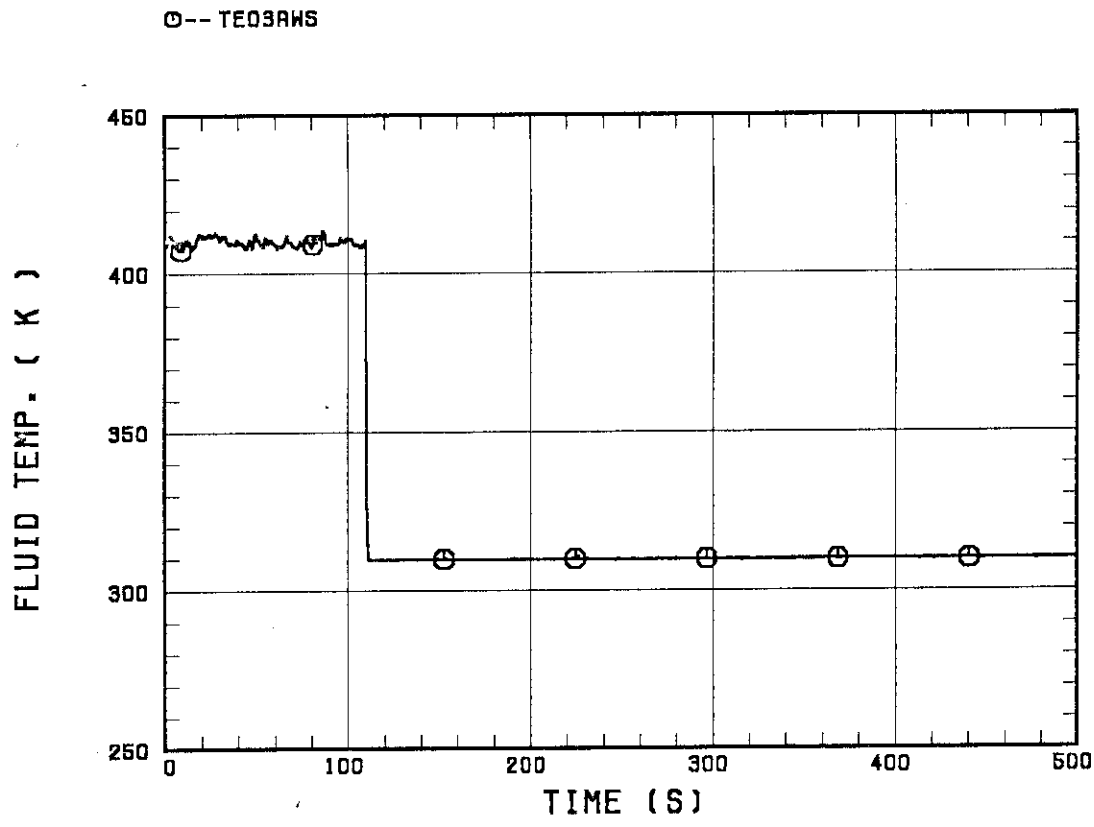

Fig. 2.9 Water temperature of cold leg injection

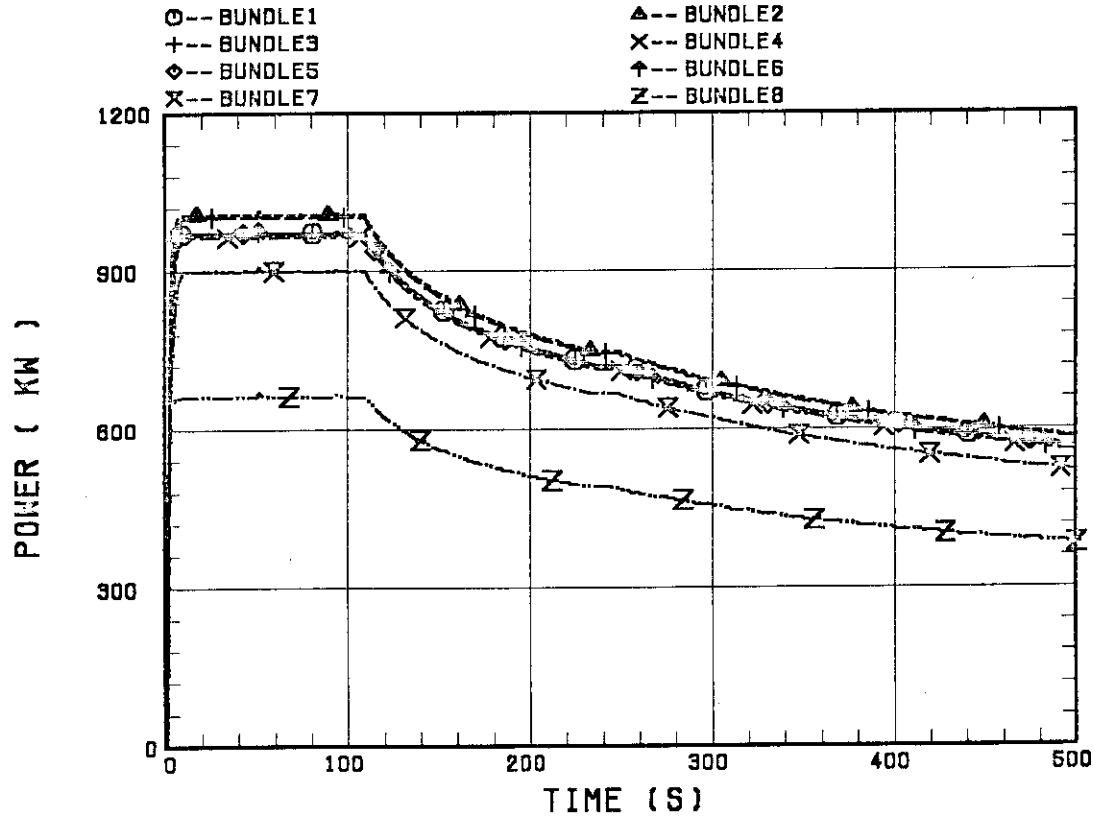

Fig. 2.10 Supplied core power

3. Test Results and Discussion

The test conditions for Test S3-20 are the same as those for Test S3-13 except the upper plenum injection rate (although the average value is set to be the same) and the small difference in the broken cold leg flow resistance as described in Sec. 2.2. Therefore, the data from Test S3-13 are utilized as the basis to investigate the effects of the intermittent ECC water delivery to the upper plenum on the water break-through and the core cooling behaviors.

3.1 Break-through Behavior

The ECC water injection rate into the upper plenum is shown in Fig. 3.1 together with that for Test S3-13. There are seven oscillations in the injection rate. The values at crests are roughly double of the average value (*i.e.* value for Test S3-13) and the values at troughs are nearly zero (*i.e.* not exact zero but about 0.8 kg/s because of the requirement of facility operation). The period of the oscillation is set to 20 s for the initial three and 40 s for the rest. Although the time-integrations were set to be the same, there observed some difference and the injected mass after the reflood initiation is larger in Test S3-20 by about 8 % at the maximum at the end of each period.

The water break-through from the upper plenum to the core is judged based on the data of the differential pressure across the tie plate, the fluid temperature just below the tie plate hole and the water mass flow rate at the tie plate. Figure 3.2 shows the differential pressures across tie plate. The ECC injection rate into the upper plenum is also shown in the Figure to show the relation between them. The differential pressure above Bundles 7 and 8 become negative corresponding exactly to the increase in the water injection rate, indicating the occurrence of the break-through. On the other hand, when the injection rate decreases, the differential pressures become zero or positive, indicating the stop of the break-through. Above the other bundles, the differential pressures increase with a little delay corresponding to the increase in the injection rate except above Bundle 6 after 70 s. This suggests the two-phase up-flow becomes higher after the break-through with a little delay in timing. Above Bundle 6, the intermittent break-through starts after 70 s and then the stable one starts after 110 s. This is considered to be the influence

of the break-through above Bundles 7 and 8.

Figure 3.3 shows the fluid temperatures just below the tie plate holes. Above Bundles 7 and 8 the temperatures become lower exactly corresponding to the increase in the injection rate, indicating the occurrence of the break-through. When the injection becomes nearly zero, the temperatures become the saturation temperature. The water mass flow rates at the tie plate shown in Fig. 3.4, which are measured with the advanced two-phase flow instrumentations provided by the USNRC, also indicates that the break-through occurs above Bundle 8 exactly corresponding to the increase in the injection rate and the break-through stops corresponding to the decrease in the injection rate. On the other hand, the upward flow increases above Bundles 4 and 5 with a little delay to the increase in the injection increase. The break-through mass flow rate is 20 ∿ 30 kg/s per bundle and is in good agreement with the injection rate. This suggests almost all the injected water falls down to Bundles 7 and 8 of the core.

3.2 Core Water Accumulation and System Behaviors

Figure 3.5 shows the core differential pressure compared with the data of Test S3-13. The data for the present test experience the oscillation or decrease during the period when the upper plenum injection is nearly zero. The reason for this oscillatory behavior is investigated in the following.

One of possible reasons is water evaporation in the core. Based on the data in Fig. 3.5, decreasing rate of the core water is estimated to be 10 ∿ 20 kg/s. Figure 3.6 shows the maximum steam generation rate of the whole core estimated from the heat release of the heater rods neglecting subcooling of core water. This value gives the possible maximum of the steam generation rate. The steam generation rate is small and about 3 kg/s during the period when the upper plenum injection is nearly zero and the core differential pressure decreases. Therefore, it becomes clear that the decreases in the core differential pressure do not correspond to the evaporation of core water.

Figure 3.7 shows the intact loop differential pressure together with the core differential pressure. It is clear that these two data show very good coincidence in the oscillation. That is, the increase in the intact loop differential pressure exactly corresponds to the decrease in the core differential pressure after the reflood initiation. Therefore, it is in-

ferred that the core differential pressure is decreased by the increase of the intact loop differential pressure. In other words, the core water is pushed down by the increase in the steam binding effect.

Figure 3.8 shows the relation among the intact loop differential pressure, the upper plenum injection rate and the core steam generation rate. Since the intact loop differential pressure is considered to be caused by the frictional pressure loss due to the steam flow, the increase and decrease of the differential pressure correspond to those of the steam flow rate in the intact loop. Accordingly, Fig. 3.8 indicates that the steam flow in the intact loop decreases during the upper plenum injection, although the core steam generation increases during the same time. This suggests the following situation: A lot of steam is generated in the core during the upper plenum injection period, but a large part of this is condensed by the injected water, and hence, the steam flow rate in the intact loop becomes low. On the other hand, when the upper plenum injection rate is nearly zero, the condensation of the steam becomes nearly zero, and hence, the steam flow in the loop increases, though the steam generation rate in the core is smaller (about one half of that in the higher injection period). Figure 3.9 shows a comparison of the intact loop differential pressure between Tests S3-20 and S3-13, and supports the discussion above.

Summarizing the discussion above, the decrease in the core water accumulation is considered to be caused by the increase in the intact loop differential pressure, which resulted from the decrease in the steam condensation in the upper plenum during the periods when the ECC water delivery to the upper plenum is nearly zero.

3.3 Core Cooling Behavior

Figure 3.10 shows the clad surface temperatures at 1.905 m elevation. The quench occurs significantly early in Bundles 7 and 8, where the breakthrough occurs. The core cooling in the other non-break-through bundles starts at the reflood initiation and it is oscillatory corresponding to the core water accumulation shown in Fig. 3.5. The heat transfer coefficients corresponding to the data shown in the previous figure are given in Fig. 3.11. These data show clearly the oscillatory core cooling in the non-break-through region.

Figure 3.12 shows a comparison of the heat transfer coefficient be-

tween Tests S3-20 and S3-13 in the non-break-through region at 1.905 m elevation. Up to 60 s, the heat transfer coefficient for Test S3-20 is higher during the injection period. However, the decrease in the heat transfer coefficient is significantly large during the nearly zero injection period. As a result, the core cooling behavior is almost the same between the two tests, although it is oscillatory and the quench time is longer by 14 s in the present test as shown in Fig. 3.13, which shows the comparison of the rod surface temperature between the two tests at 1.905 m elevation. Figure 3.14 shows comparisons of the rod surface temperature at nine axial elevations of the core in the non-break-through bundle (Bundle 2). It also indicates that the core cooling behavior is almost the same, though the quench time is slightly later in the present test at every elevation.

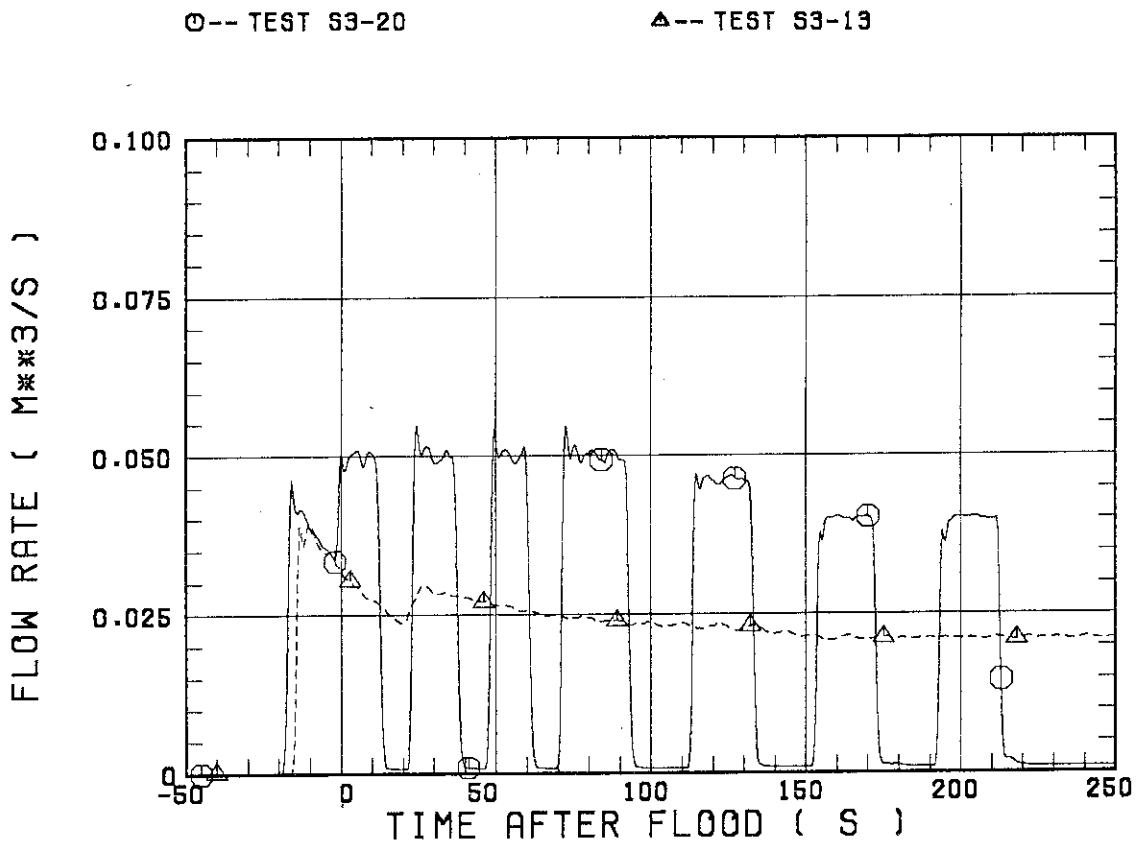

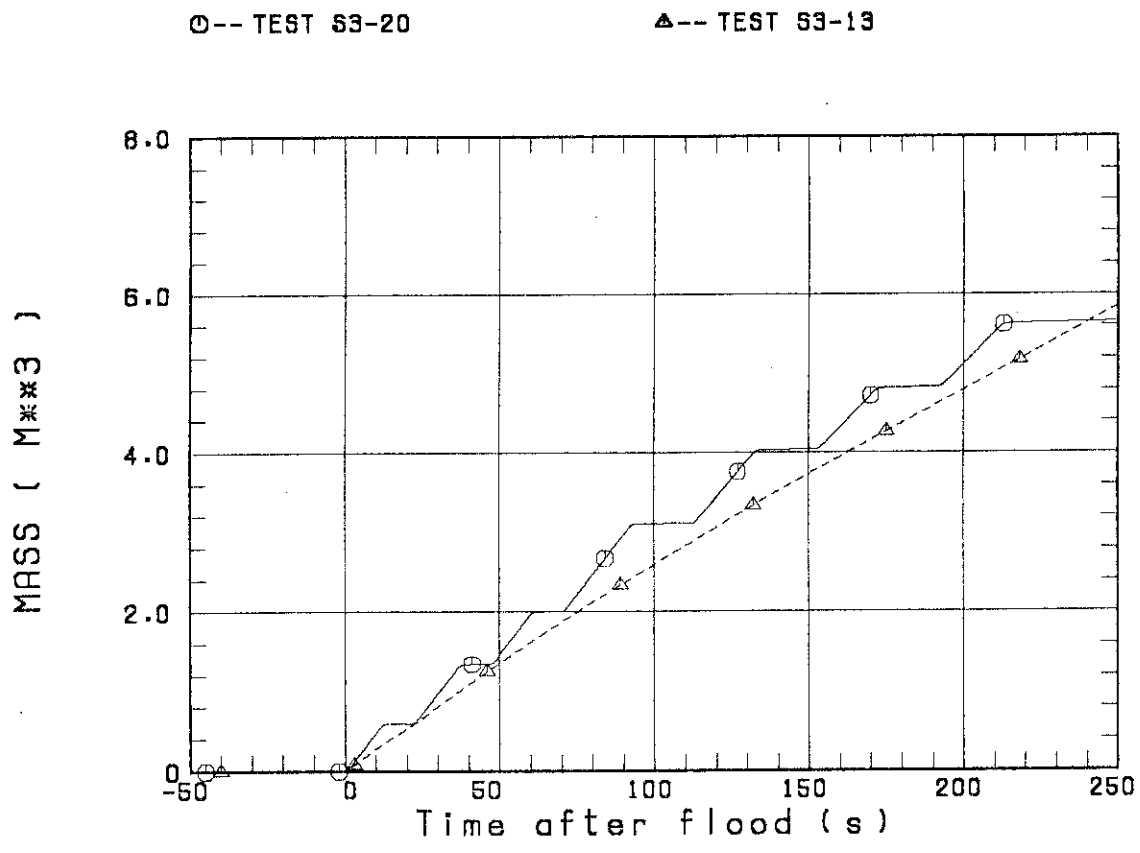

Fig. 3.1 ECC water injection rates into upper plenum and their time-integrations

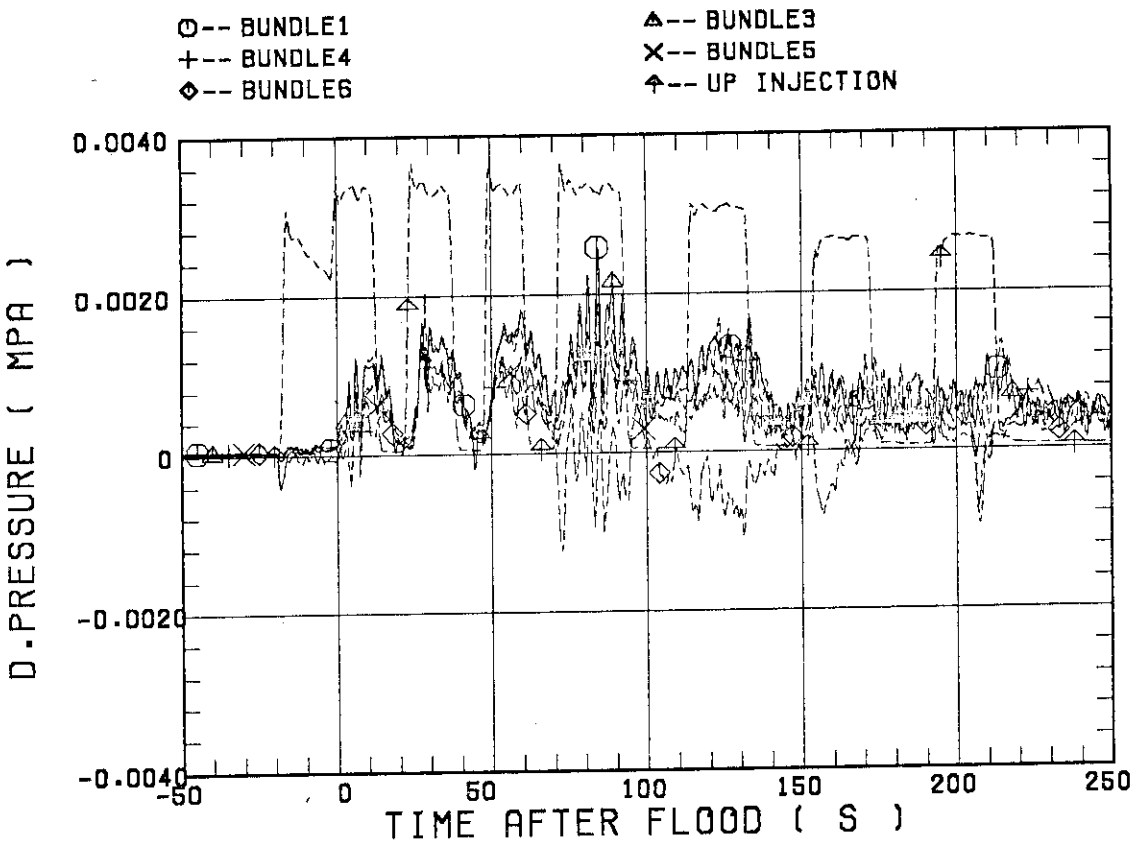

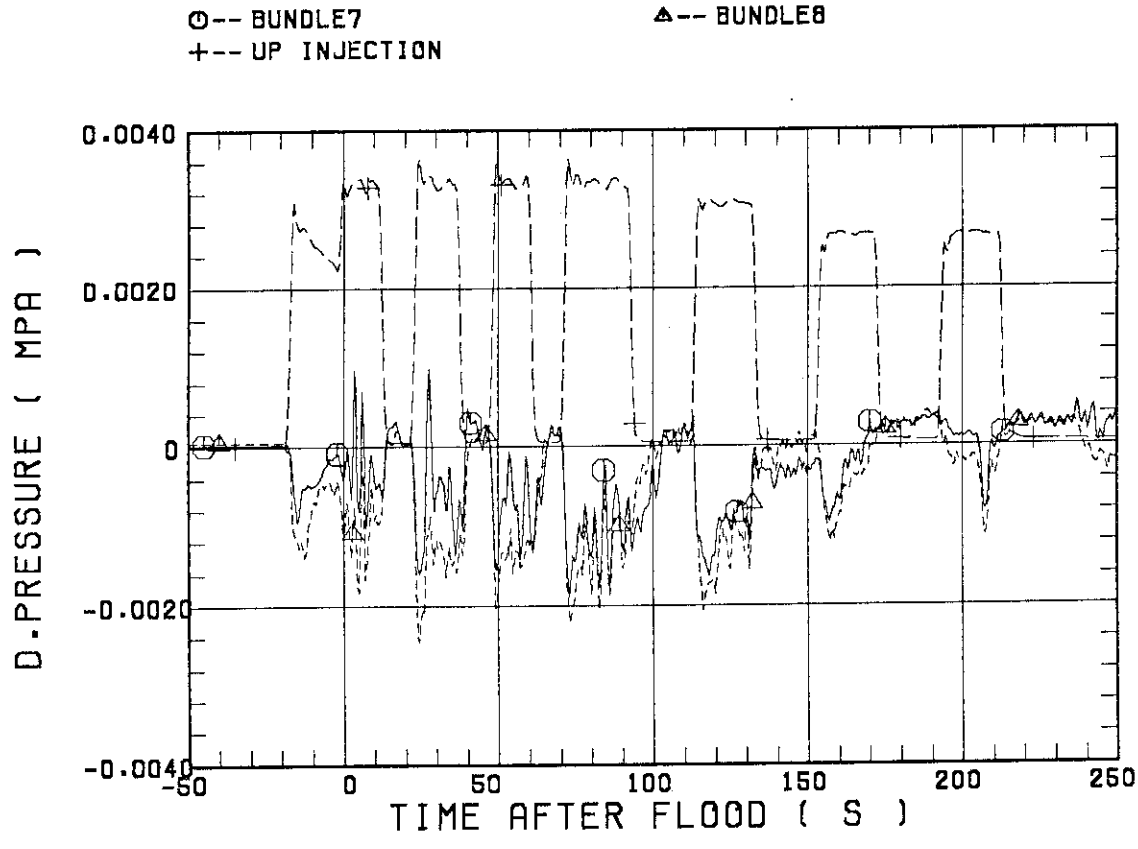

Fig. 3.2 Differential pressures across tie plate

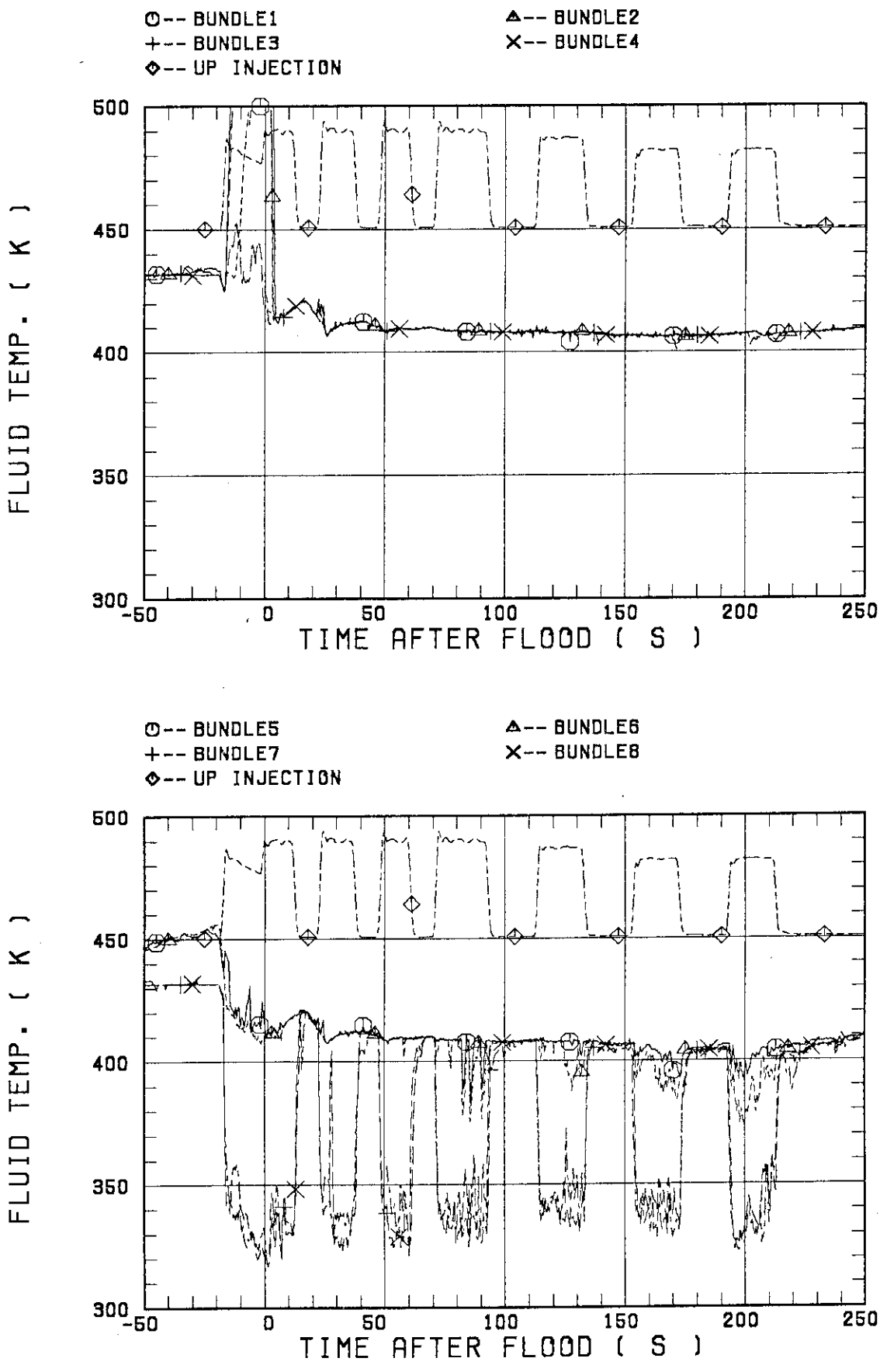

Fig. 3.3 Fluid temperatures just below tie plate holes

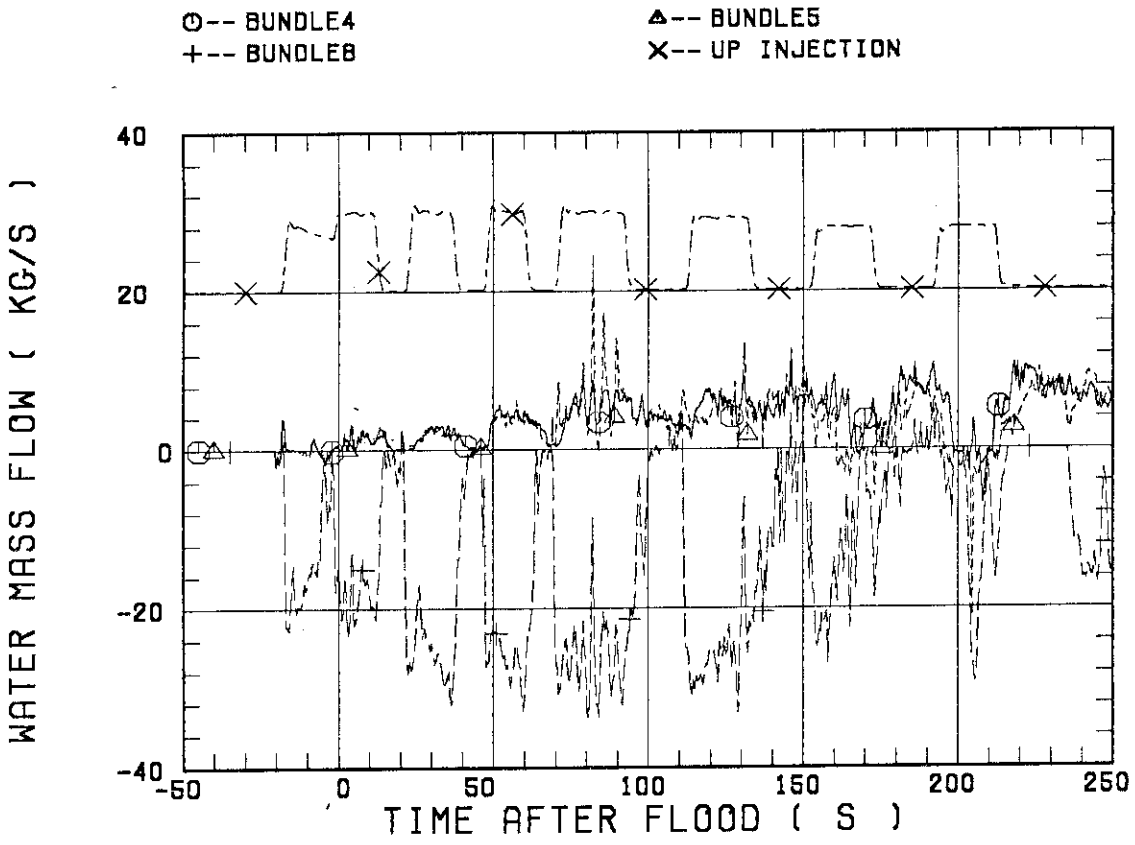

Fig. 3.4 Water mass flow rates at tie plate

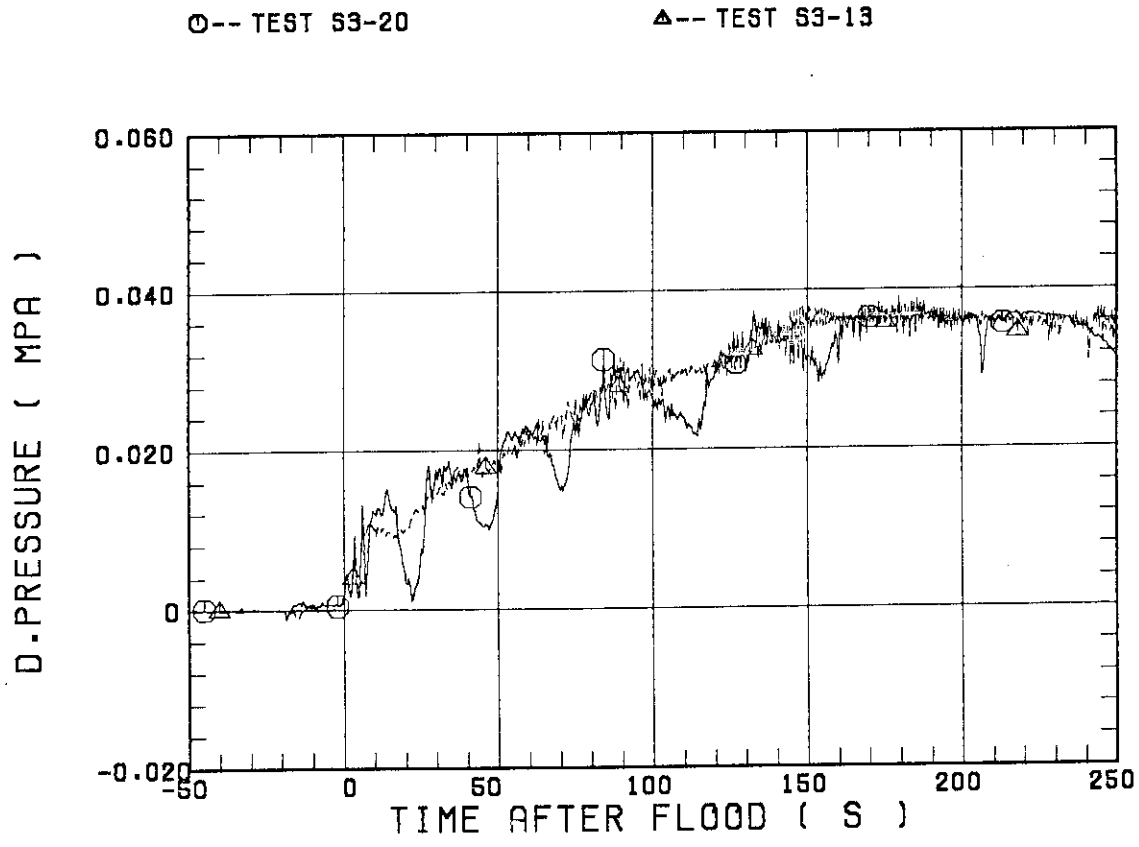

Fig. 3.5 Core differential pressures

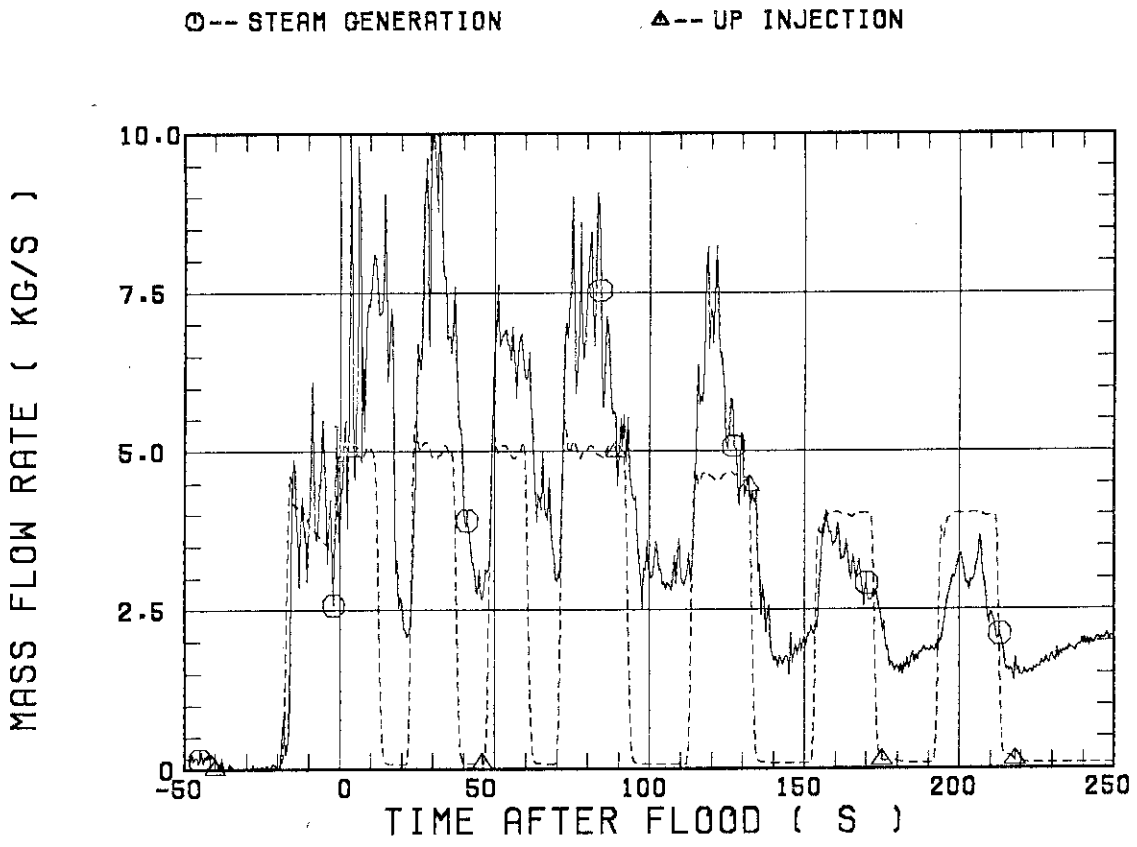

Fig. 3.6 Estimated steam generation rate in core

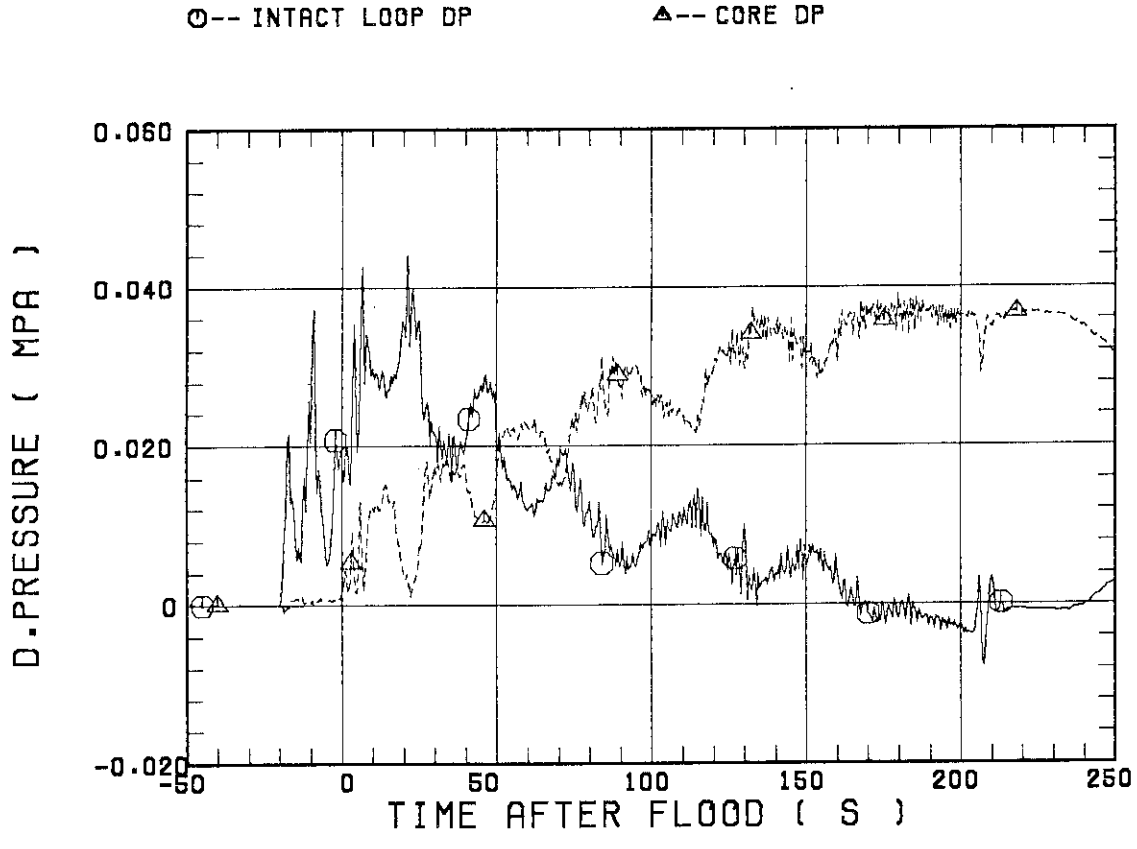

Fig. 3.7 Comparison of intact loop differential pressure with core differential pressure

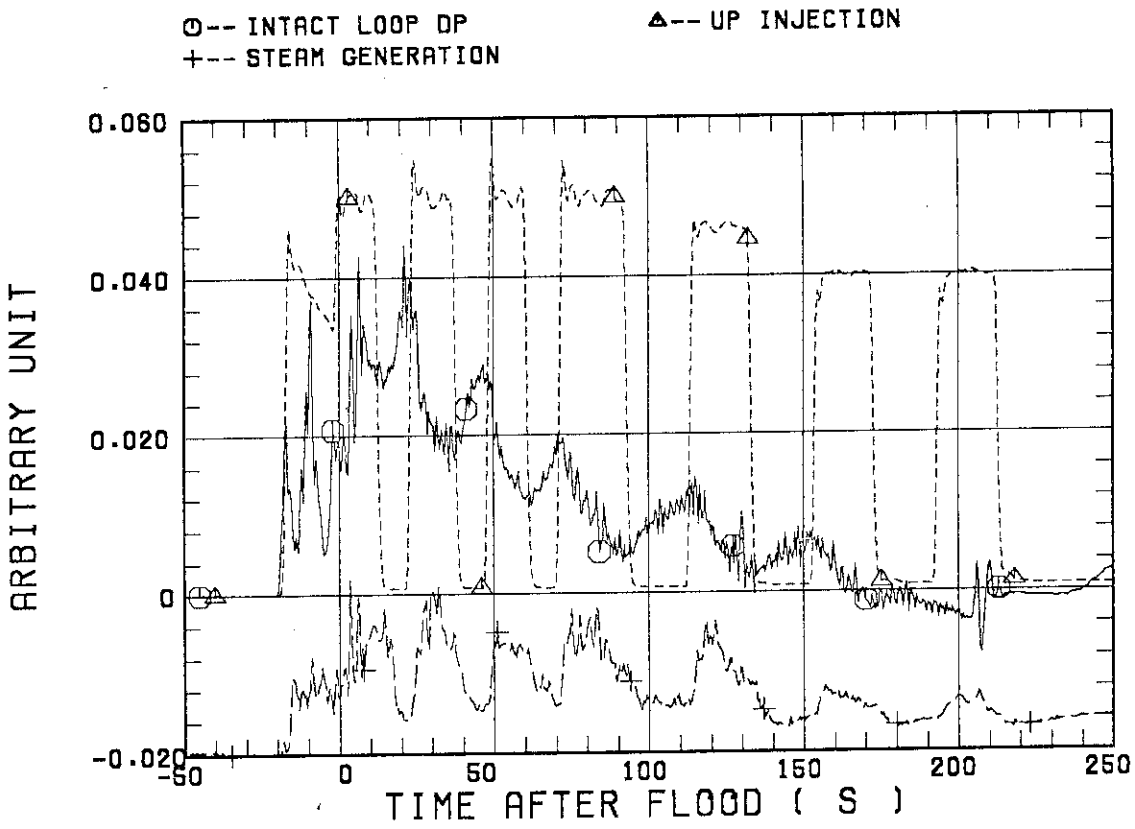

Fig. 3.8 Relation among intact loop differential pressure, upper plenum injection rate and core steam generation rate

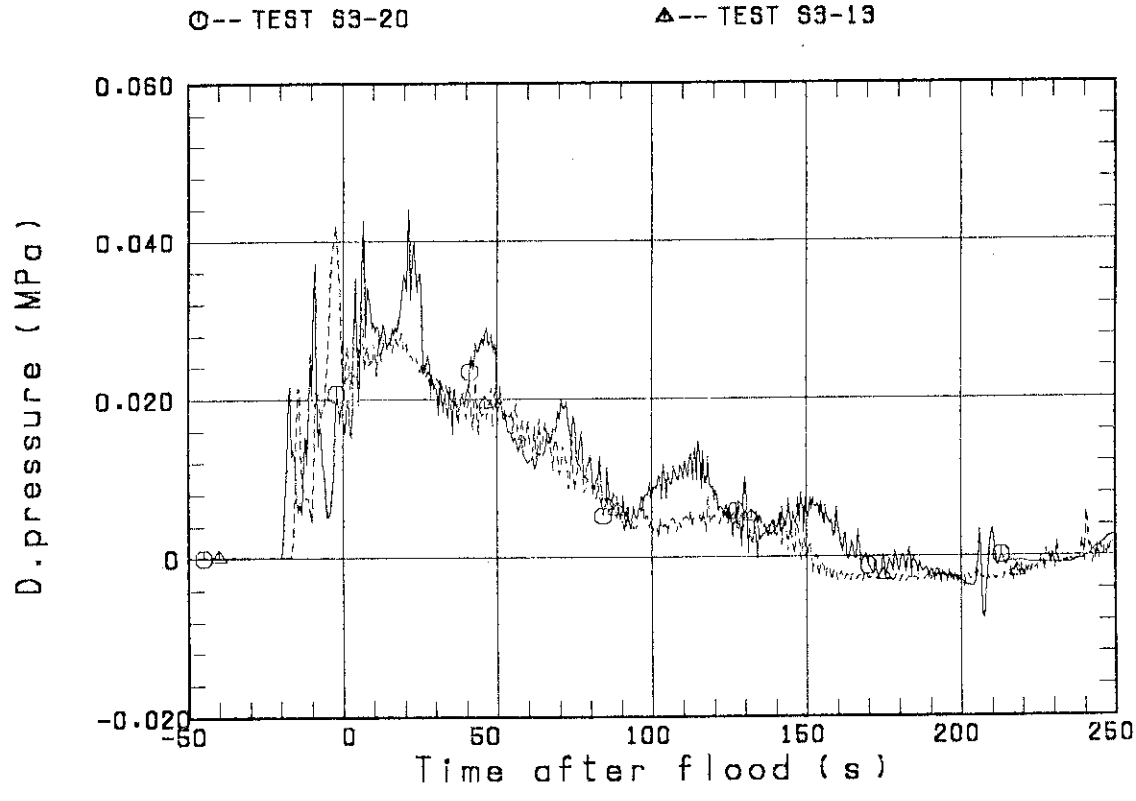

Fig. 3.9 Intact loop differential pressures

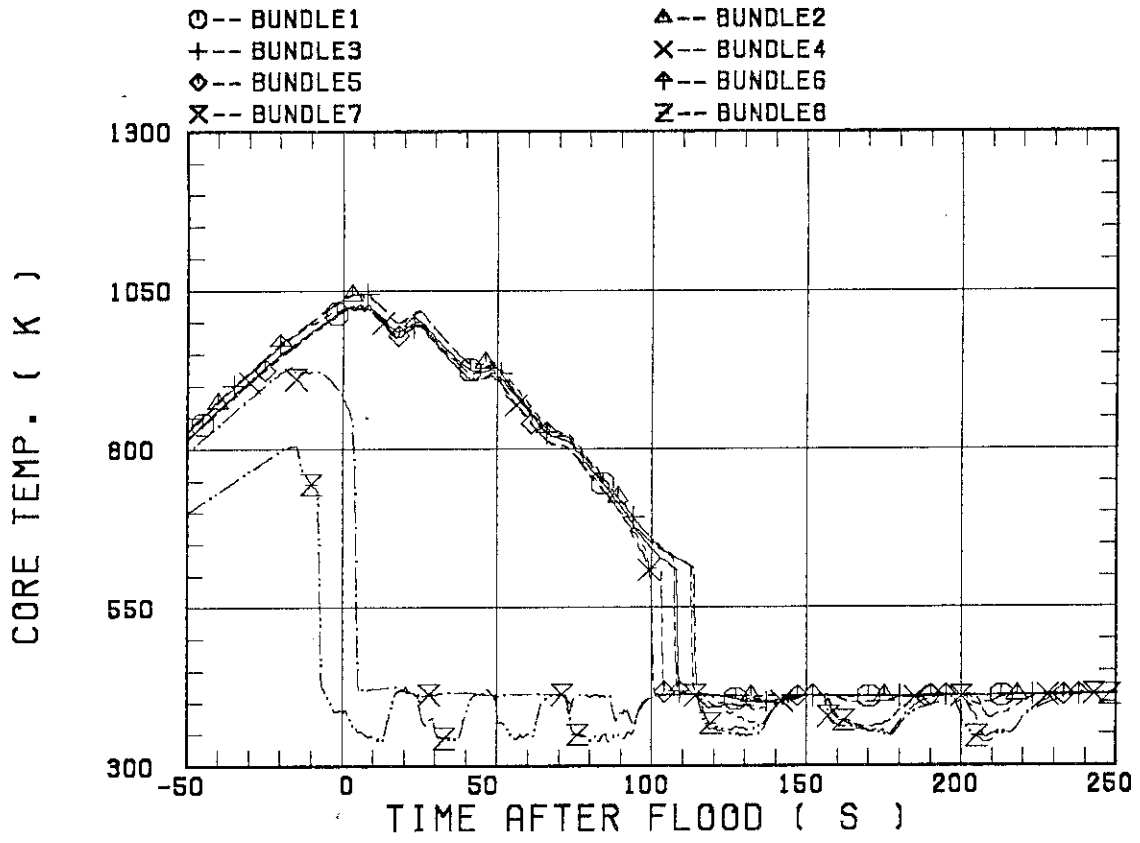

Fig. 3.10 Rod surface temperatures at 1.905 m elevation

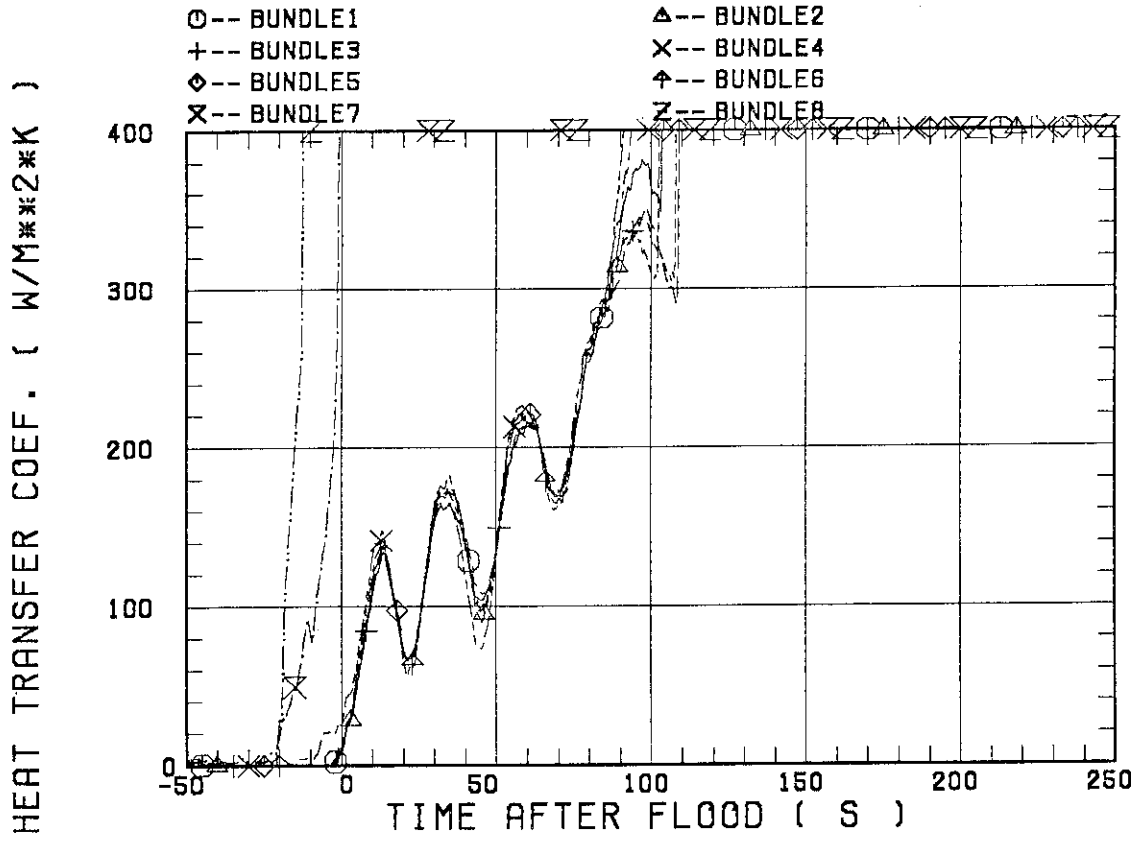

Fig. 3.11 Heat transfer coefficients at 1.905 m elevation

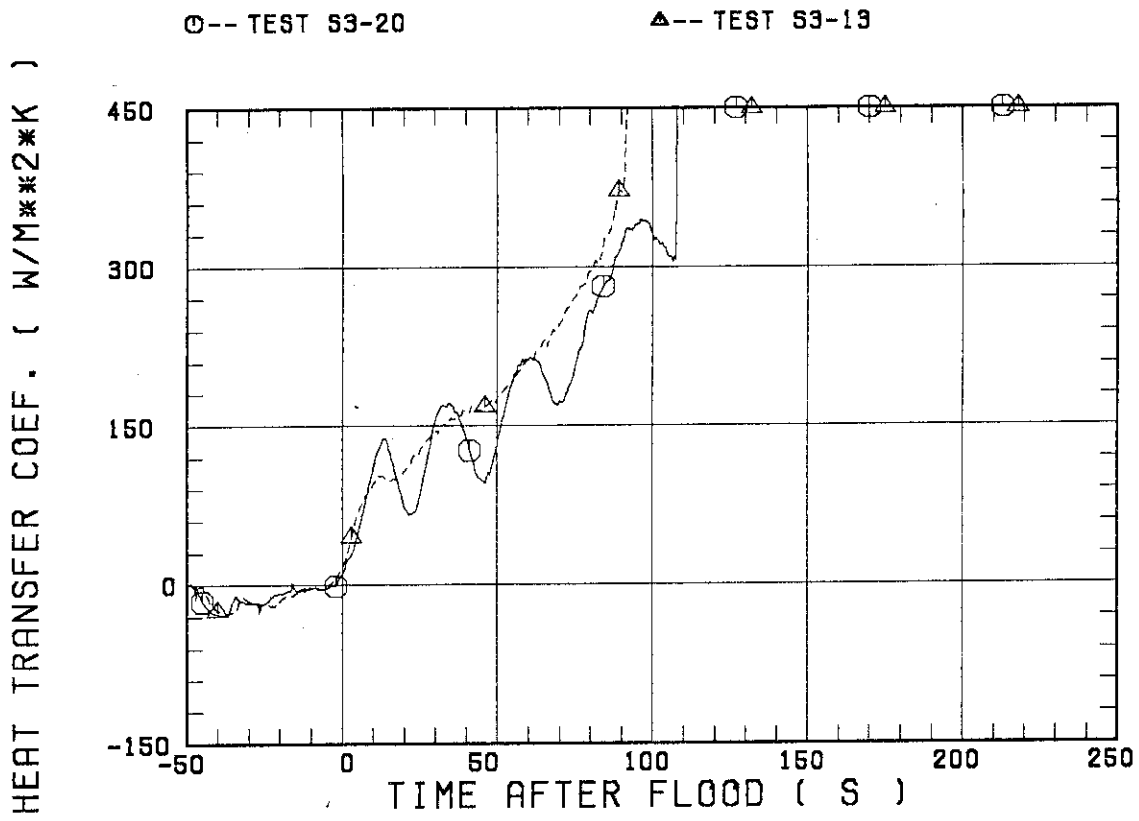

Fig. 3.12 Comparison of heat transfer coefficient at 1.905 m elevation in Bundle 2 between Tests S3-20 and S3-13

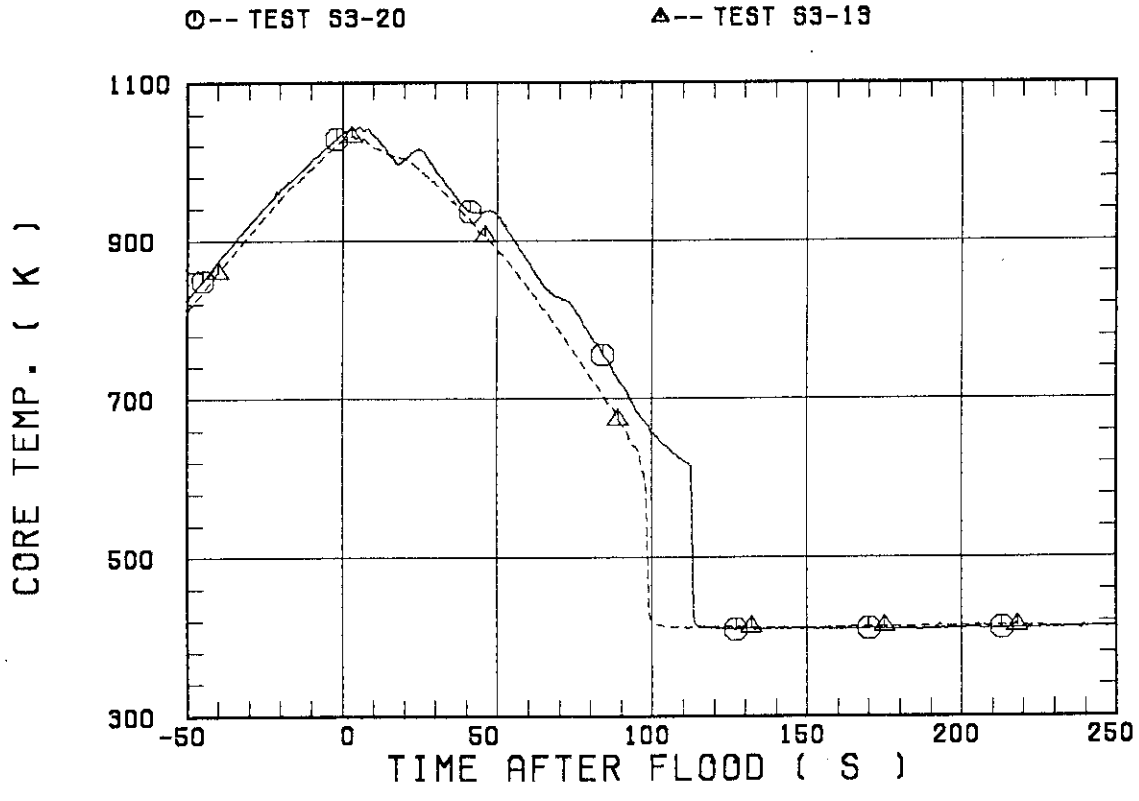

Fig. 3.13 Comparison of rod surface temperature at 1.905 m elevation in Bundle 2 between Tests S3-20 and S3-13

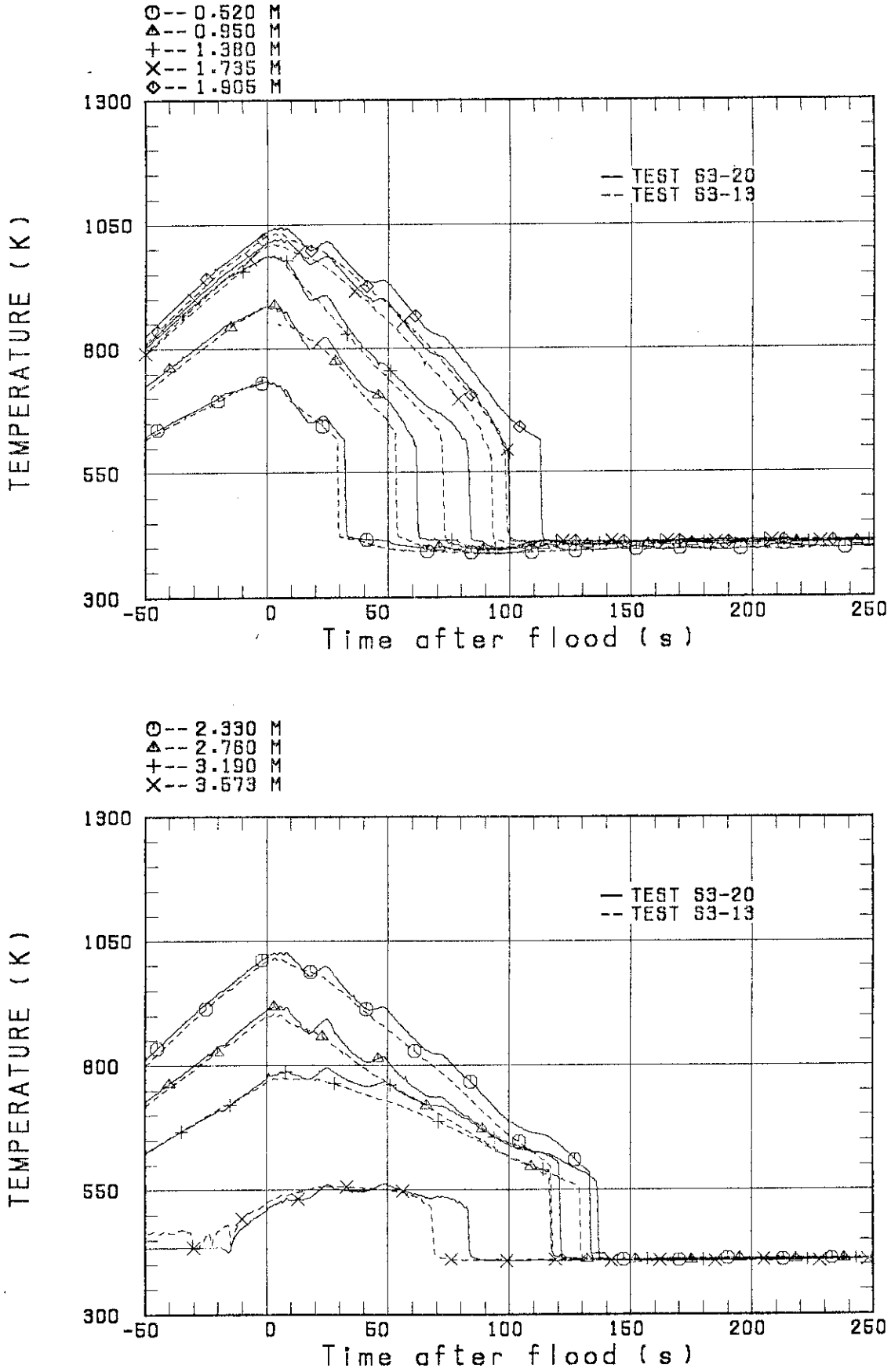

Fig. 3.14 Comparison of rod surface temperature at nine axial elevations in Bundle 2 between Tests S3-20 and S3-13

4. Conclusions

In order to investigate the effects of the intermittent ECC water delivery to the upper plenum on the break-through and the core cooling behaviors, SCTF Test S3-20 has been conducted. Analyzing the data of the present test together with those of Test S3-13, the following conclusions are obtained:

(1) The break-through occurred intermittently immediately corresponding to the intermittent ECC water injection. When the break-through occurred, there observed two different thermo-hydrodynamic behaviors between the break-through region and the non-break-through region.

(2) During the periods when the ECC water injection was nearly zero, the core water head decreased and this resulted in degradation of the core cooling in those periods. The reason of the decrease in the core water head is considered to be the increase in the intact loop differential pressure due to the decrease in the steam condensation in the upper plenum.

(3) Although the core cooling behavior was oscillatory, it has been found to be nearly identical to that for the continuous injection case.

Acknowledgments

The authors would like to express their appreciation to Messrs. A. Kamoshida, T. Oyama, Y. Niitsuma, K. Nakajima, T. Chiba, K. Komori, H. Sonobe and A. Owada for their contribution to the test conduction.

This work was performed under a contract with the Atomic Energy Bureau of Science and Technology Agency of Japan.

References

[1] Hirano, K. and Murao, Y.: "Large Scale Reflood Test", Nihon-Genshiryoku-Gakkai Shi (J. At. Energy Soc. Jpn.) [in Japanese], 22[10], 681(1980).

[2] Adachi, H. et al.: "Design of Slab Core test Facility (SCTF) in Large Scale Reflood Test Program, Part I: Core-I", JAERI-M 83-080 (1983).

[3] Sobajima, M. et al.: "Design of Slab Core Test Facility (SCTF) in Large Scale Reflood Test Program, Part II: Core-II", To be published as a JAERI-M report.

[4] Adachi, H. et al.: "Design of Slab Core Test Facility (SCTF) in Large Scale Reflood test Program, Part III: Core-III", To be published as a JAERI-M report.

[5] Weiss, P.A. and Hertlein, R.J.: "UPTF First Integral Test with Combined ECC Injection", NUREG/CP-0091, Vol. 4 (1988)

[6] Cappiello, M.W.: Private communication.

[7] Iguchi, T. et al.: "Evaluation Report on SCTF Core III Test S3-13 (Observed Reflood Phenomena in Test S3-13 under Combined Injection Mode for German-type PWR)", To be published as a JAERI-M report.

Acknowledgments

The authors would like to express their appreciation to Messrs. A. Kamoshida, T. Oyama, Y. Niitsuma, K. Nakajima, T. Chiba, K. Komori, H. Sonobe and A. Owada for their contribution to the test conduction.

This work was performed under a contract with the Atomic Energy Bureau of Science and Technology Agency of Japan.

References

[1] Hirano, K. and Murao, Y.: "Large Scale Reflood Test", Nihon-Genshiryoku-Gakkai Shi (J. At. Energy Soc. Jpn.) [in Japanese], 22[10], 681(1980).

[2] Adachi, H. et al.: "Design of Slab Core test Facility (SCTF) in Large Scale Reflood Test Program, Part I: Core-I", JAERI-M 83-080 (1983).

[3] Sobajima, M. et al.: "Design of Slab Core Test Facility (SCTF) in Large Scale Reflood Test Program, Part II: Core-II", To be published as a JAERI-M report.

[4] Adachi, H. et al.: "Design of Slab Core Test Facility (SCTF) in Large Scale Reflood test Program, Part III: Core-III", To be published as a JAERI-M report.

[5] Weiss, P.A. and Hertlein, R.J.: "UPTF First Integral Test with Combined ECC Injection", NUREG/CP-0091, Vol. 4 (1988)

[6] Cappiello, M.W.: Private communication.

[7] Iguchi, T. et al.: "Evaluation Report on SCTF Core III Test S3-13 (Observed Reflood Phenomena in Test S3-13 under Combined Injection Mode for German-type PWR)", To be published as a JAERI-M report.

Appendix A

Description of SCTF Core—III

A.1 Test Facility

The overall schematic diagram of SCTF is shown in Fig. A-1. The principal dimensions of the facility is shown in Table A-1, and the comparison of dimensions between SCTF and the reference PWR is shown in Fig. A-2.

A.1.1 Pressure Vessel

The pressure vessel is of slab geometry as shown in Fig. A-3. The height of the components in the pressure vessel is almost the same as the reference reactor's, and the flow area and the fluid volume of each component are scaled down based on the nominal core flow area scaling, 1/21.

The core consists of 8 bundles arranged in a row and each bundle includes heater rods and non-heated rods with 16×16 array. The core is enveloped by the honeycomb thermal insulator which is attached on the back surface of core wall plate.

The downcomer is located at one end of the pressure vessel which corresponds to the periphery of the actual reactor pressure vessel. The core baffle region located between the core and the downcomer is isolated for Core-III to minimize uncertainty in actual core flow. The cross sections of the pressure vessel at the upper head, upper plenum, core and lower plenum are shown in Fig. A-4.

A.1.2 Interface between Core and Upper Plenum

The interface between the core and the upper plenum consists of upper core support plate (UCSP), end box and various structures in the end box such as control rod spider which is paired with the control rod guid assembly (CRGA) and its support column bottom and special baffle plate spider which is paired with the hold-down bridge. These structures are exactly the same as those for a German PWR except some minor modifications.

Figure A-5 shows arrangement of the UCSP, the end box and the top grid spacer. The configuration of the end box is shown in Fig. A-6.

Detail of the end boxes with drag transducer device and other internals is shown in Fig. A-7. The UCSP shown in Fig. A-8 has two kinds of holes, i.e., the square holes correspond to the end boxes with control rod spider and the circular holes correspond to the end boxes with special baffle plate spider.

A.1.3 Upper Plenum and Upper Head

The vertical and horizontal cross sections of the upper plenum are shown in Figs. A-9 and A-4, respectively. In the SCTF Core-III, the slab cut of the upper plenum of a German (KWU) PWR is simulated. The splitted and staggered arrangement of the CRGA support columns was chosen to make good simulation of horizontal flow in the upper plenum.

As shown in Fig. A-10, there are three kinds of CRGA support column. Support column-1 is installed above Bundles 3 and 5 and connected to the CRGA support column bottom with the transition cone. Cross section of the CRGA support calumn changes from a circle to a half circle in this transition cone. Support column 2 is installed above Bundles 6 and 7 and the bottom is closed with the half conical bottom seal plate with many flow holes. Support column 3 is essentially the same as support column 2 but the edge of one side is cut off in order to install above Bundle 1. Each CRGA support column has ten or eleven baffle plates with flow holes. Top flow paths to the upper head bottom and to the upper plenum top are also provided.

Figure A-11 shows vertical cross section of the bottom part of the upper plenum and the interface between the core and the upper plenum. There are eight side flow injection nozzles and eight side flow extraction nozzles just at the opposite side of the upper plenum bottom, corresponding to each bundle.

The upper plenum is separated from the upper head by an upper support plate. Four top injection nozzles penetrate the upper head and open the top of upper plenum as shown in Fig. A-12. Outlet part of the top injection nozzle has a rectangular cross section and double mesh screen with 45 degree cross angle is attached at the mouth.

A.1.4 Simulated Core

The simulated core for the SCTF Core-III consists of 8 heater rod bundles arranged in a row. Each bundle has 236 electrically heated rods and 20 non-heated rods. The arrangement of rods in a bundle is shown in Fig. A-13. The dimensions of the heater rods are based on 15×15 fuel rods bundle for a PWR and the heated length and the outer diameter of each heater rod are 3.613 m and 10.7 mm, respectively. A heater rod consists of a nichrome heater element, boron nitride (BN) or magnesium oxide (MgO) depending on elevation in the heated zone and Nichrofer 7216 (equivalent to Inconel 600) sheath. The sheath thickness is about 1.0 mm and is thicker than the actual fuel cladding because of the requirements for thermocouple installation. The heater element is a helical coil and has a 17 step chopped cosine axial power profile as shown in Fig. A-14. The peaking factor is 1.4.

Non-heated rods are either pipes or solid rods of stainless steel with 13.8 mm O.D. The heater rods and non-heated rods are fixed at the top of the core allowing downward expansion. In Fig. A-15, relative elevation of rods and spacers is shown.

For better simulation of flow resistance in the lower plenum, the simulated fuel rods end in the lower plenum and do not penetrate through the bottom plate of the lower plenum as shown in Fig. A-15.

A.1.5 Primary Loops

Primary loops consist of a hot leg equivalent to four hot legs in area, a steam/water separator for simulating single steam phase flow downstream of the steam generator and for measuring flow rate of carry over water, an intact cold leg equivalent to three intact loops, a broken cold leg on the pressure vessel side and a broken cold leg on the steam/water separator side. These two broken cold legs are connected to two containment tanks through break valves, respectively. The arrangement of the primary loops is shown in Fig. A-16. The flow area of each loop is scaled down based on the core flow area scaling, 1/21. It should be emphasized that the cross section of the hot leg is an elongated circle with an actual height to realize proper flow pattern in the hot leg. The steam/water separator has a steam generator inlet plenum simulator to correctly simulate the flow

characteristics of carryover water into the U-tubes. The cross section of the hot leg and the configuration of the steam genrator inlet plenum simulator are shown in Fig. A-17.

A pump simulator and a loop seal part are provided for the intact cold leg. The arangement of the intact cold leg is shown in Fig. A-18. The pump simulator consists of the casing and duct simulators and an orifice plate as shown in Fig. A-19. The loop resistance is adjusted with the orifice plates attached to the intact cold leg, the steam/water separator side and pressure vessel side broken cold legs and the pump simulator.

A.1.6 ECC Water Injection System

Three kinds of ECCSs are provided, i.e., the accumulator injection system (Acc), low pressure coolant injection system (LPCI) and combined injection system. Available injection locations for the former two are the intact and broken cold legs, the hot leg, the lower plenum and the downcomer. On the other hand, those for the last one are the top and bottom-side of the upper plenum and the intact and broken cold legs.

A.1.7 Containment Tanks and Auxiliary System

Two containment tanks are provided to SCTF. The containment tank-I is connected with the downcomer through the pressure vessel side broken cold leg and the containment tank-II is connected with the steam/water separator through the steam/water separator side broken cold leg. Especially in the containment tank-I, carryover water from the downcomer is measured by the differentiation of the liquid level. These containment tanks and auxiliary system such as a pressurizer for injecting water from the Acc tanks, etc. are shared with CCTF.

A.2 Instrumentation

The instrumentation in SCTF has been provided both by JAERI and USNRC. The JAERI-provided instrumentation includes the measurement of temperatures, pressures, differential pressures, liquid levels, flow velocities, and heating powers. USNRC has provided film probes, impedance probes, string probes, liquid level detectors (LLDs), fluid distribution grids (FDGs), turbine meters, drag disks, densitometers, spool pieces, drag bodies, break through detectors and video optical probes. Locations of the JAERI-provided instruments are shown in Figs. A-20 through A-43.

Table A-1 Principal Dimensions of the SCTF

1. Core Dimension		
(1) Quantity of Bundle	8 Bundles	
(2) Bundle Array	1 × 8	
(3) Bundle Pitch	230 mm	
(4) Rod Array in a Bundle	16 × 16	
(5) Rod Pitch in a Bundle	14.3 mm	
(6) Quantity of Heater Rod in a Bundle	236 rods	
(7) Quantity of Non-Heated Rod in a Bundle	20 rods	
(8) Total Quantity of Heater Rods	236×8=1,888 rods	
(9) Total Quantity of Non-Heated Rods	20×8=160 rods	
(10) Effective Heated Length of Heater Rod	3613 mm	
(11) Diameter of Heater Rod	10.7 mm	
(12) Diameter of Non-Heated Rod	13.8 mm	
2. Flow Area & Fluid Volume		
(1) Core Flow Area	0.25	m^2
(2) Core Fluid Volume	0.903	m^3
(3) Baffle Region Flow Area (isolated)	(0.096)	m^2
(4) Baffle Region Fluid Volume (nominal)	0.355	m^3
(5) Cross-Sectional Area of Core Additional Fluid Volumes Including Gap between Core Barrel and Pressure Vessel Wall and Various Penetration Holes	0.07 ~ 0.10	m^2
(6) Downcomer Flow Area	0.158	m^2
(7) Upper Annulus Flow Area	0.158	m^2
(8) Upper Plenum Horizontal Flow Area (max.)	0.541	m^2
(9) Upper Plenum Vertical Flow Area	0.525	m^2
(10) Upper Plenum Fluid Volume	1.156	m^3
(11) Upper Head Fluid Volume	0.86	m^3
(12) Lower Plenum Fluid Volume (excluding below downcomer)	1.305	m^3
(13) Steam Generator Inlet Plenum Simulator Flow Area	0.626	m^2
(14) Steam Generator Inlet Plenum Simulator Fluid Volume	0.931	m^3
(15) Steam Water Separator Fluid Volume	5.3	m^3
(16) Flow Area at the Top Plate of Steam Generator Inlet Plenum Simulator	0.195	m^2
(17) Hot Leg Flow Area	0.0826	m^2

Table A-1 (continue)

(18)	Intact Cold Leg Flow Area (Diameter = 297.9 mm) Inverted U-Tube with 0.0314 m^2 Cross-Sectional Area (Diameter = 200 mm) and 10 m Height from the Top of Steam Generator Inlet Plenum Simulator Can Be Added As an Option.	0.0697 m^2
(19)	Broken Cold Leg Flow Area (Diameter = 151.0 mm)	0.0197 m^2
(20)	Containment Tank-I Fluid Volume	30 m^3
(21)	Containment Tank-II Fluid Volume	50 m^3
(22)	Flow Area of Exhausted Steam Line from Containment Tank-II to the Atmosphere	see Fig. 3-63

3. Elevation & Height

(1)	Top Surface of Upper Core Support Plate (UCSP)	0 mm
(2)	Bottom Surface of UCSP	- 40 mm
(3)	Top of the Effective Heated Length of Heater Rod	- 444 mm
(4)	Bottom of the Effective Heated Length of Heater Rod	-4,057 mm
(5)	Bottom of the Skirt in the Lower Plenum	-5,270 mm
(6)	Bottom of Intact Cold Leg	+ 724 mm
(7)	Bottom of Hot Leg	+1,050 mm
(8)	Top of Upper Plenum	+2,200 mm
(9)	Bottom of Steam Generator Inlet Plenum Simulator	+1,933 mm
(10)	Centerline of Loop Seal Bottom	-2,281 mm
(11)	Bottom Surface of End Box	- 263 mm
(12)	Top of Upper Annulus of Downcomer	+2,234 mm
(13)	Height of Steam Generator Inlet Plenum Simulator	1,595 mm
(14)	Height of Loop Seal	3,140 mm
(15)	Inner Height of Hot Leg Pipe	737 mm
(16)	Bottom of Lower Plenum	-5,772 mm
(17)	Top of Upper Head	+2,887 mm

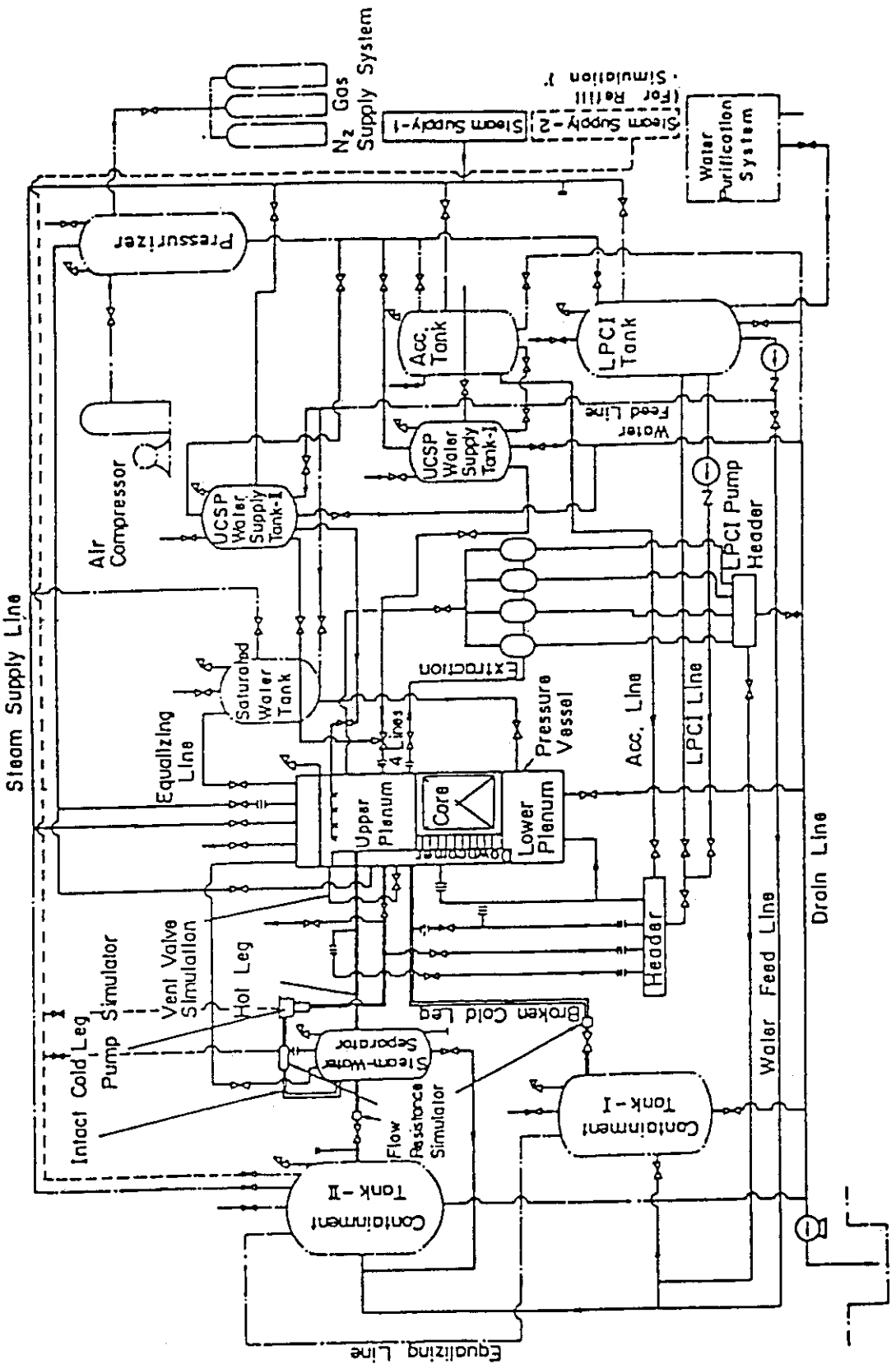

Fig. A-1 Schematic Diagram of Slab Core Test Facility

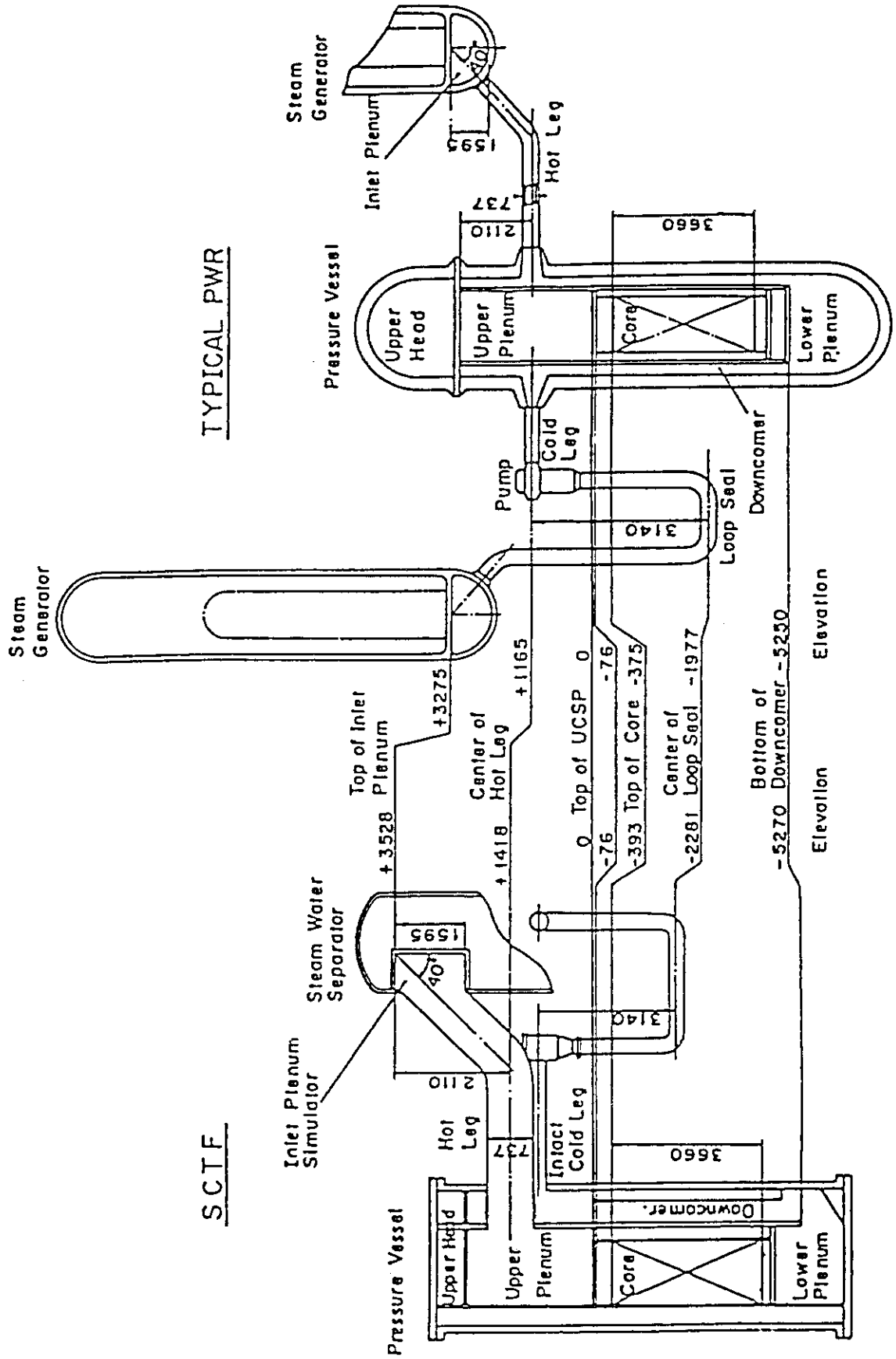

Fig. A-2 Comparison of Dimensions between SCTF and a Reference PWR

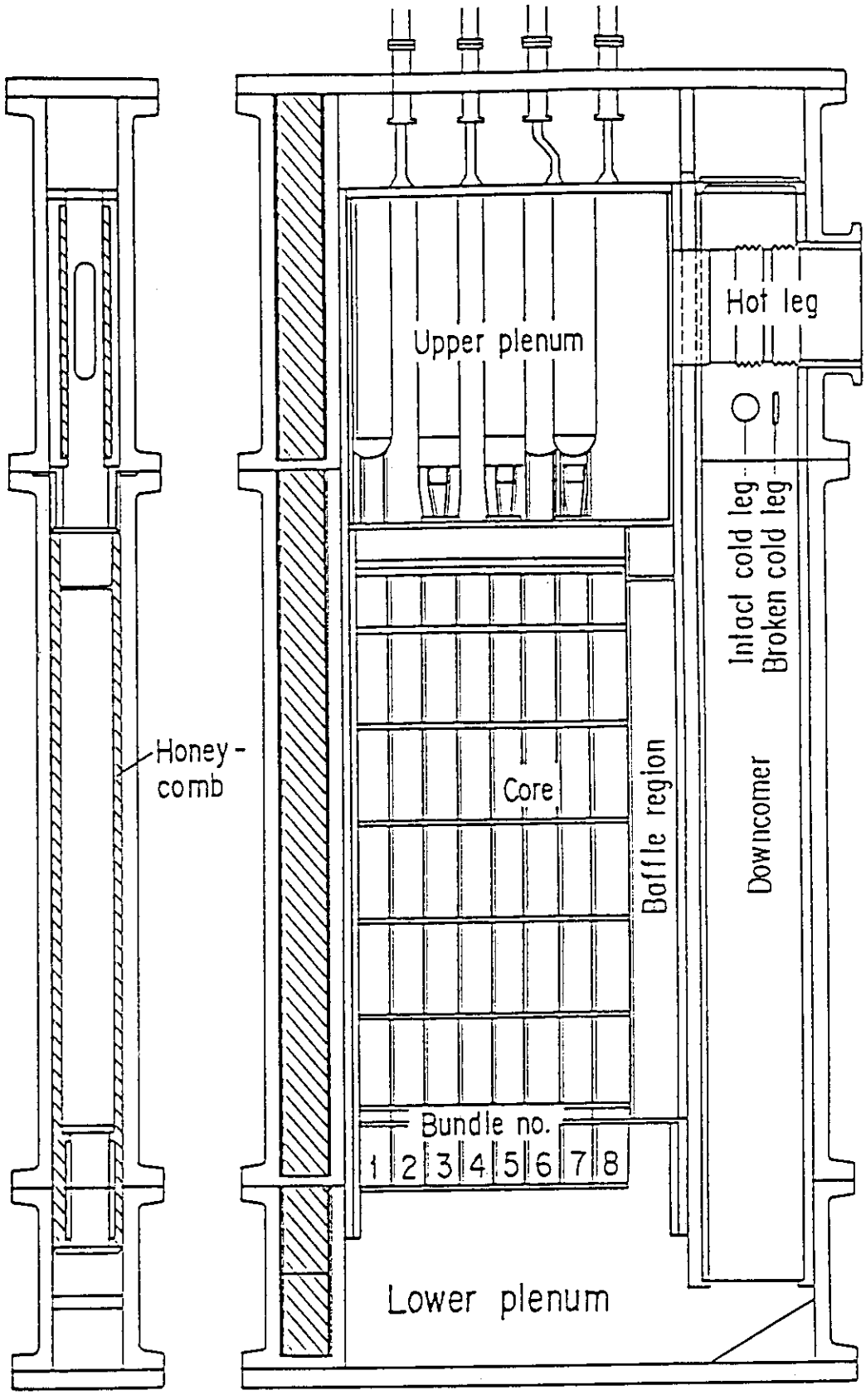

Fig. A-3 Vertical Cross Sections of Pressure Vessel

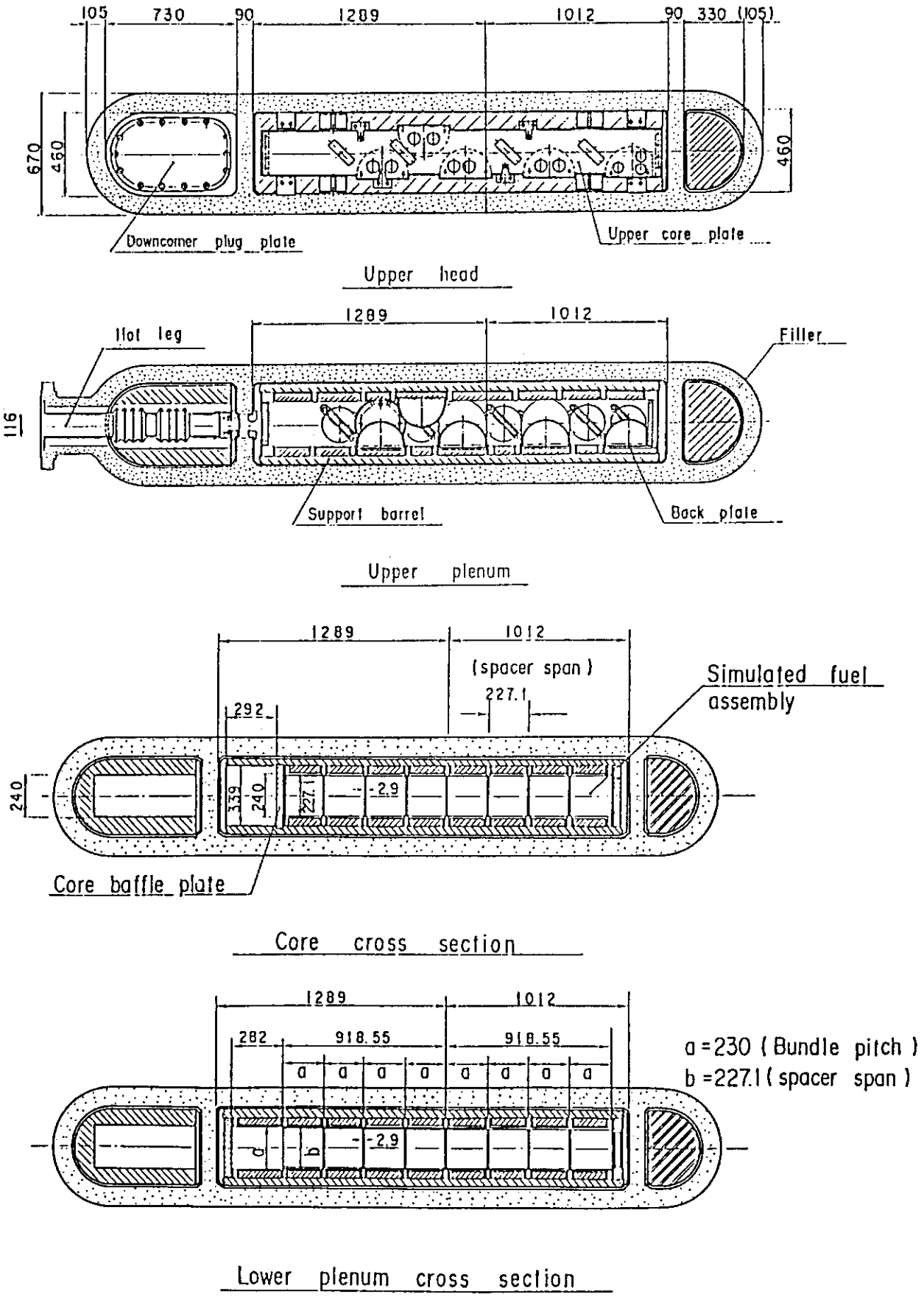

Fig. A-4 Horizontal Cross Sections of Pressure Vessel

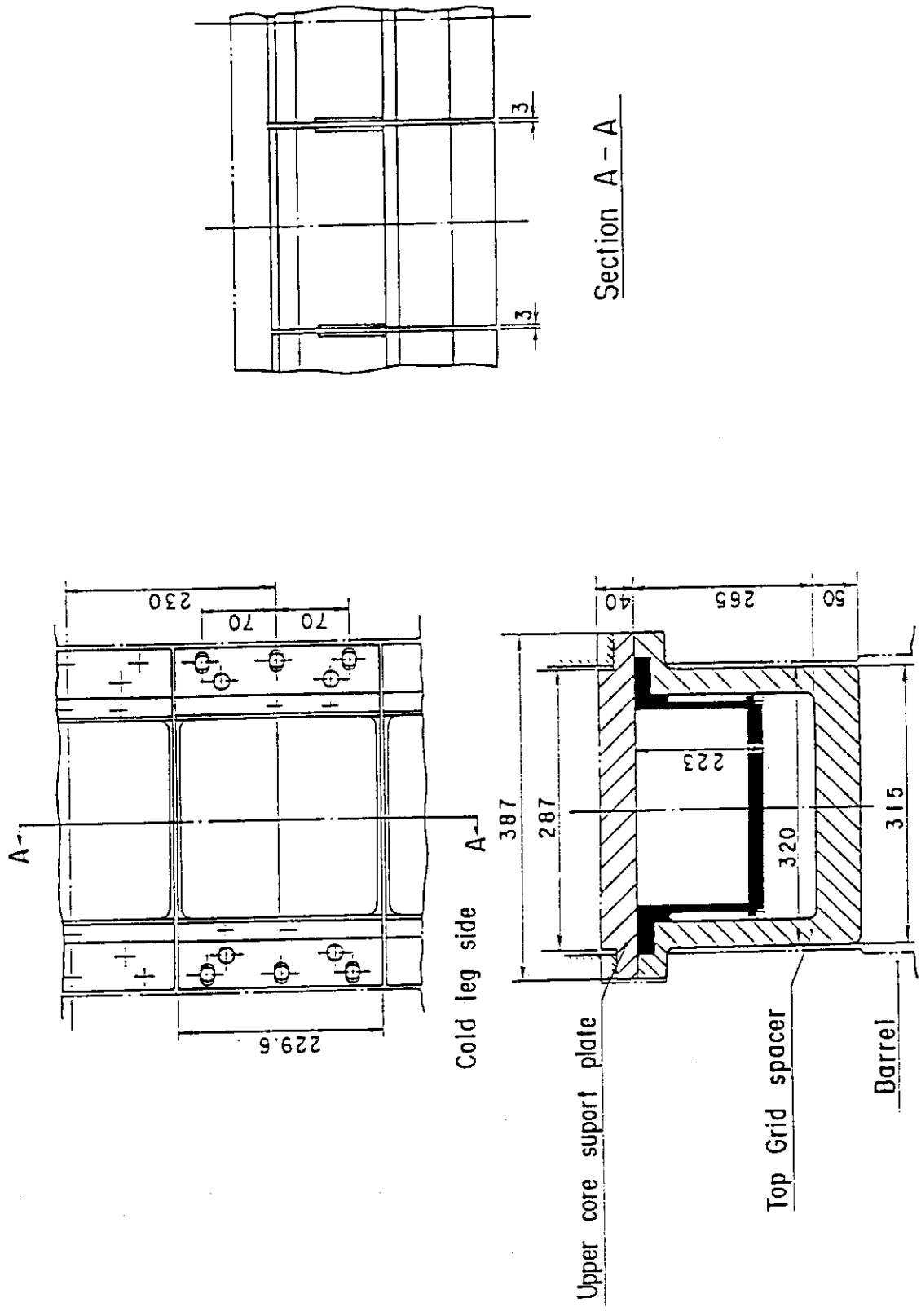

Fig. A-5 Arrangement and Principal Dimension of End Boxes and Top Grid Spacers

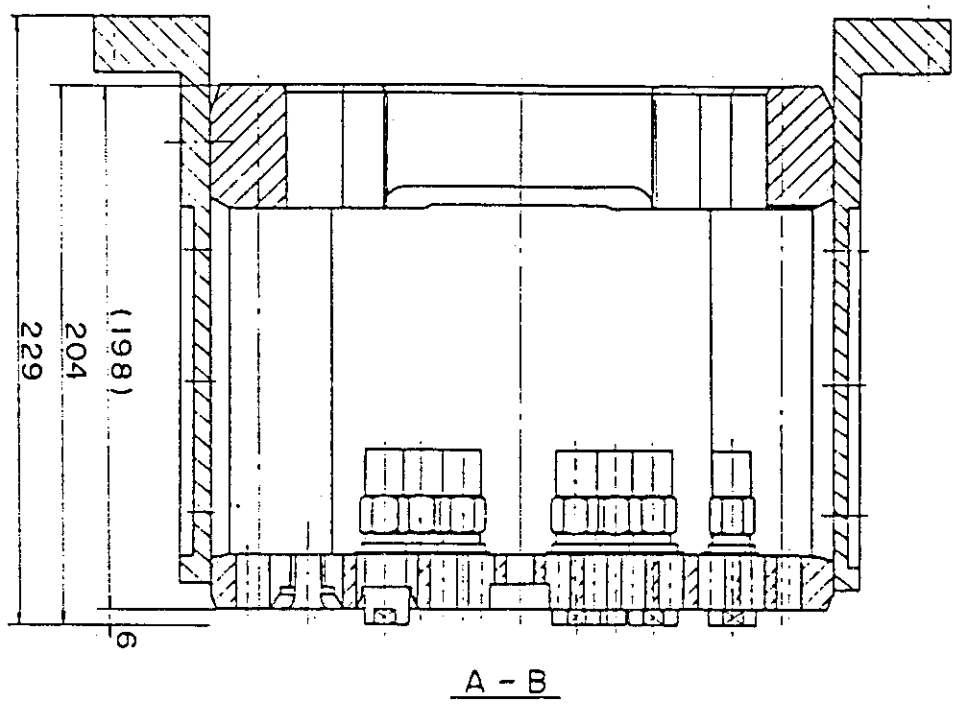

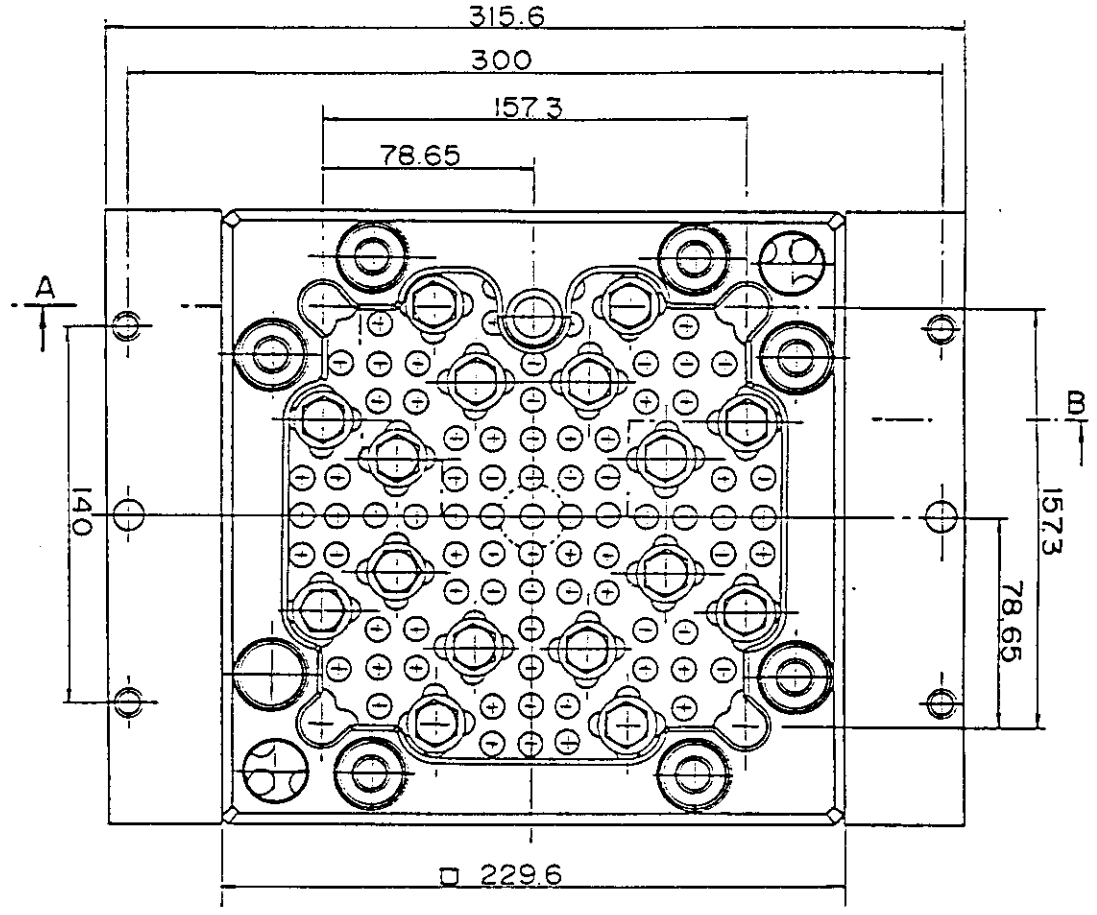

Fig. A-6 Configuration and Dimension of End Boxes

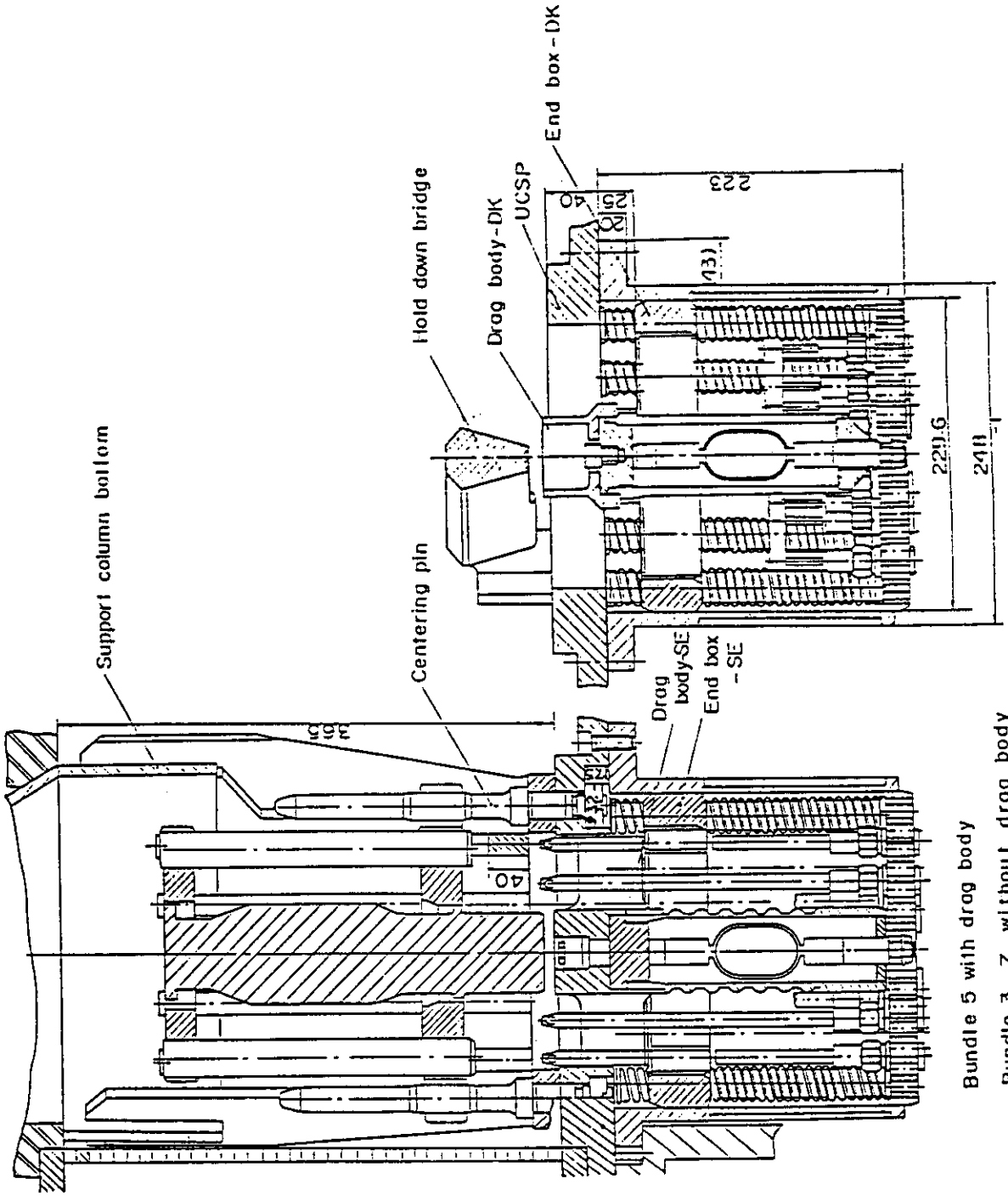

Fig. A-7 Detail of End Boxes with Drag Bodies

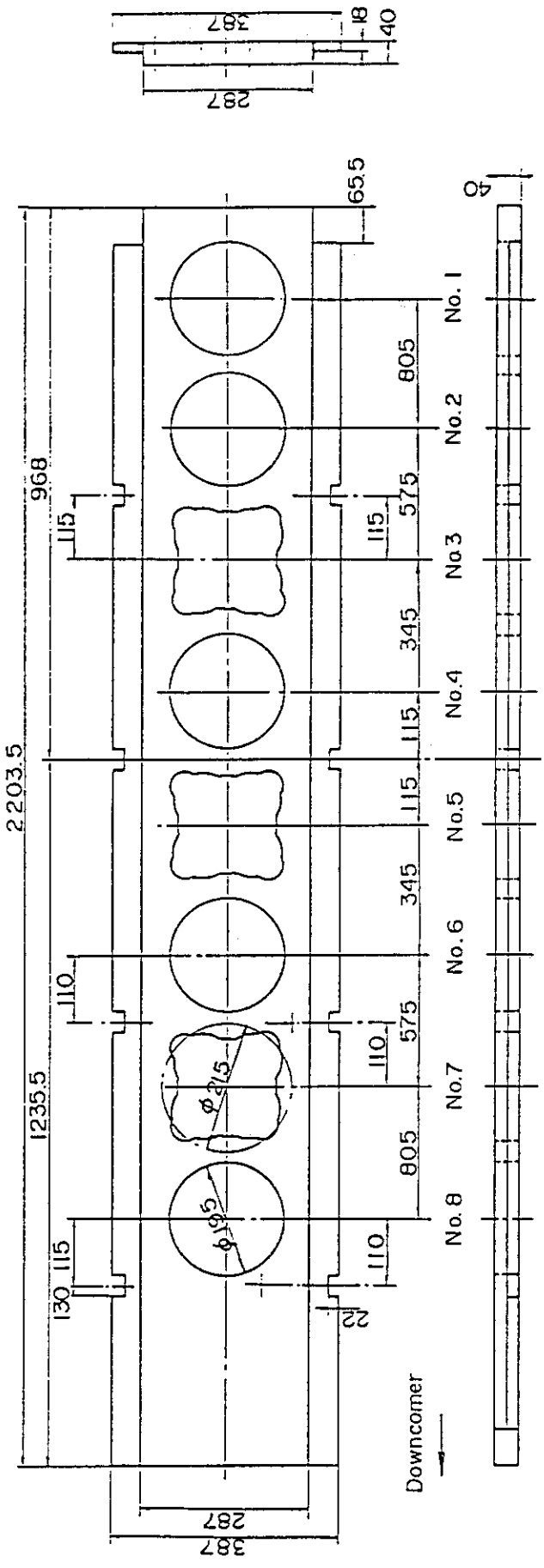

Fig. A-8 Dimension of Upper Core Support Plate

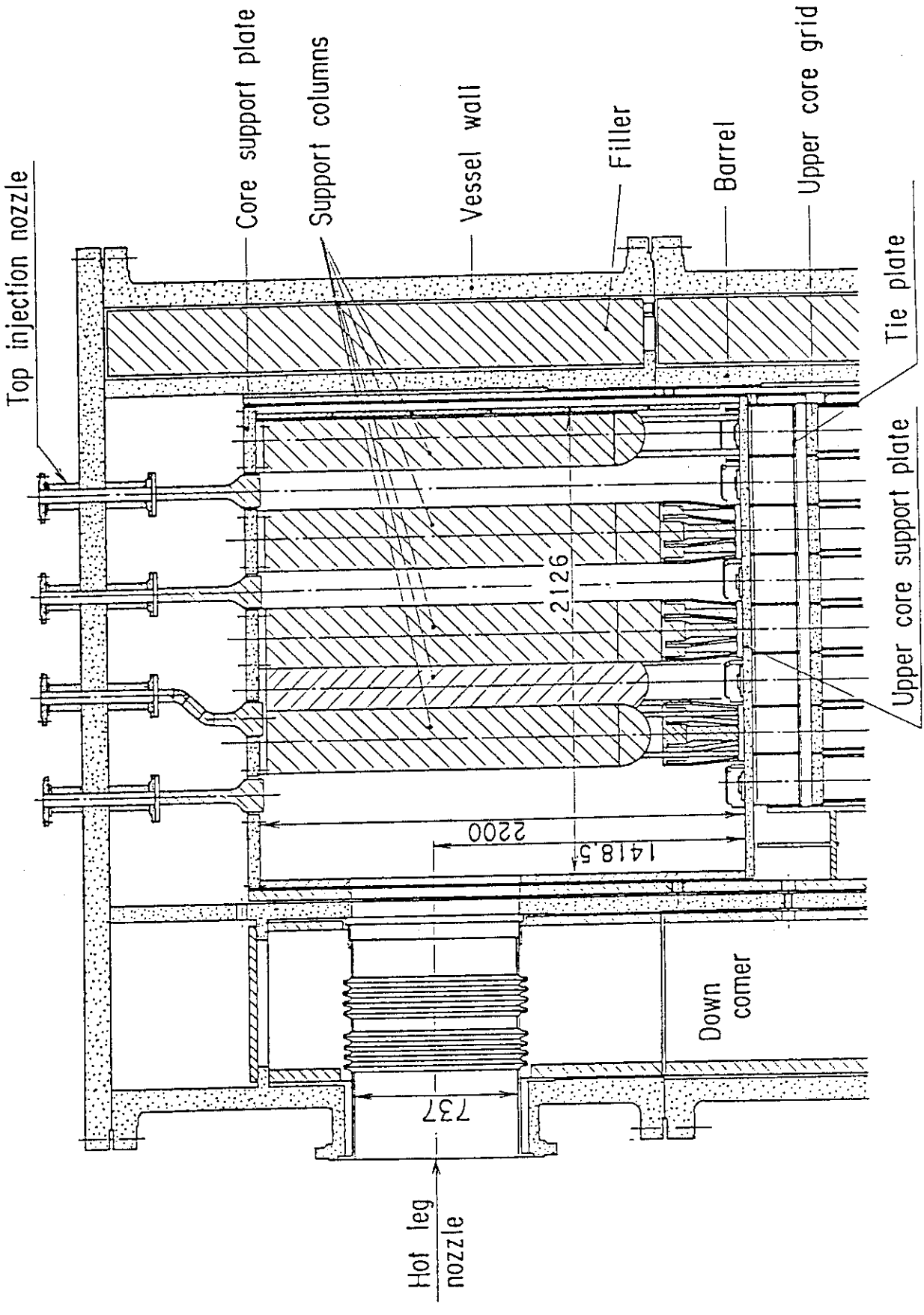

Fig. A-9 Vertical Cross Section of Upper Plenum Internals

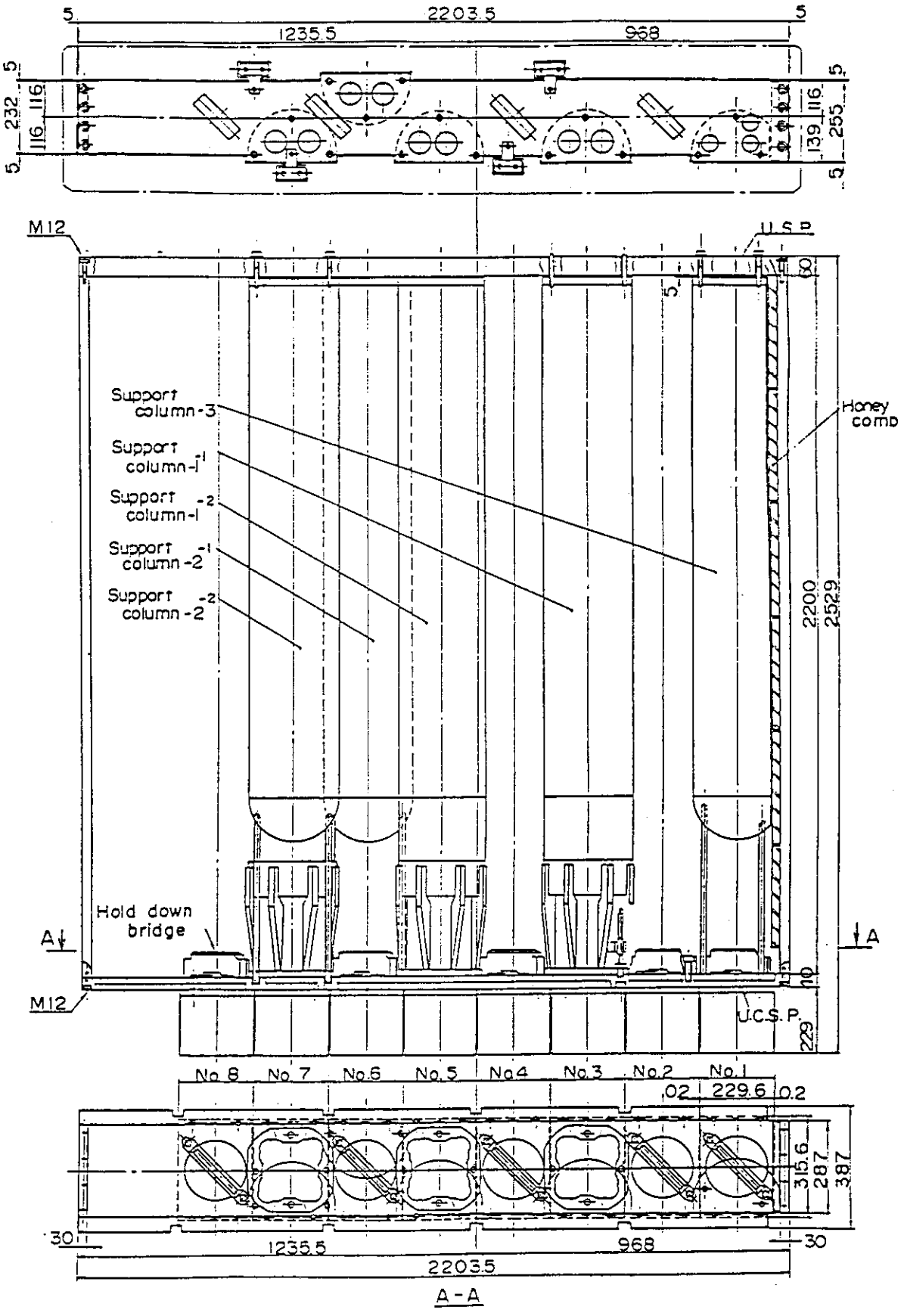

Fig. A-10 Three Kinds of CRGA Support Column

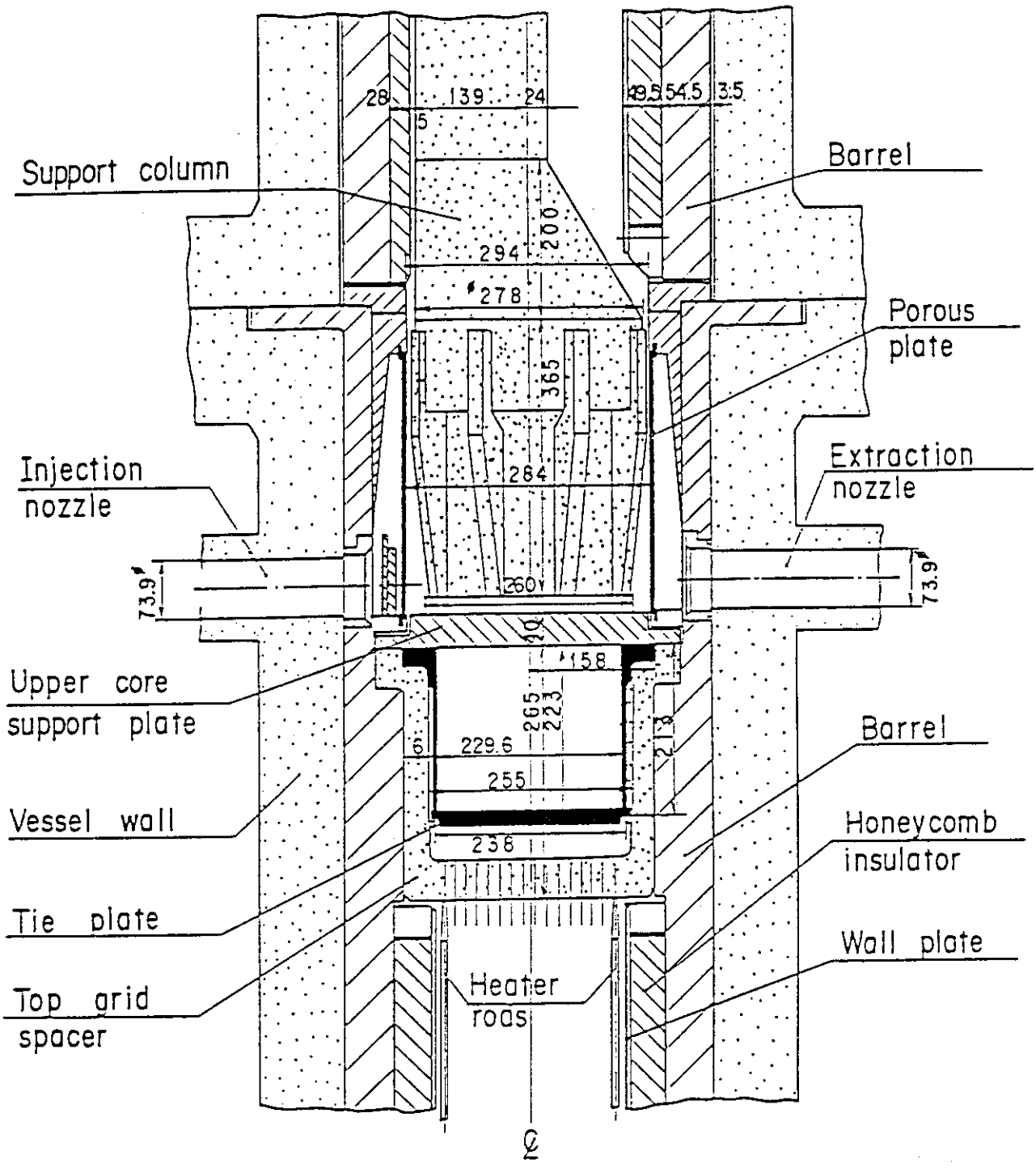

Fig. A-11 Vertical Cross Section of Interface between Core and Upper Plenum

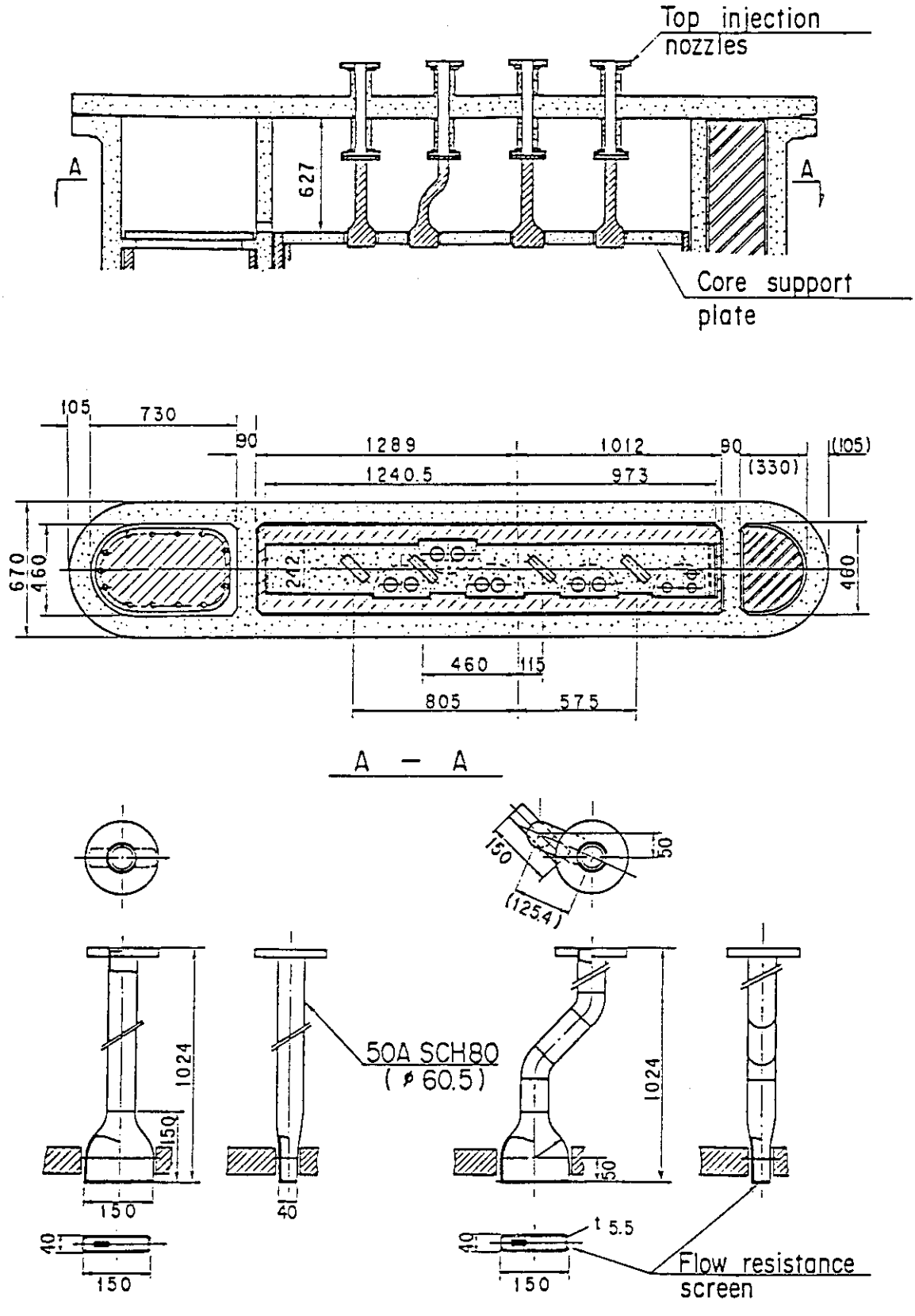

Fig. A-12 Schematic of Upper Head

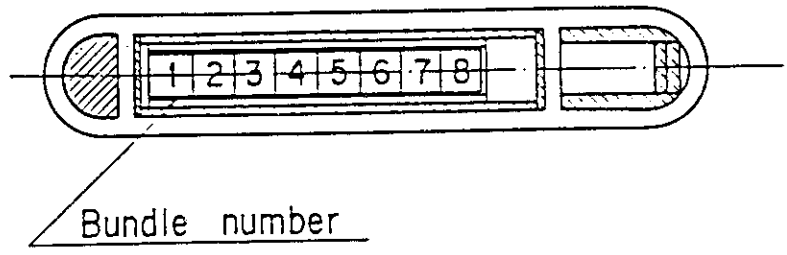

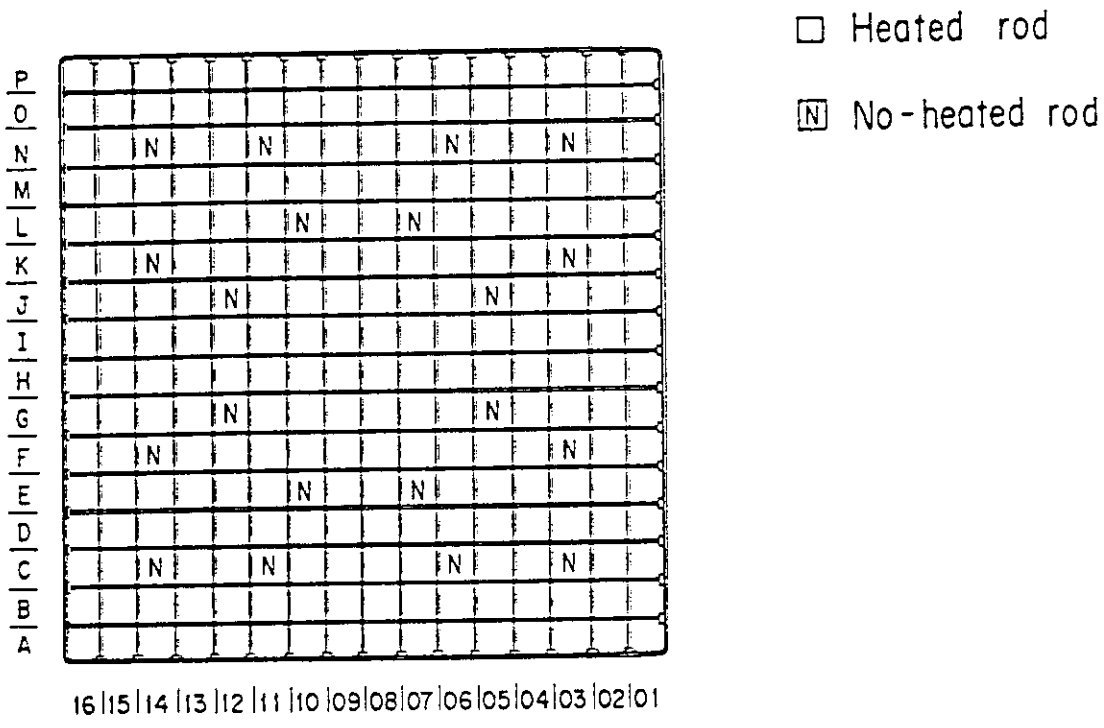

Fig. A-13 Arrangement of Heater Rod Bundles

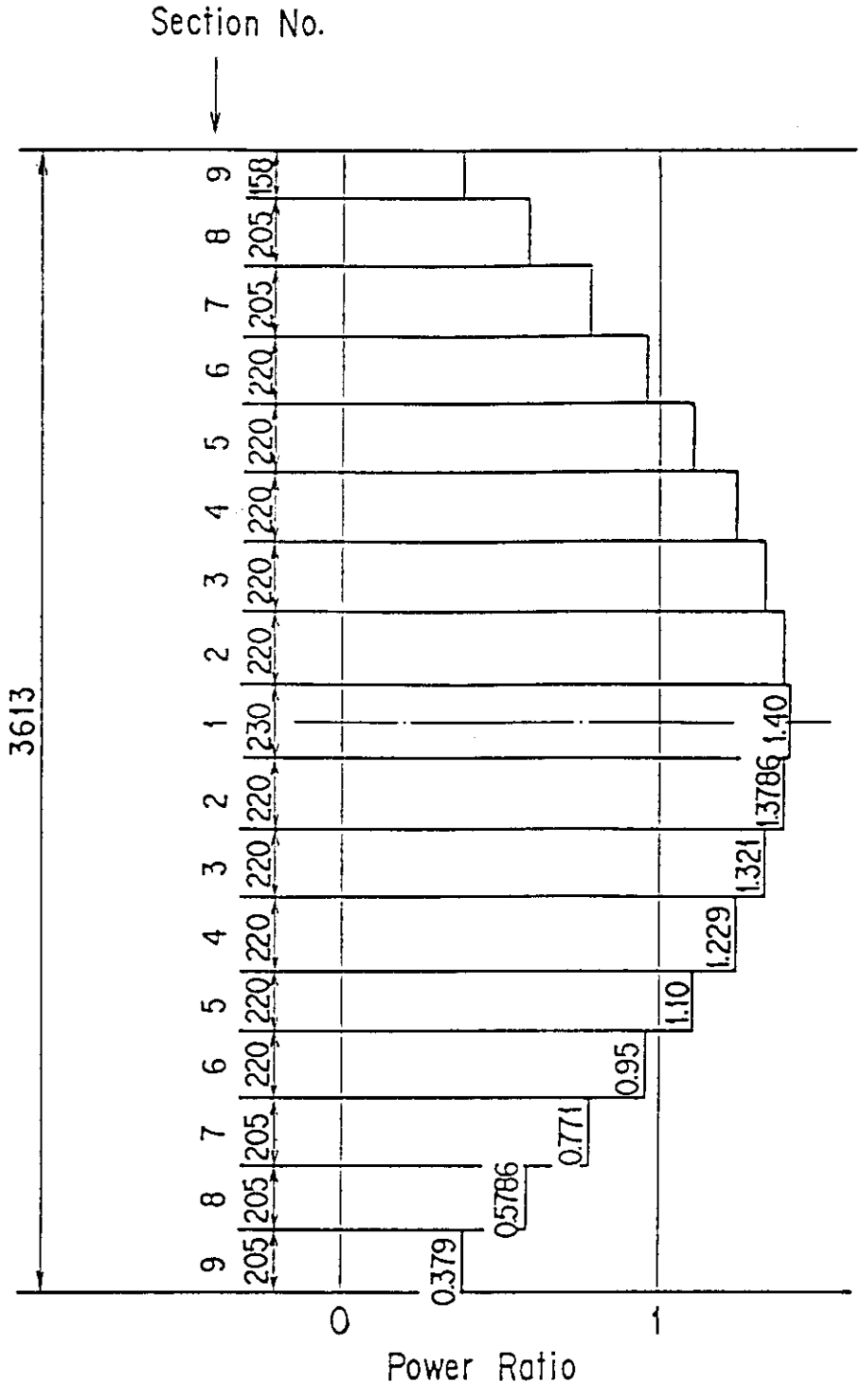

Fig. A-14 Axial Power Distribution of Heater Rods

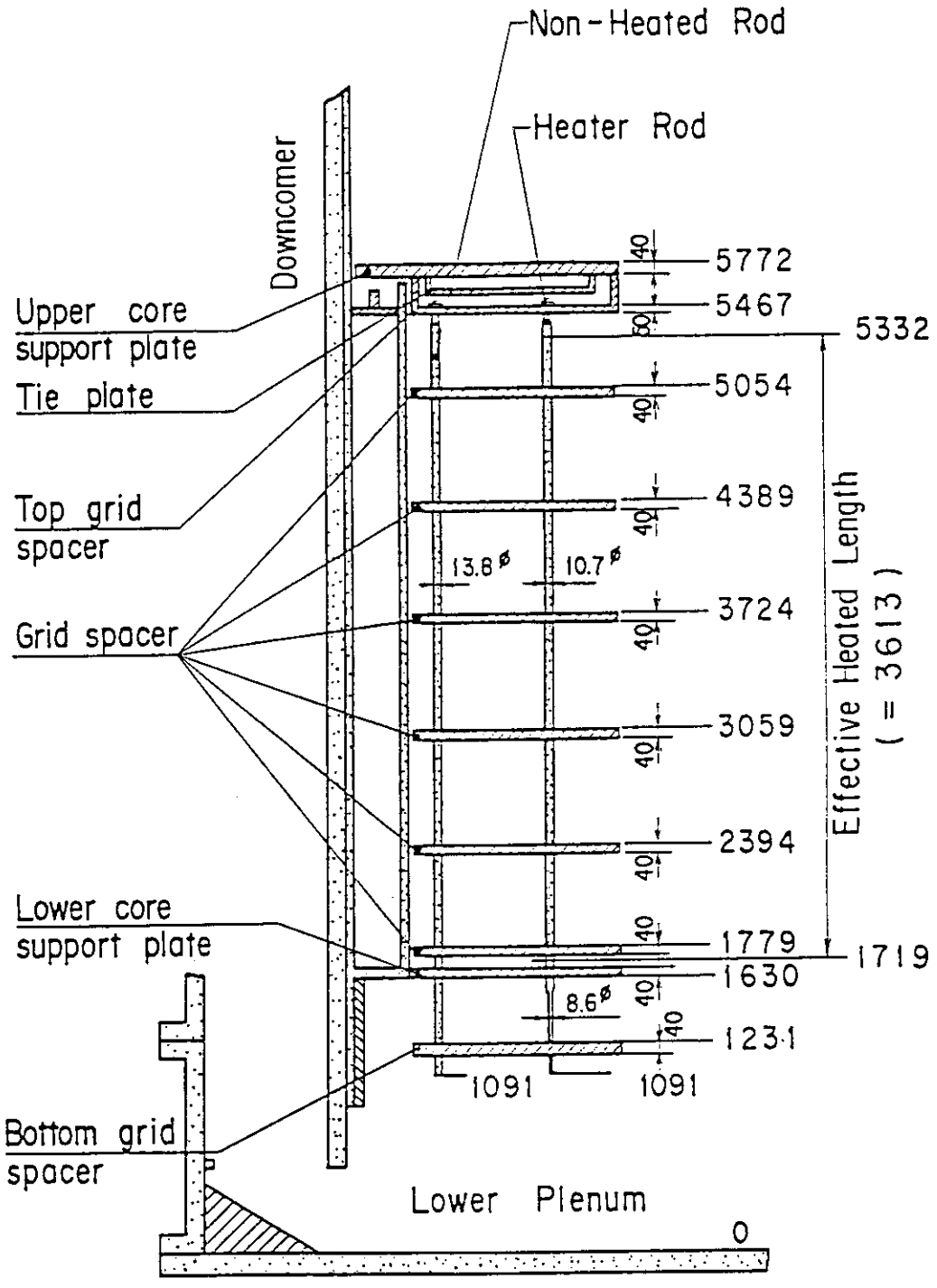

Fig. A-15 Relative Elevation and Dimension of Core

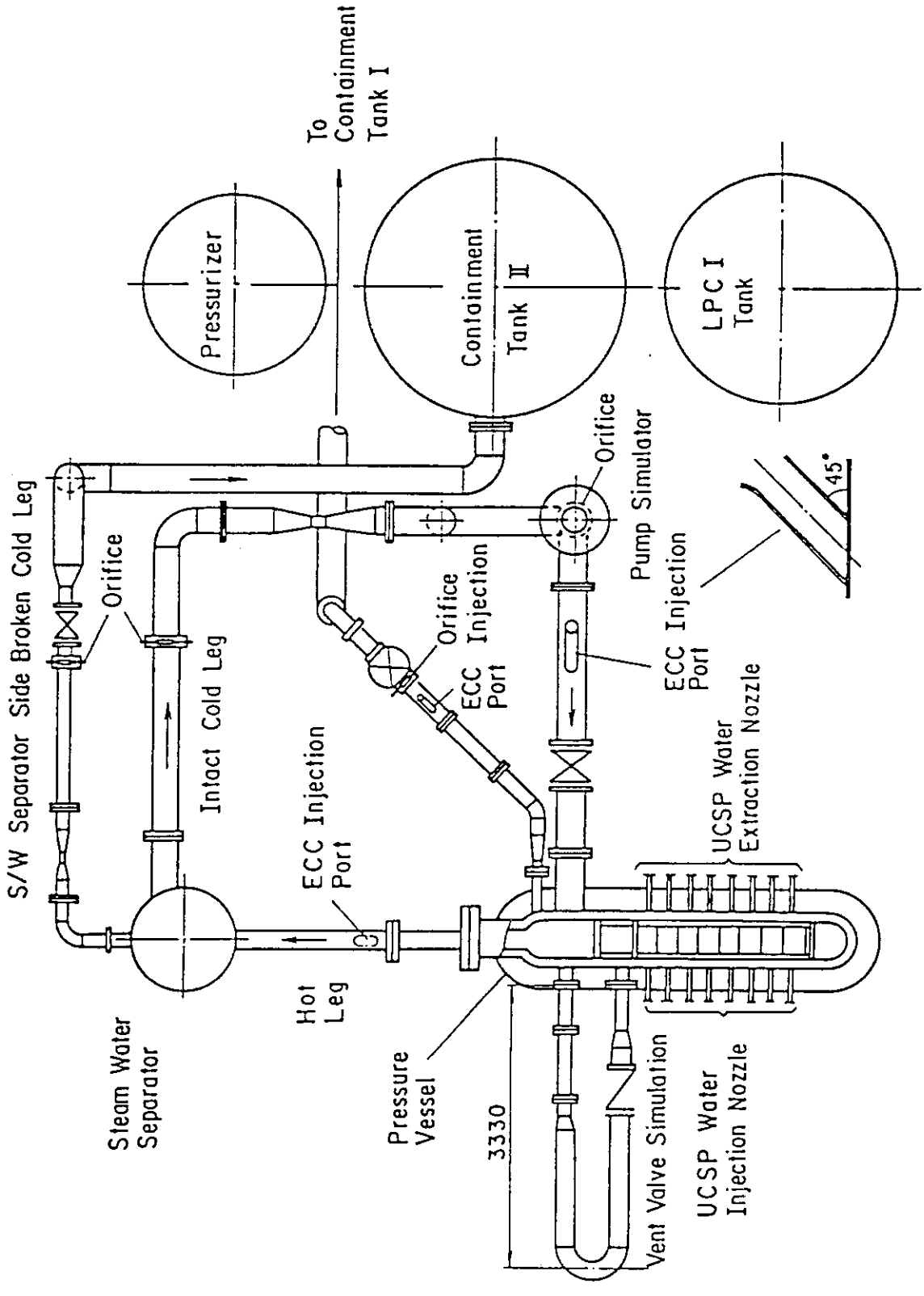

Fig. A-16 Overview of the Arrangements of SCTF

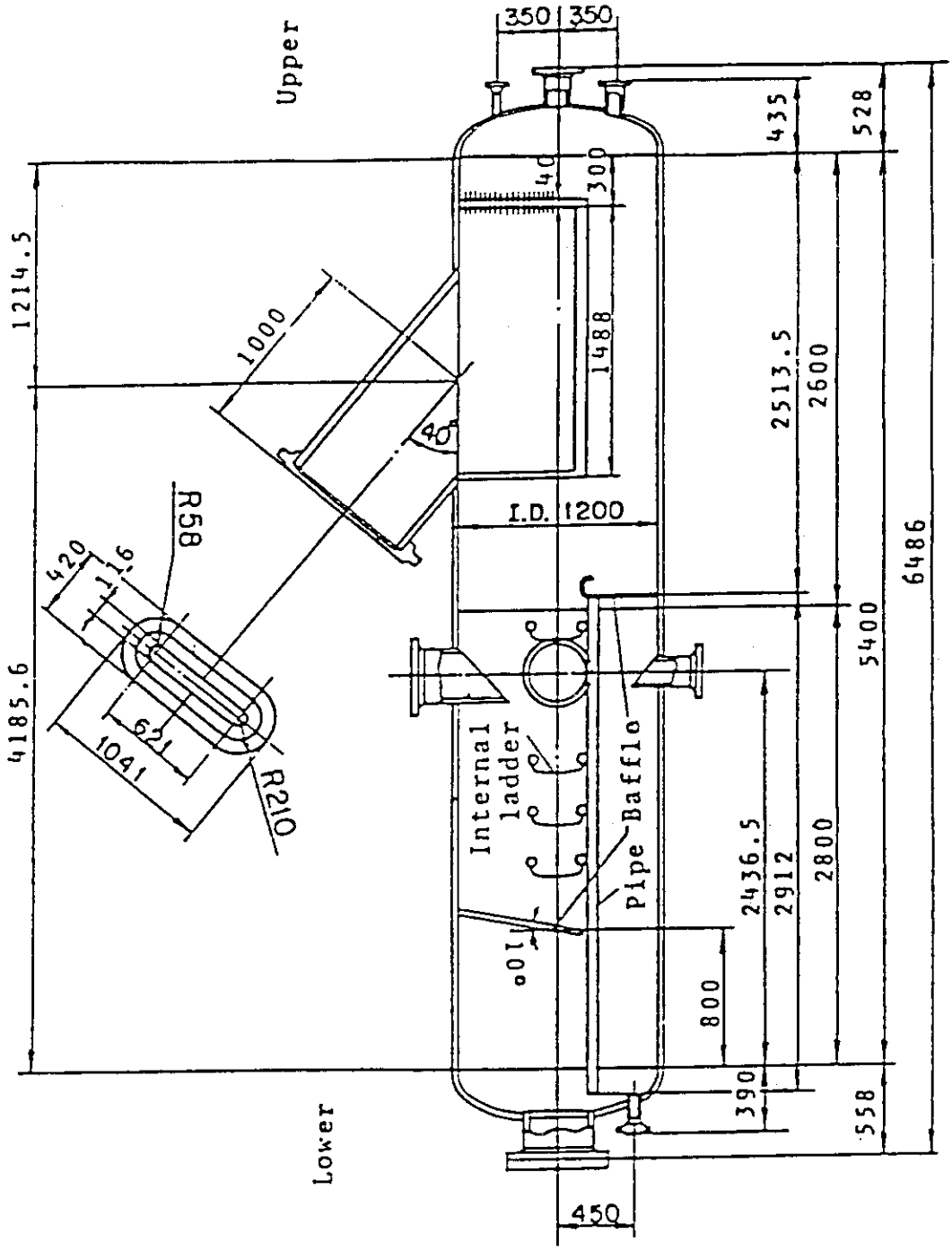

Fig. A-17 Steam/Water Separator

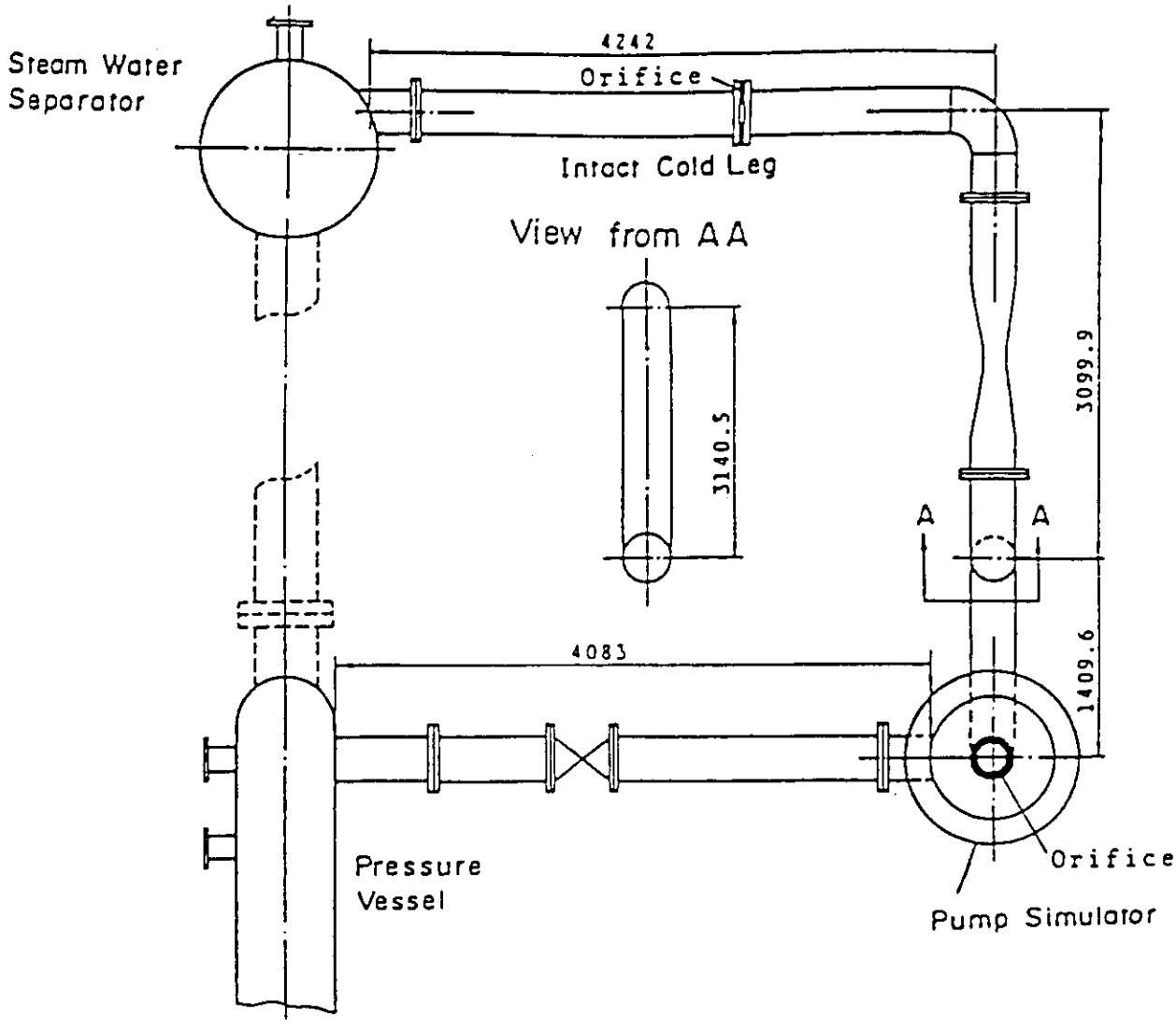

Fig. A-18 Arrangement of Intact Cold Leg

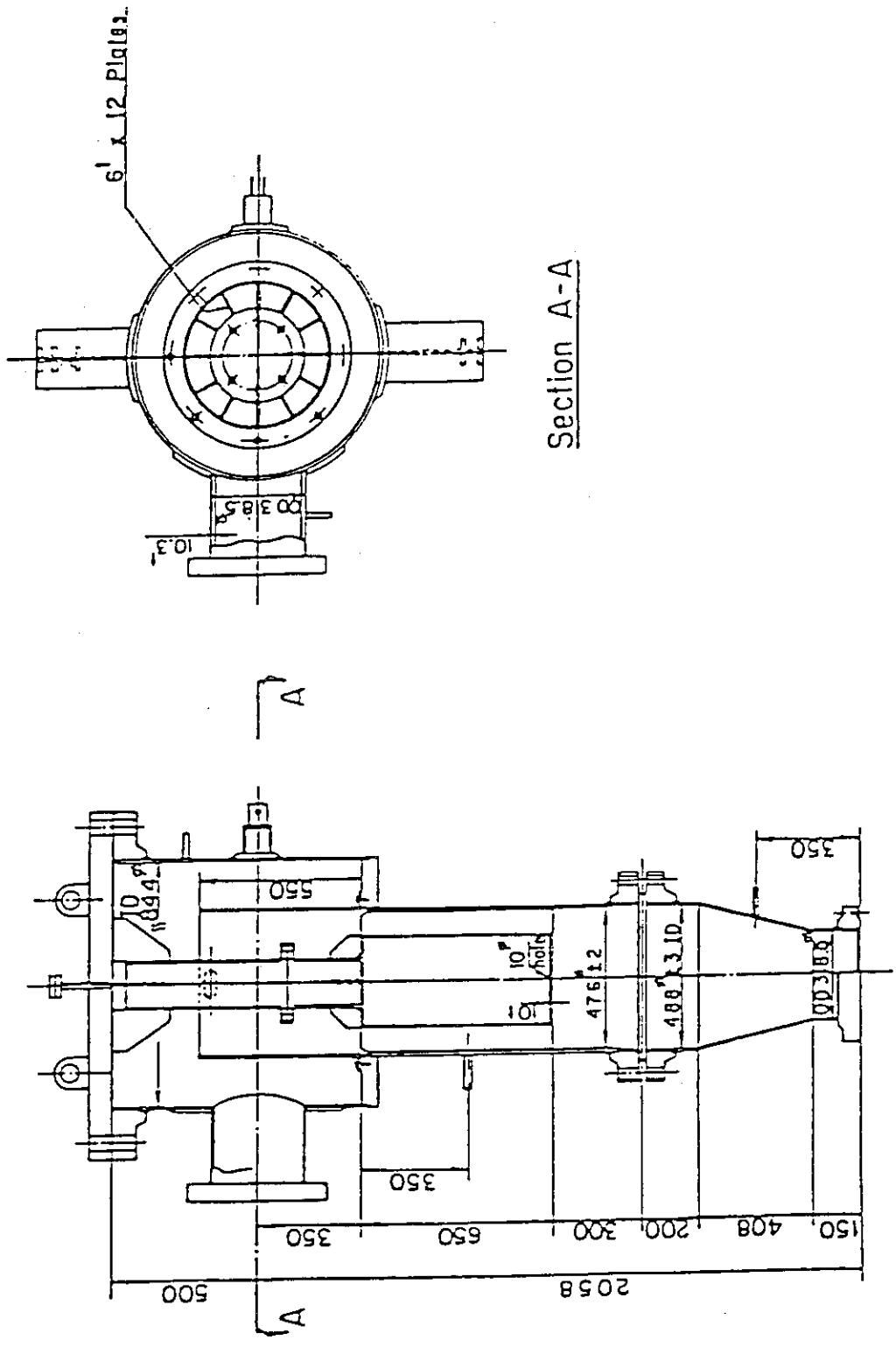

Fig. A-19 Configuration and Dimension of Pump Simulator

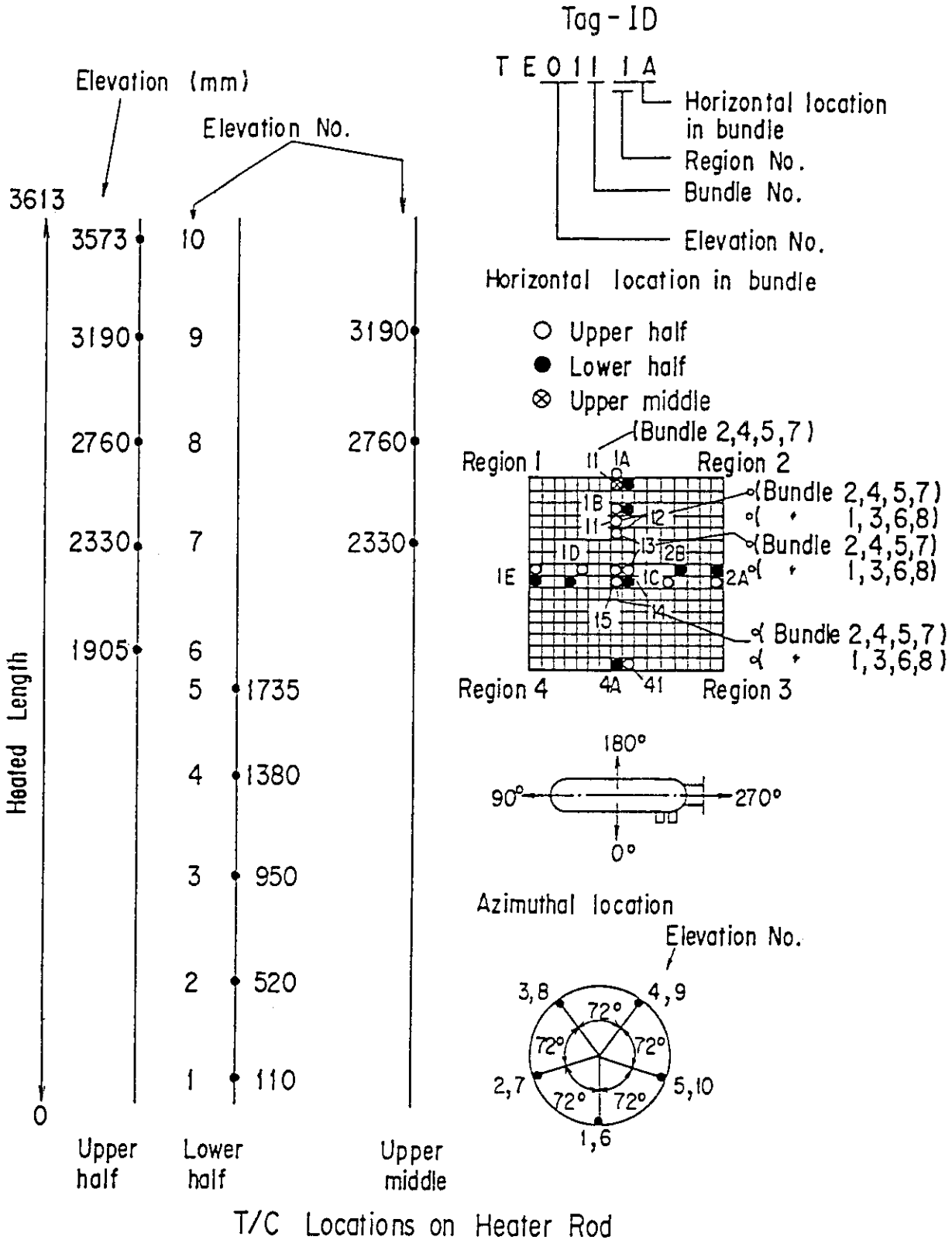

Fig. A-20 Thermocouple Locations of Heater Rod Surface Temperature Measurements

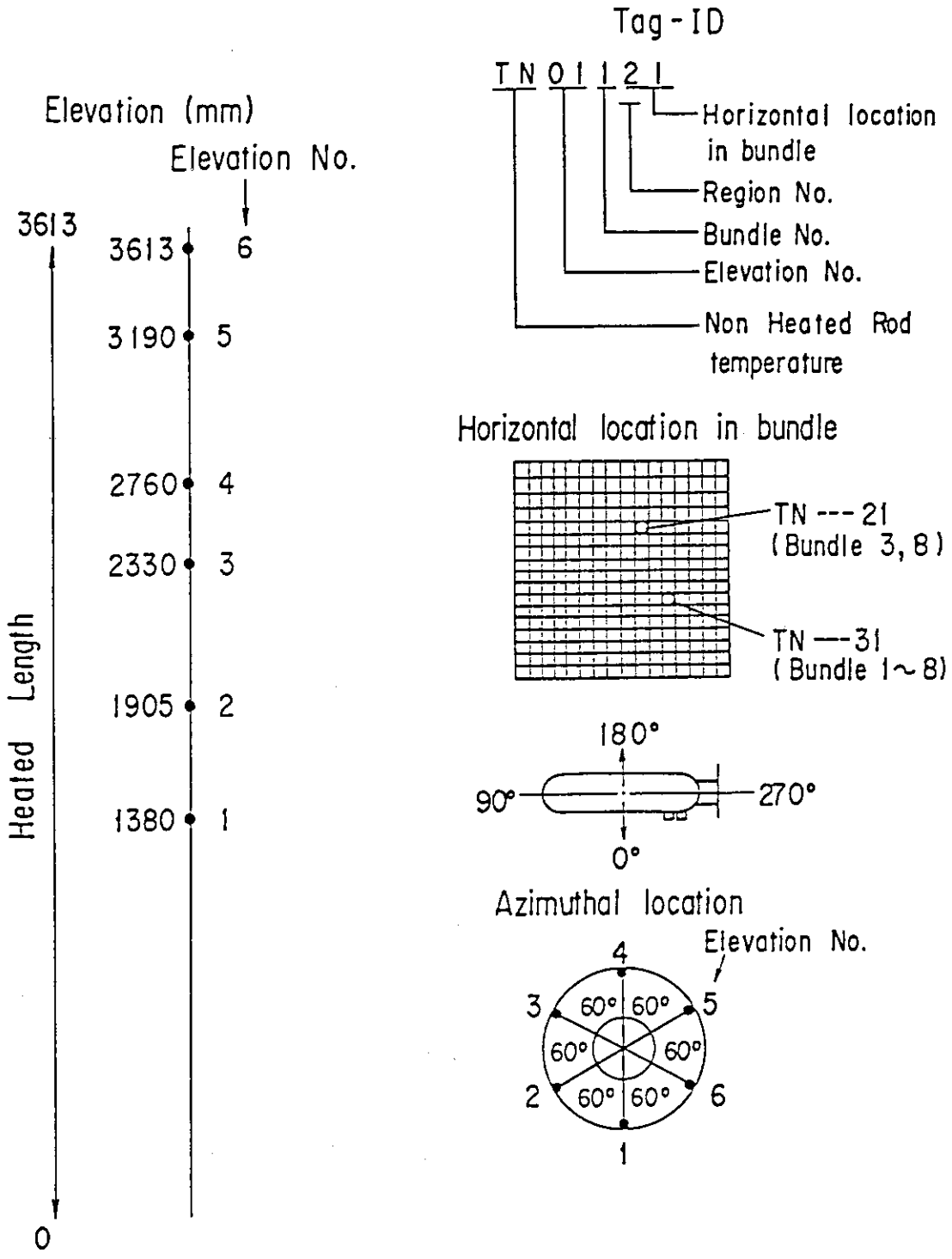

Fig. A-21 Thermocouple Locations of Non-Heated Rod Surface temperature Measurements

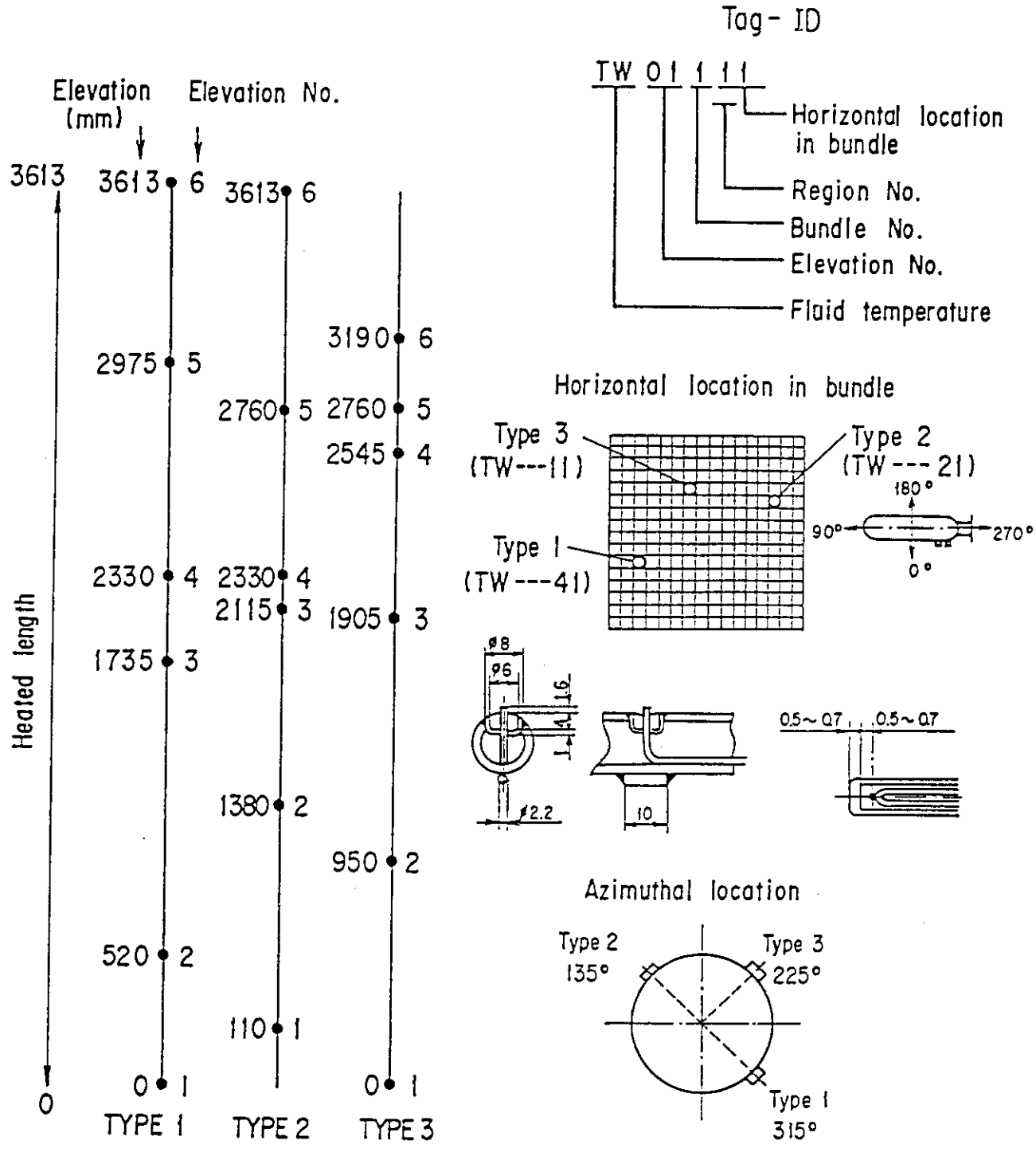

Fig. A-22 Thermocouple Locations of Fluid Temperature Measurements in Core

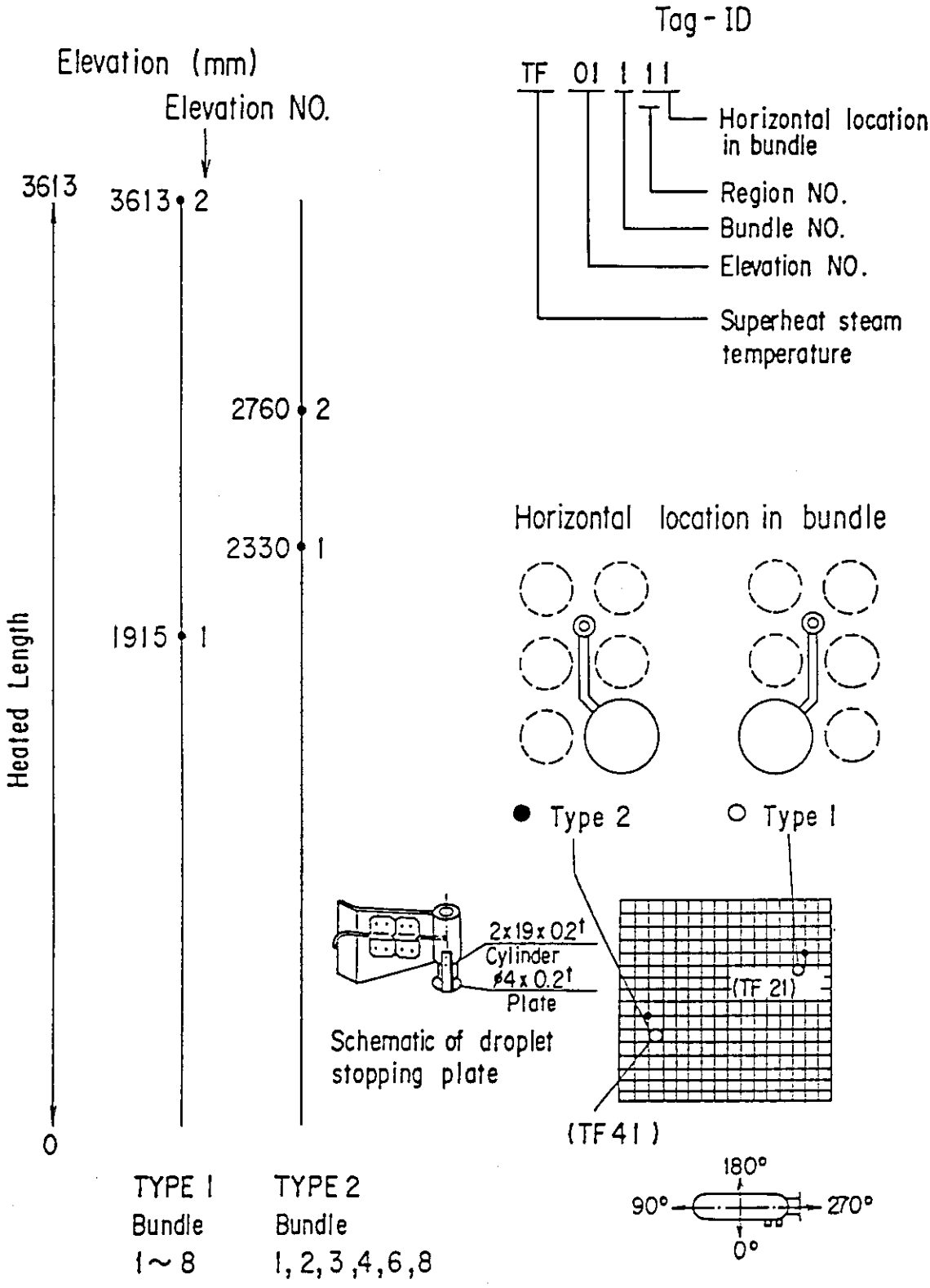

Fig. A-23 Thermocouple Locations of Steam Temperature Measurements in Core

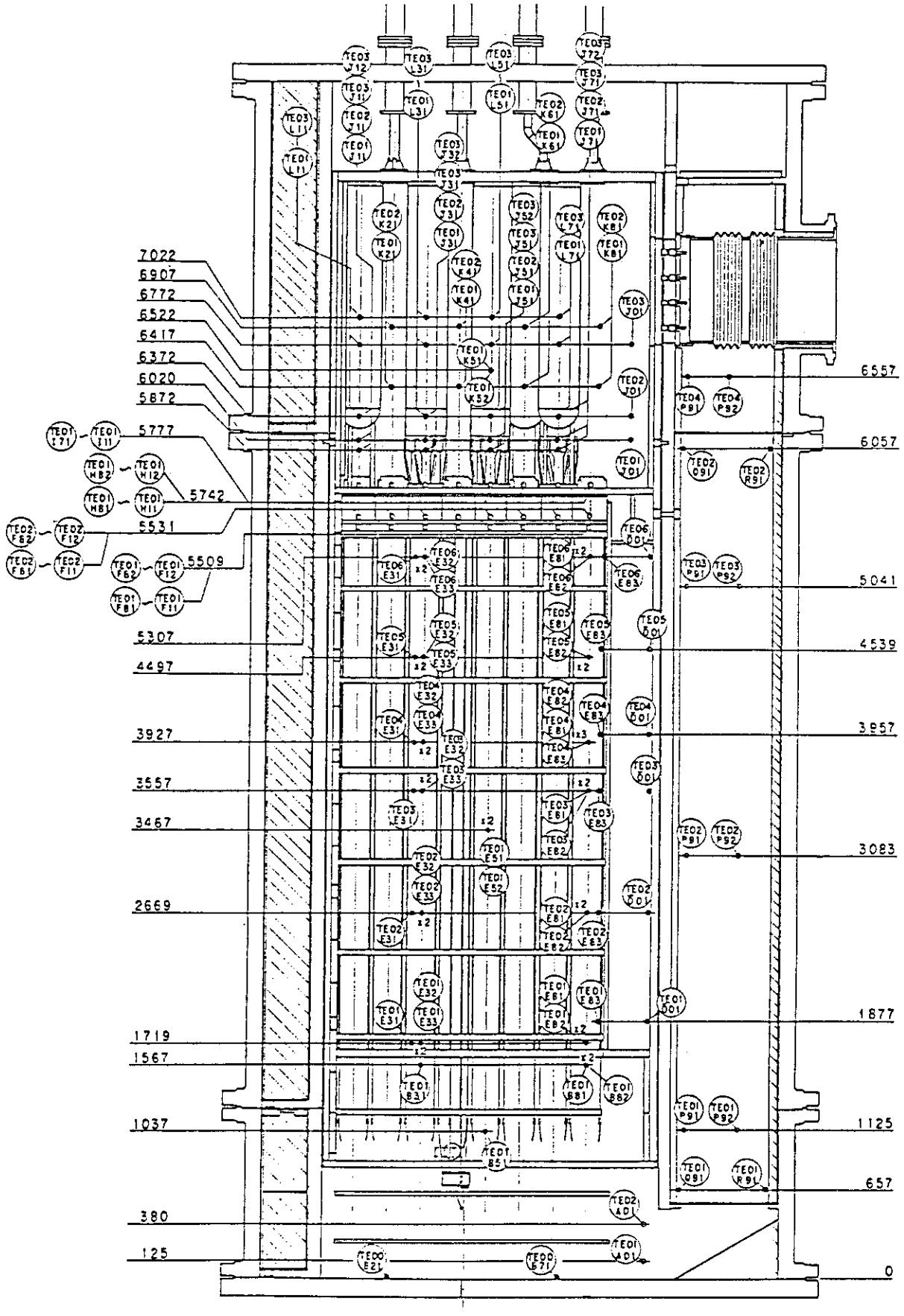

Fig. A-24 Thermocouple Locations of Temperature Measurements in Pressure Vessel except Core Region (Vertical View)

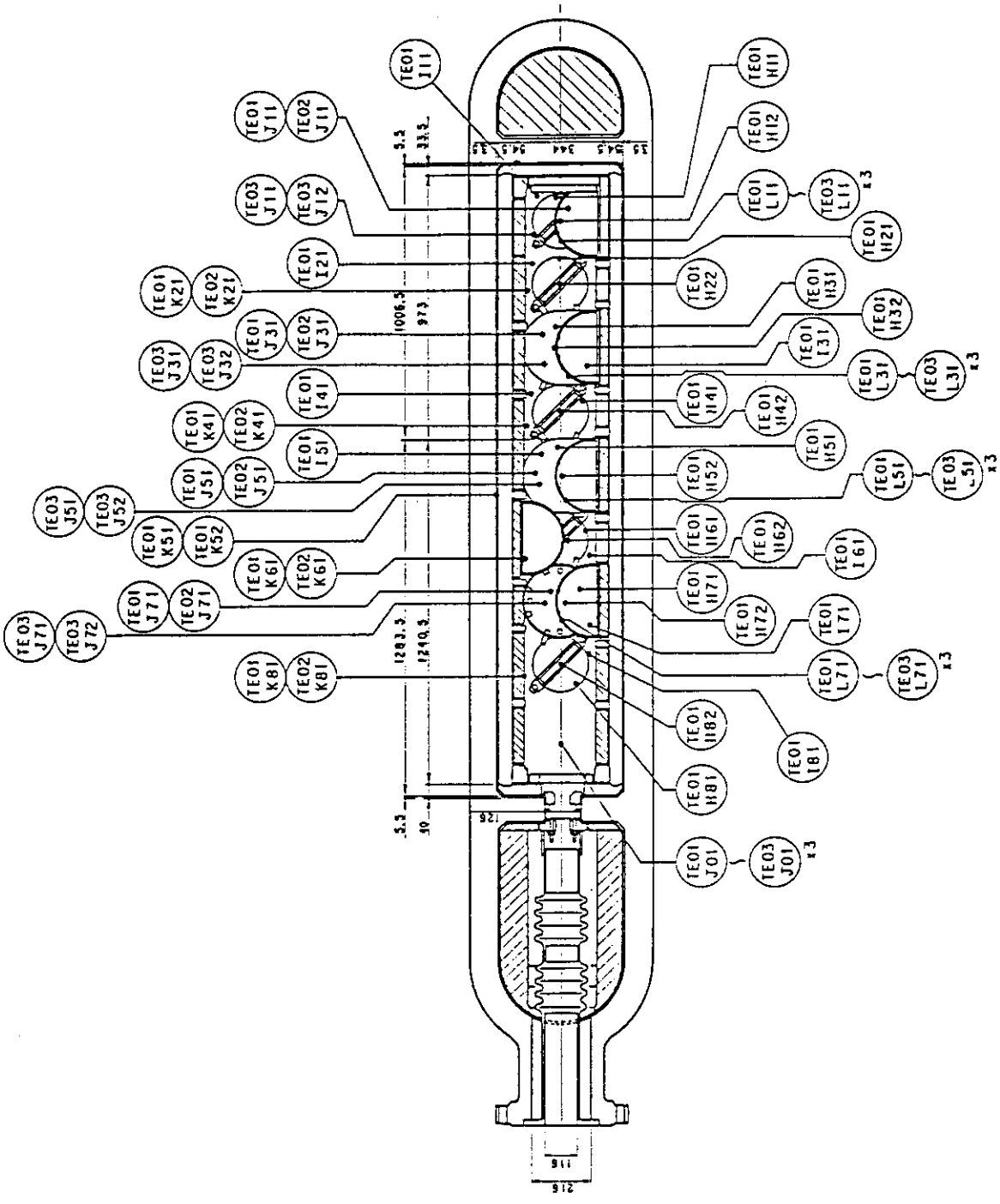

Fig. A-25 Thermocouple Locations of Temperature Measurements in Upper Plenum (Horizontal View)

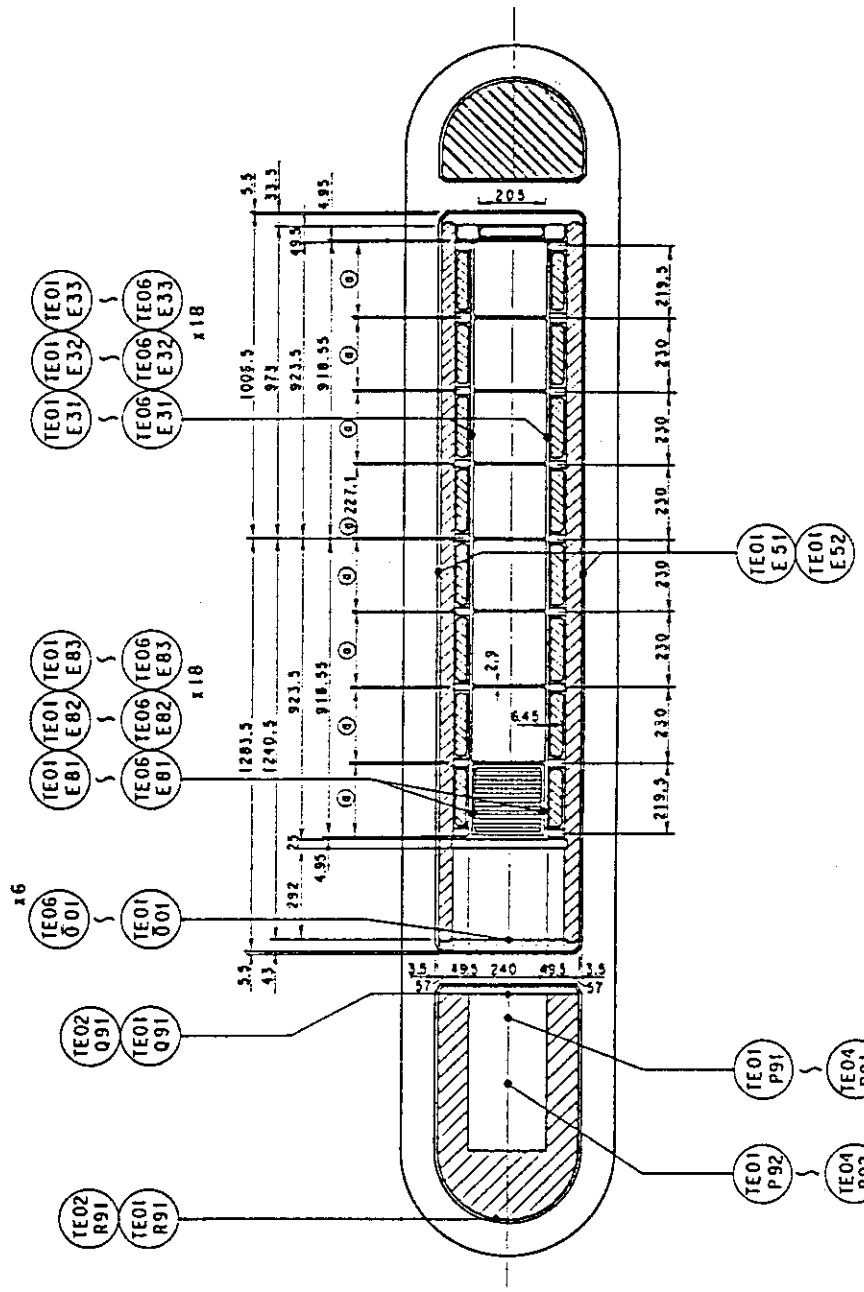

Fig. A-26 Thermocouple Locations of Temperature Measurements in Pressure Vessel except Upper Plenum (Horizontal View)

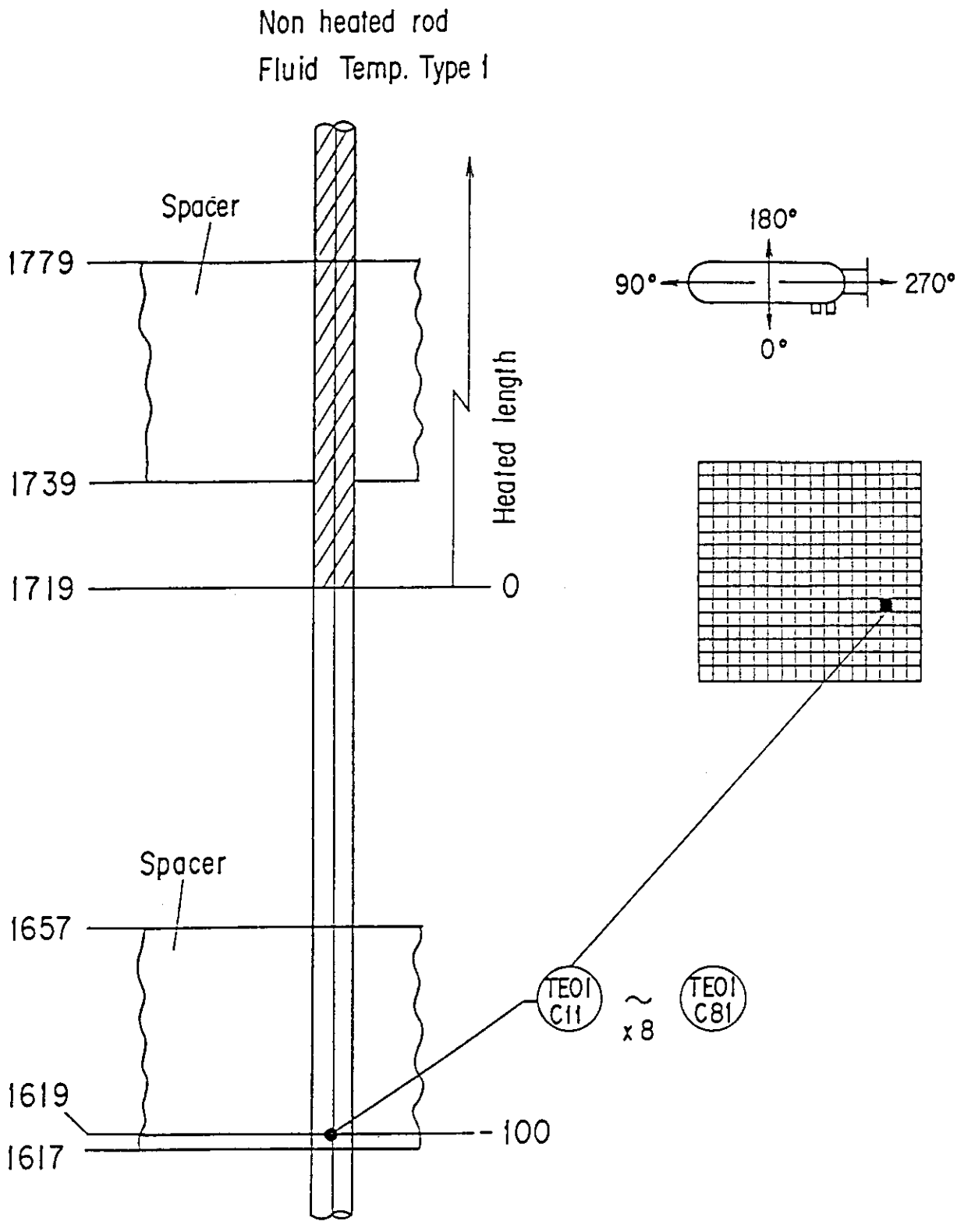

Fig. A-27 Thermocouple Locations of Fluid Temperature Measurements at Core Inlet

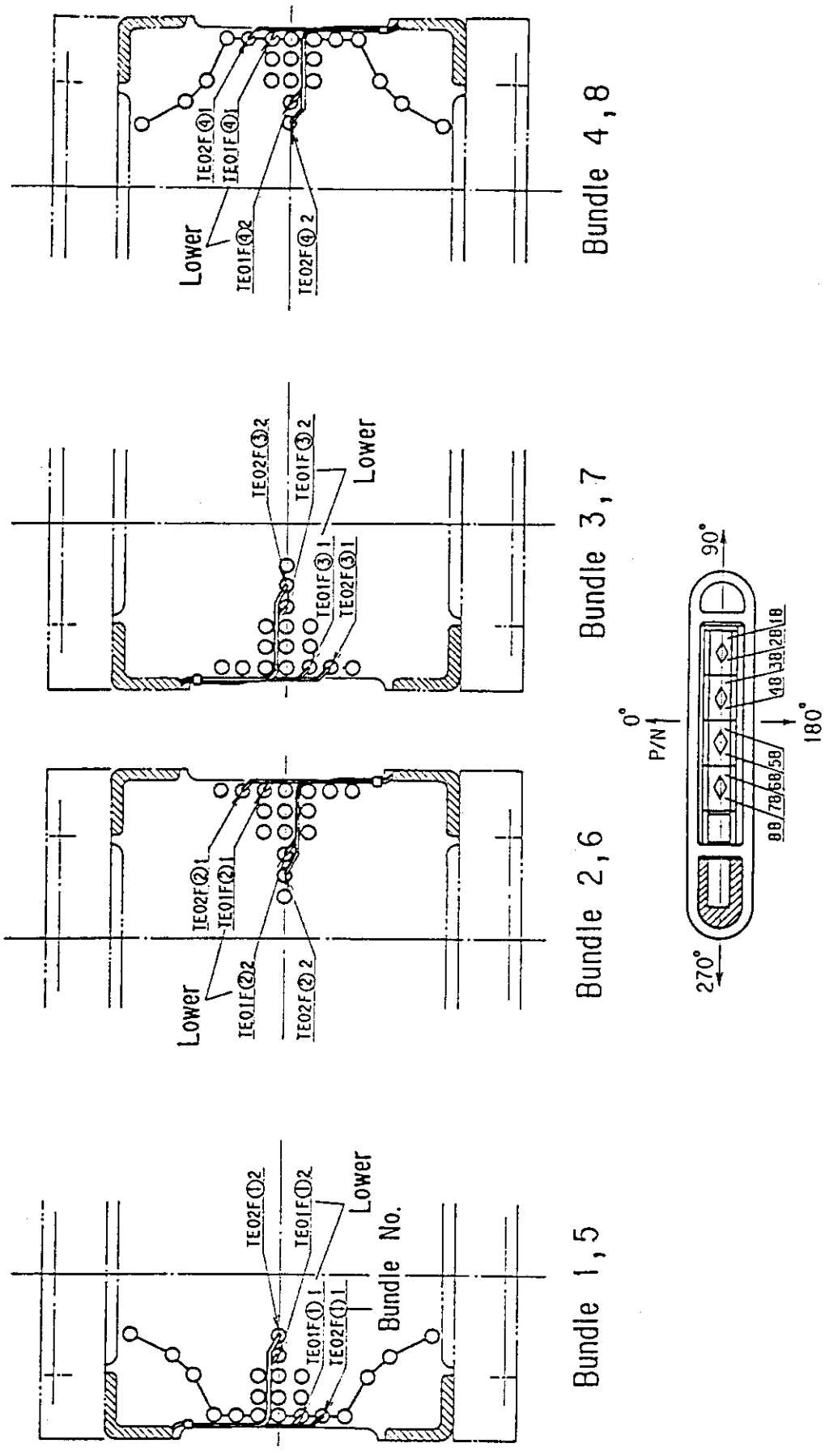

Fig. A-28 Thermocouple Locations of Fluid Temperature Measurements just above and below End Box Tie Plates

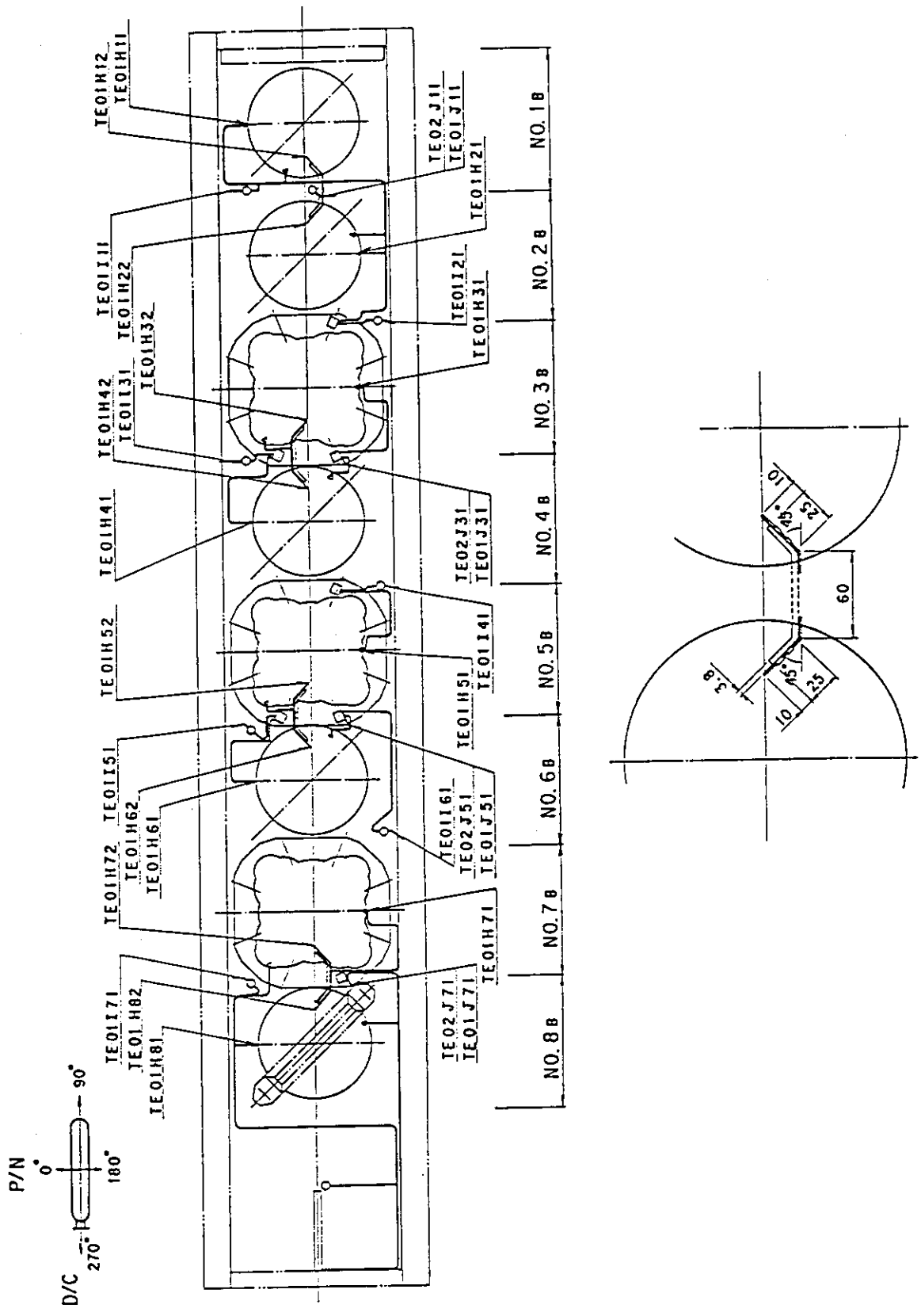

Fig. A-29 Thermocouple Locations of Fluid Temperature Measurements on UCSP and at Inside and Periphery of UCSP Holes

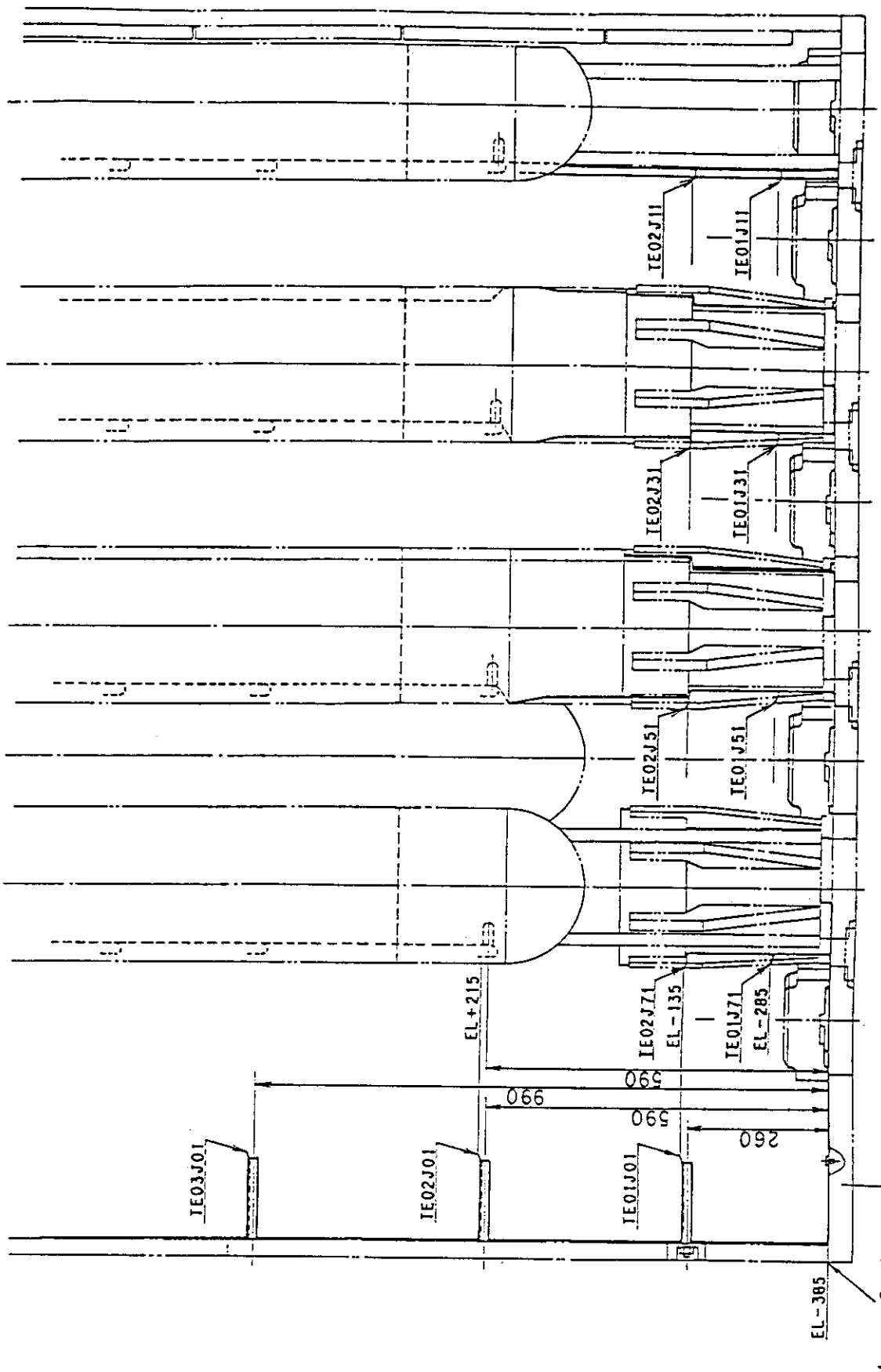

Fig. A-30 Thermocouple Locations of Fluid Temperature Measurements on and above UCSP

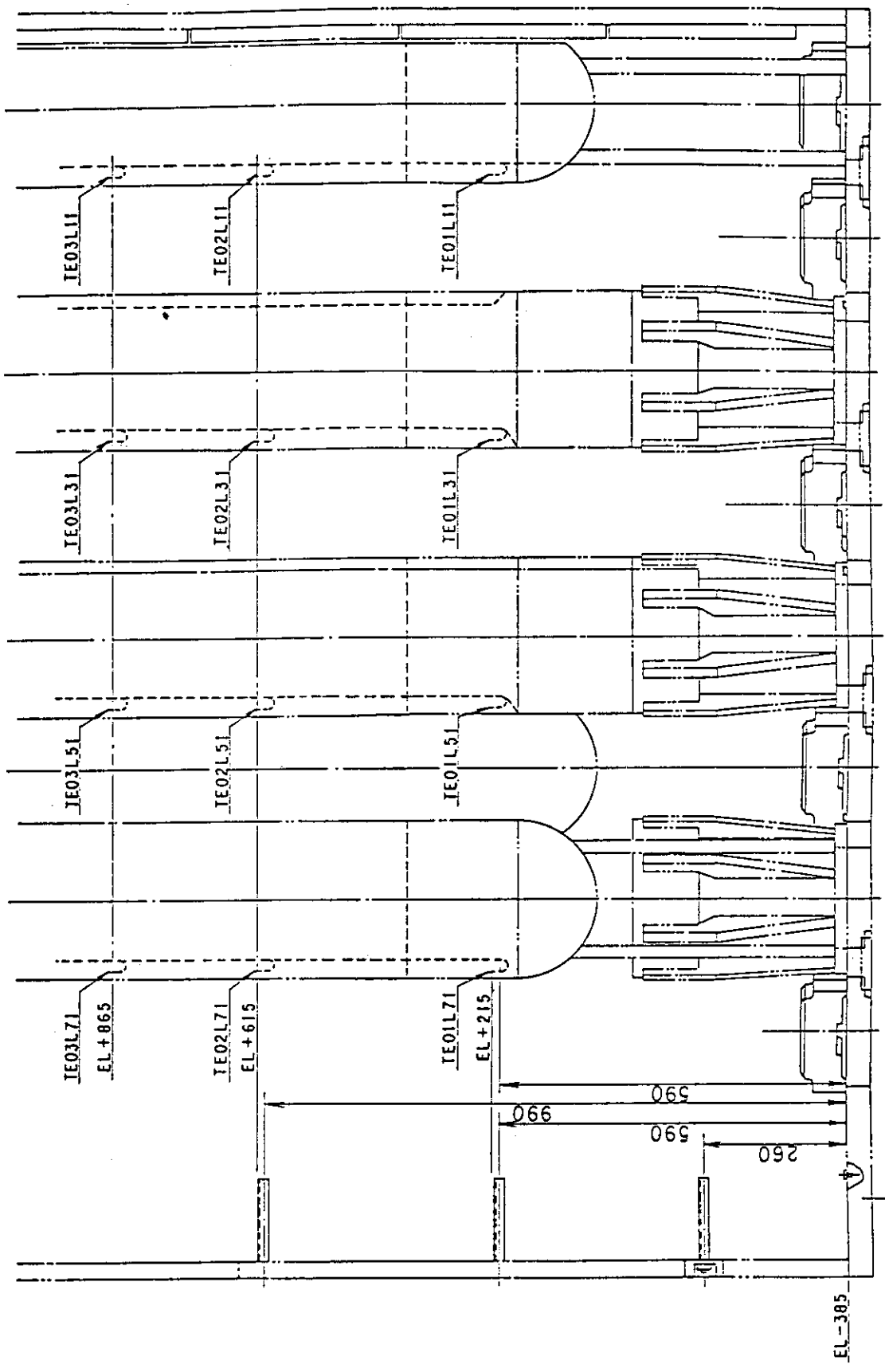

Fig. A-31 Thermocouple Locations of Surface Temperature Measurements of Upper Plenum Structures

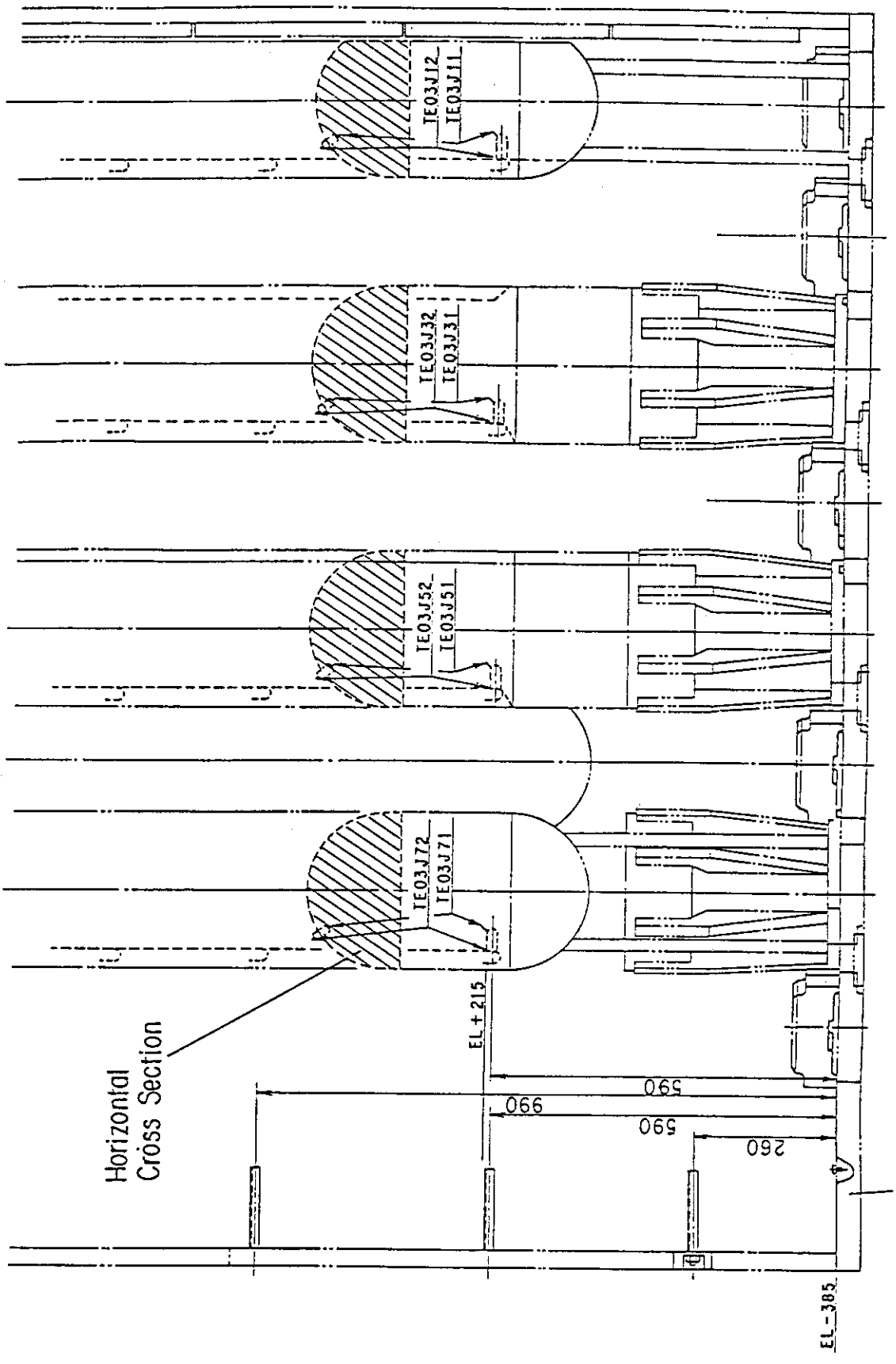

Fig. A-32 Thermocouple Locations of Steam Temperature Measurements above UCSP Holes

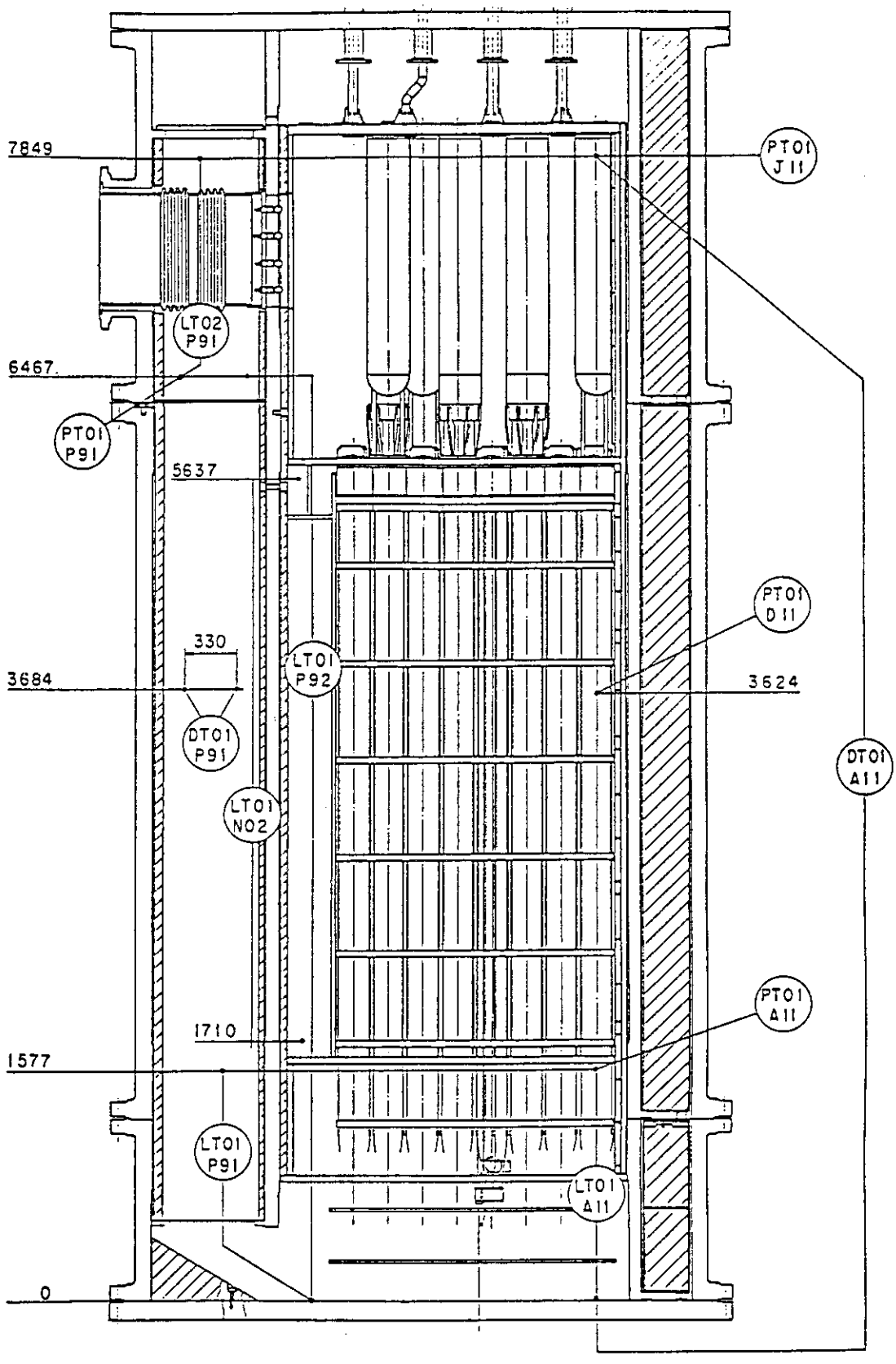

Fig. A-33 Locations of Pressure Measurements in Pressure Vessel, Differential Pressure Measurements between Upper and Lower Plenums and Liquid Level Measurements in Downcomer and Lower Plenum

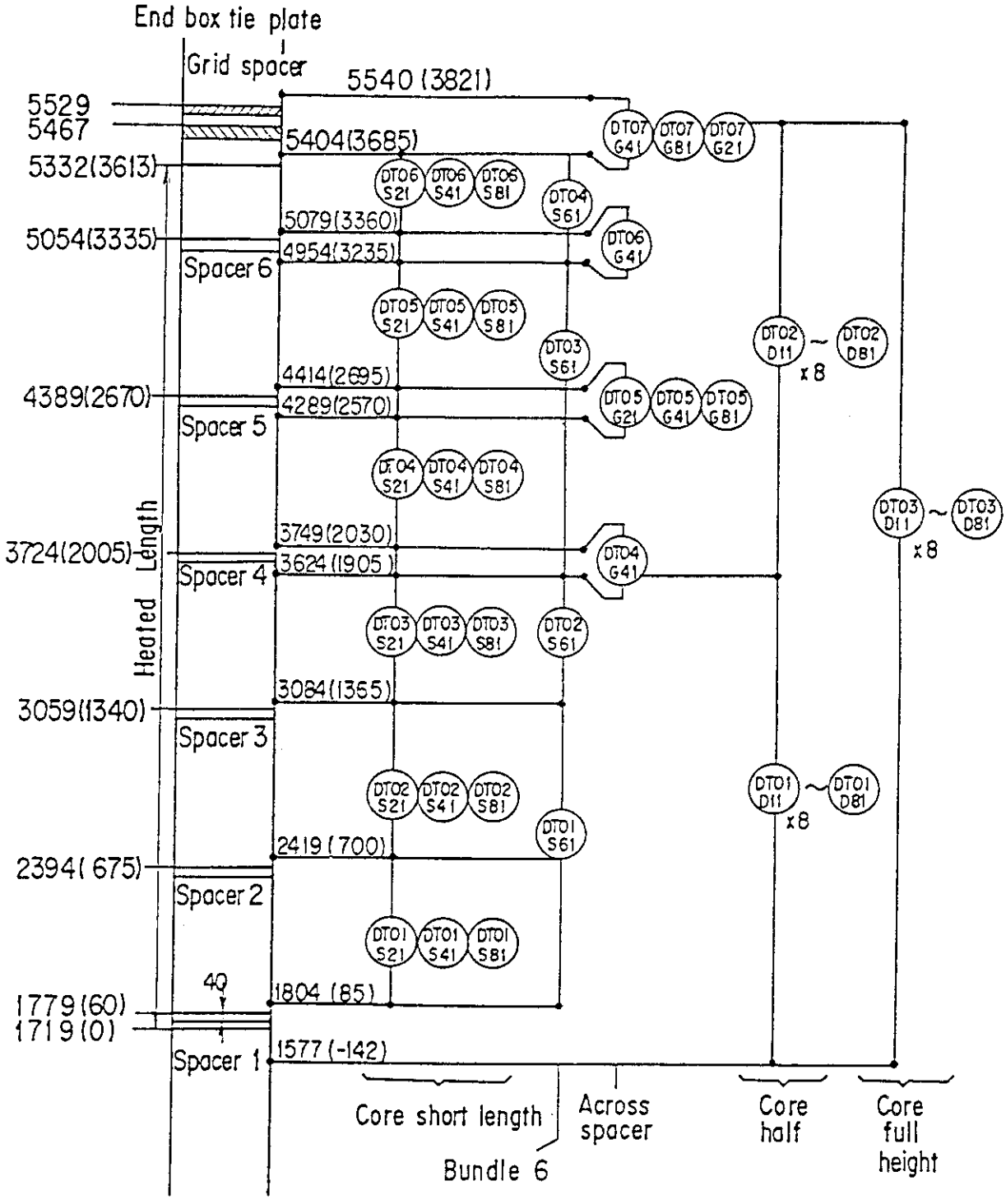

Fig. A-34 Locations of Vertical Differential Pressure Measurements in Core

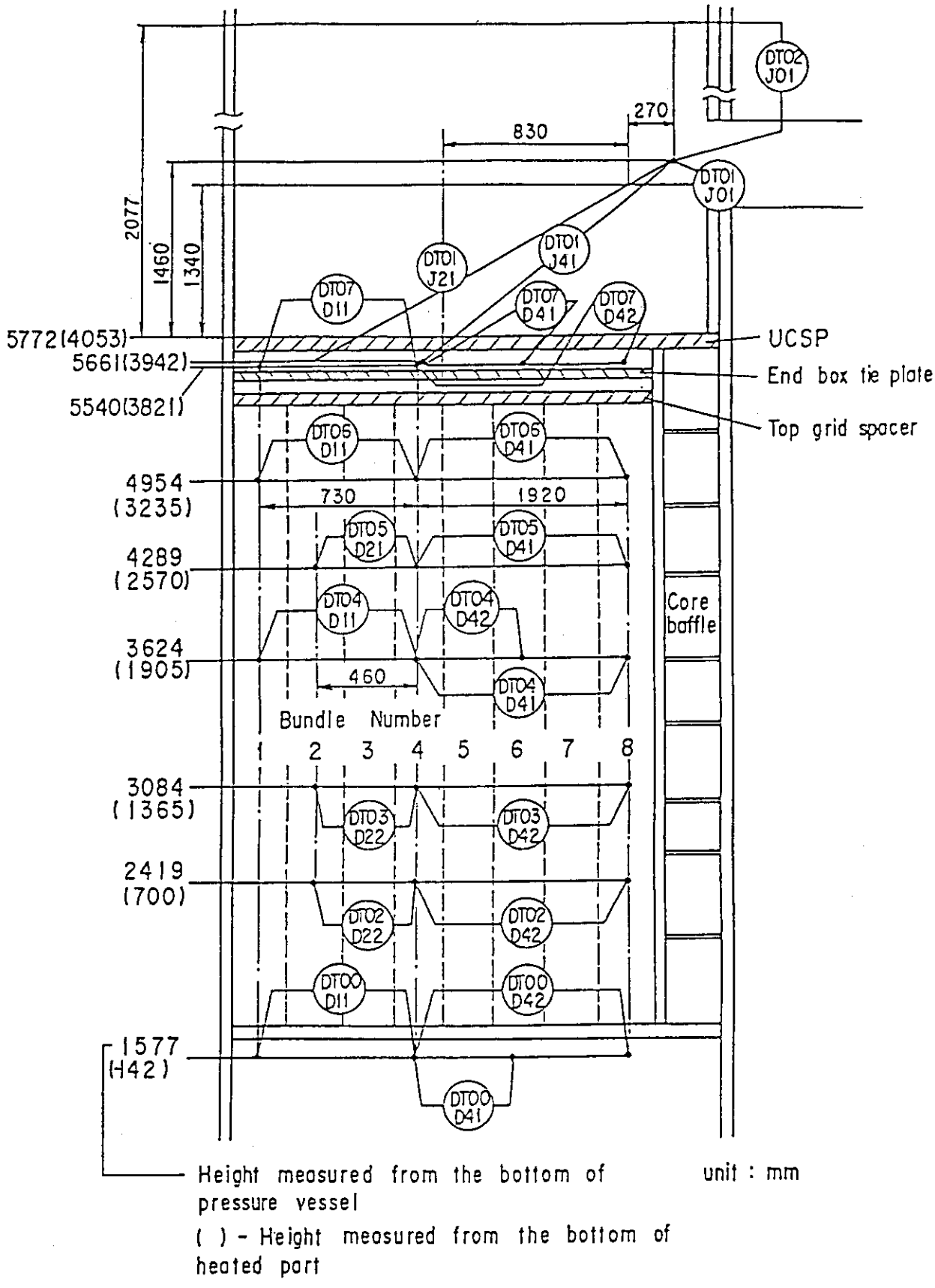

Fig. A-35 Locations of Horizontal Differential Pressure Measurements in Core and Differential Pressure Measurements between End Boxes and Inlet of Hot Leg

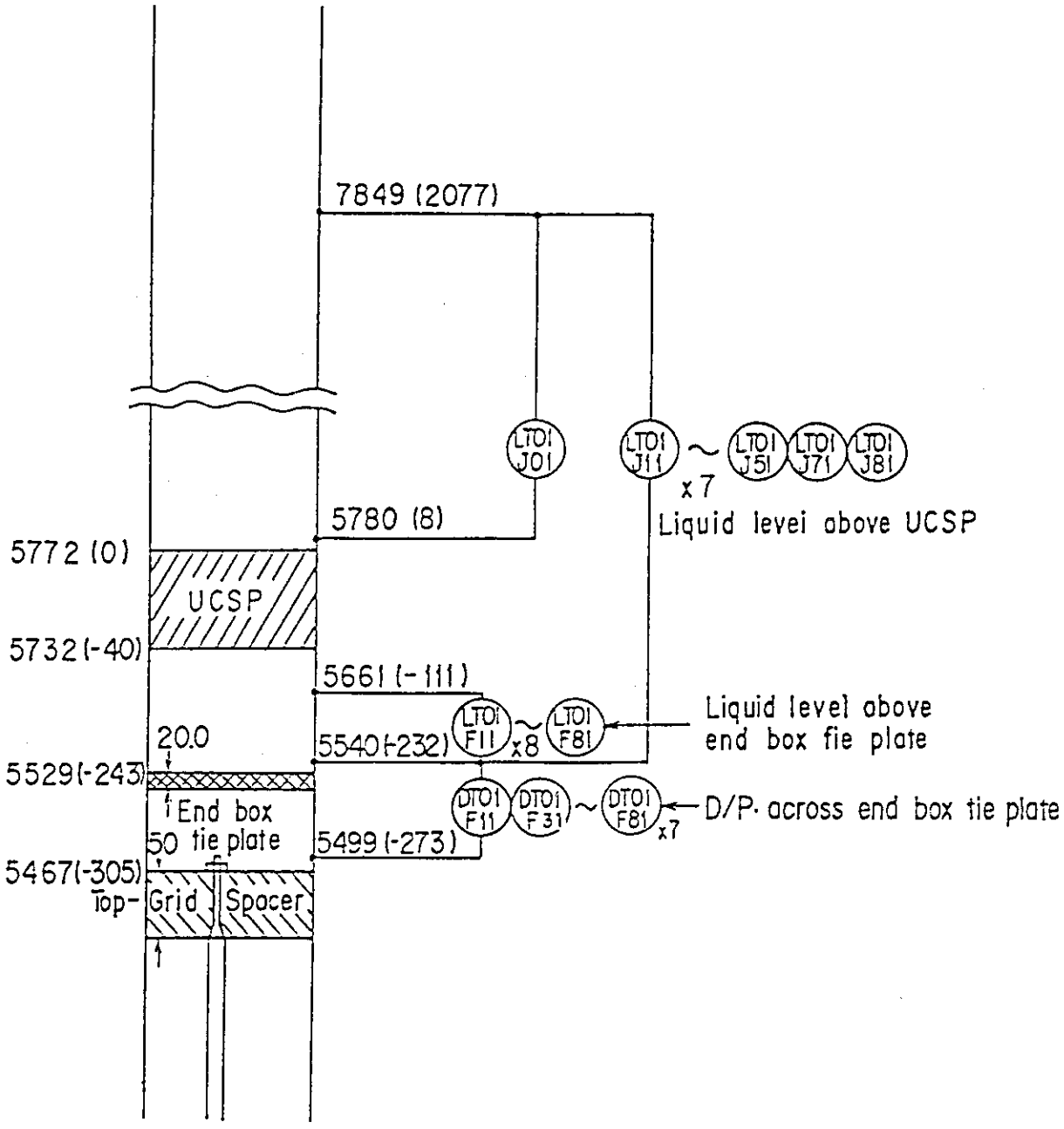

Fig. A-36 Locations of Differential Pressure Measurements across End Box Tie Plate

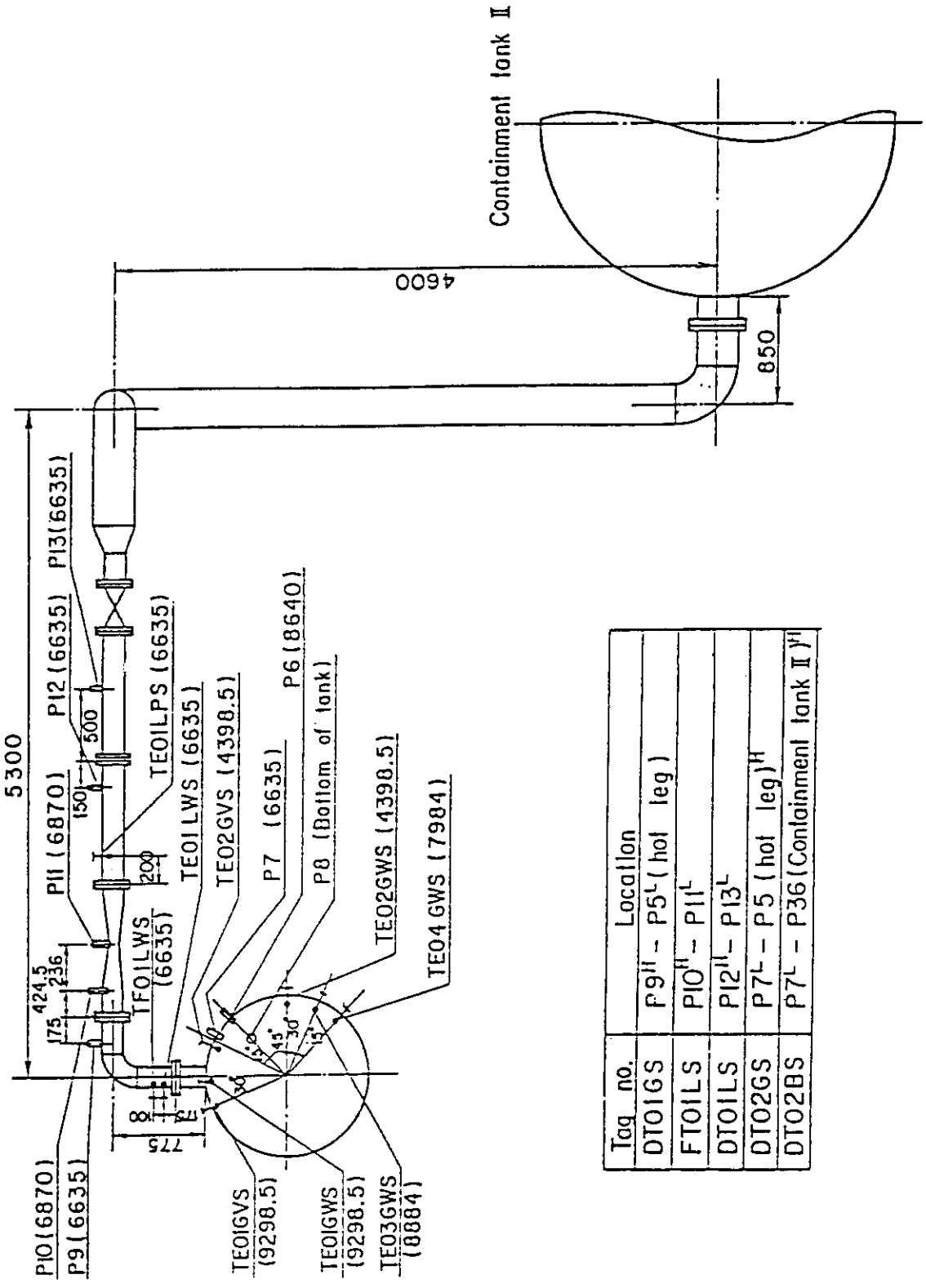

Tag no.	Location
DT01GS	$P9^{H}$ – $P5^{L}$ (hot leg)
FT01LS	$P10^{H}$ – $P11^{L}$
DT01LS	$P12^{H}$ – $P13^{L}$
DT02GS	$P7^{L}$ – P5 (hot leg)^{H}
DT02BS	$P7^{L}$ – P36 (Containment tank II)^{H}

Fig. A-37 Locations of Broken Cold Leg Instruments (Steam-Water Separator Side)

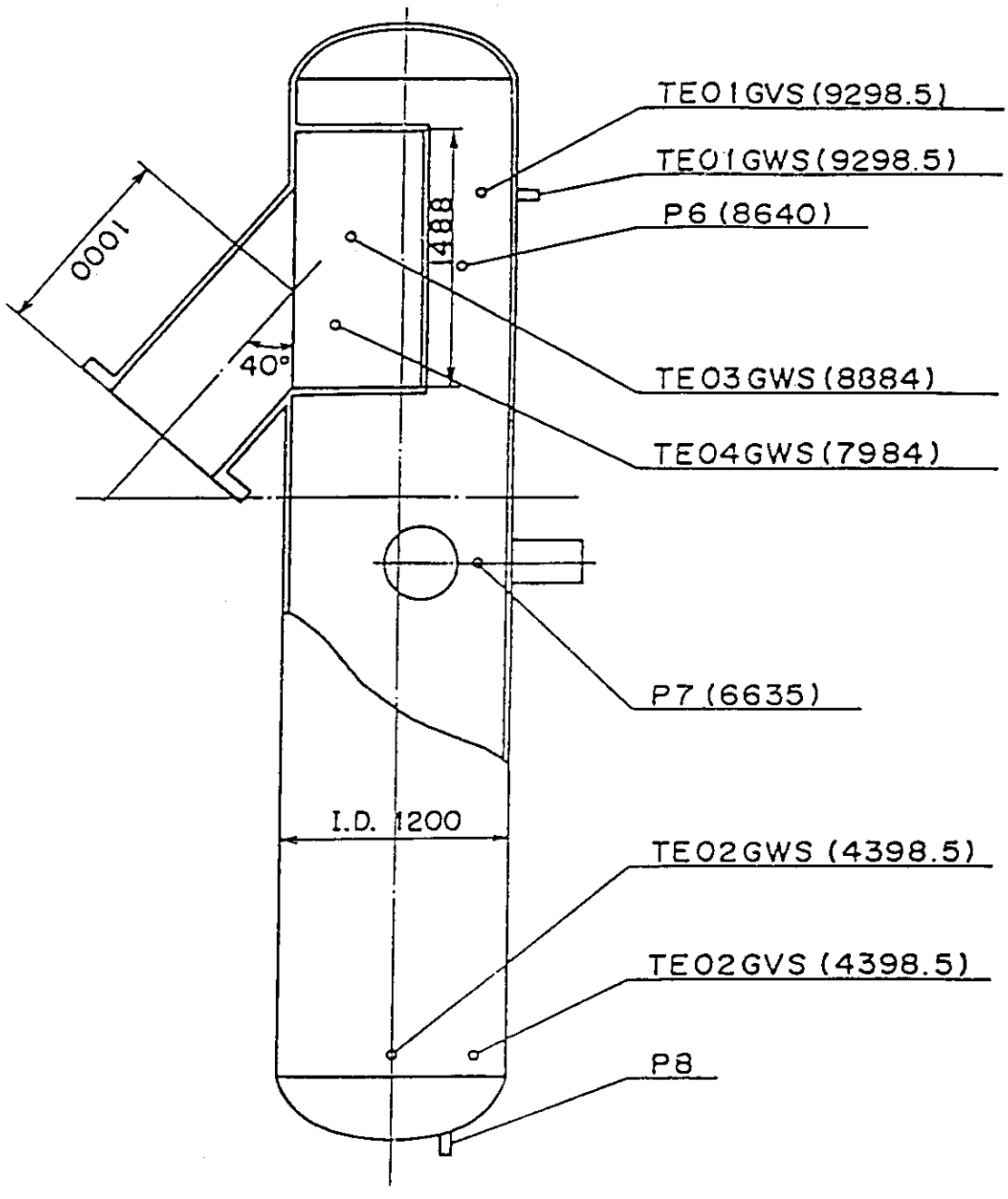

Fig. A-38 Locations of Steam-Water Separator Instruments

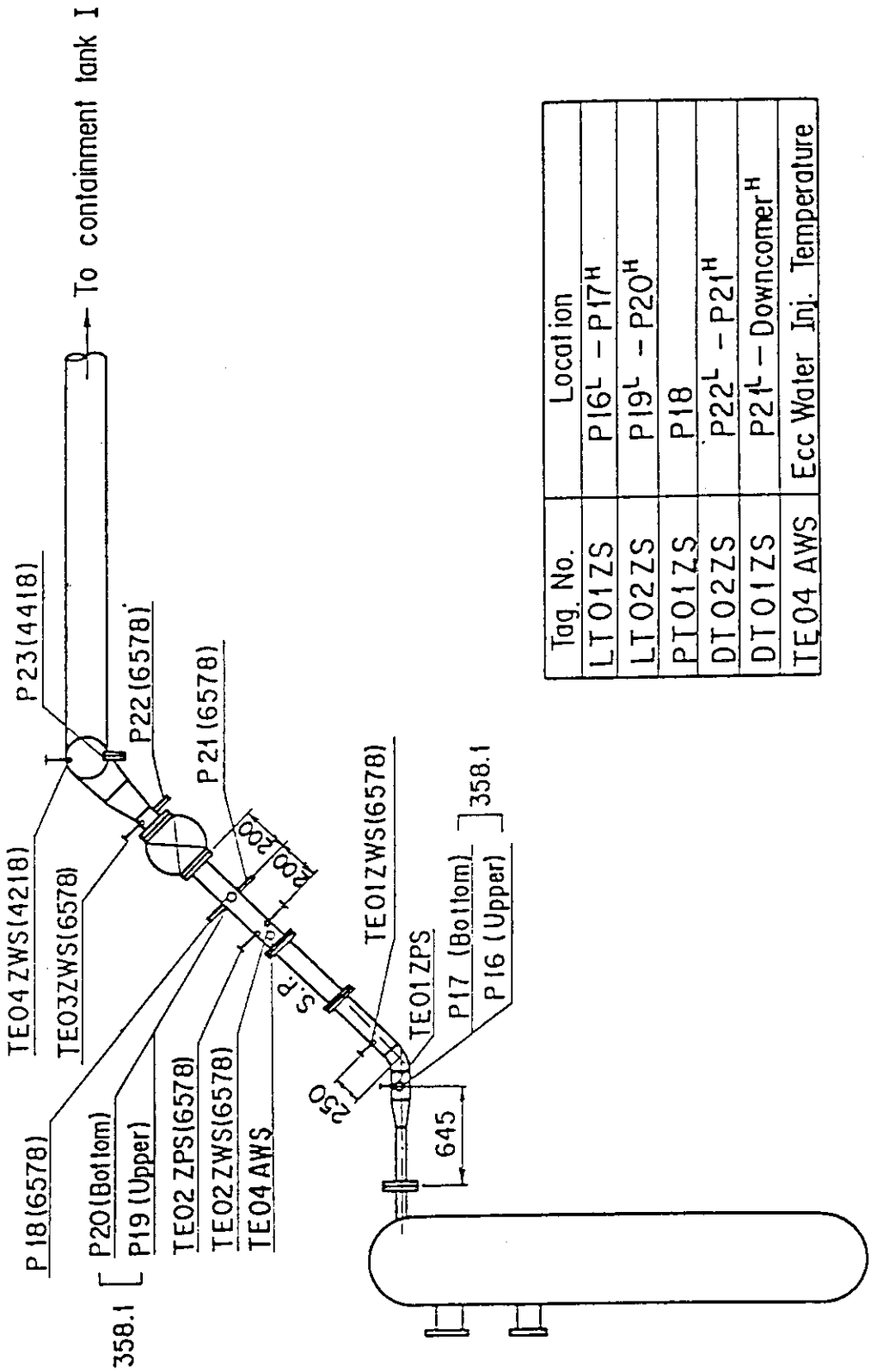

Tag. No.	Location
LT01ZS	$P16^{L} - P17^{H}$
LT02ZS	$P19^{L} - P20^{H}$
PT01ZS	P18
DT02ZS	$P22^{L} - P21^{H}$
DT01ZS	$P21^{L}$ – Downcomer^{H}
TE04AWS	Ecc Water Inj. Temperature

Fig. A-39 Locations of Broken Cold Leg Instruments (Pressure Vessel Side)

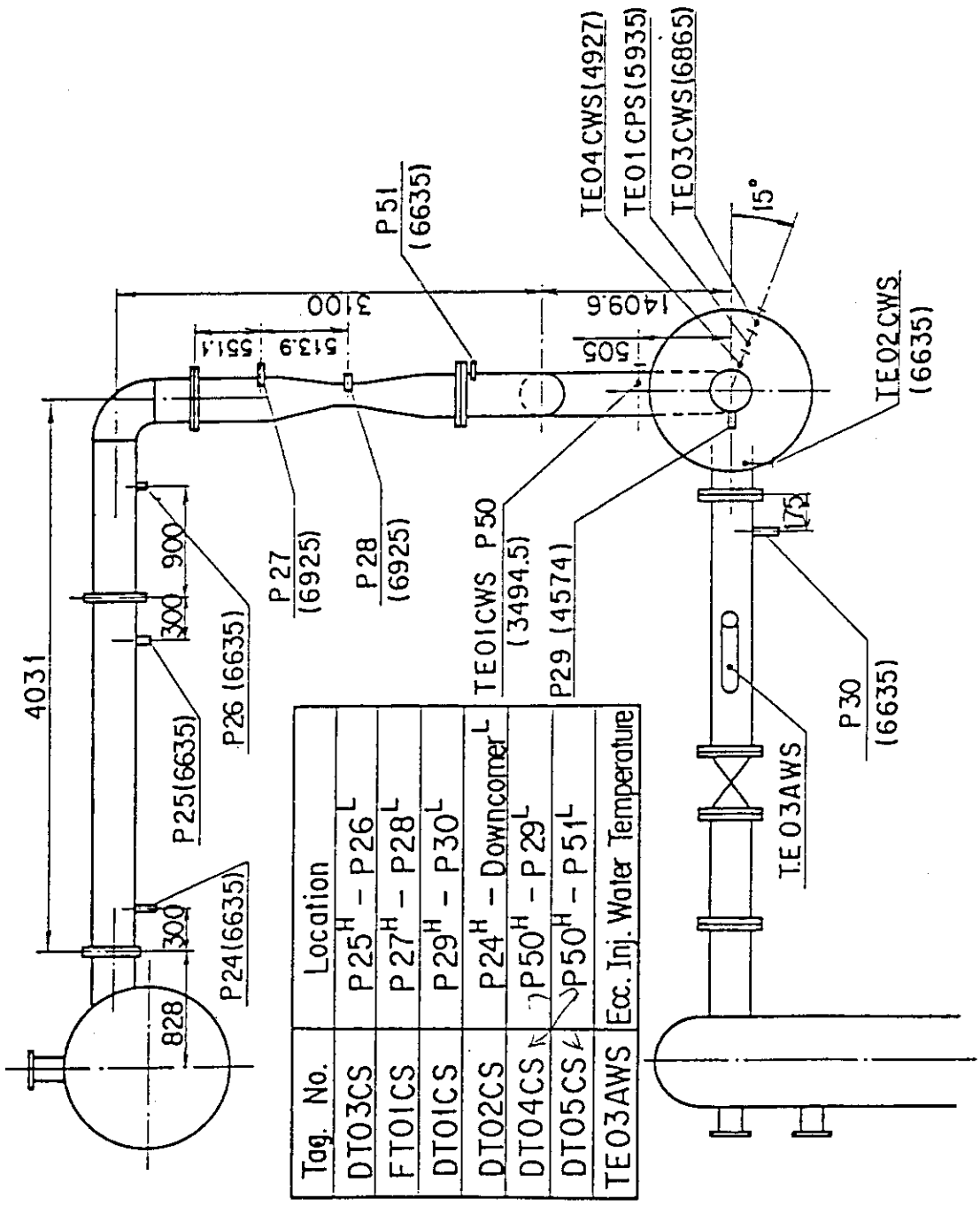

Fig. A-40 Locations of Intact Cold Leg Instruments

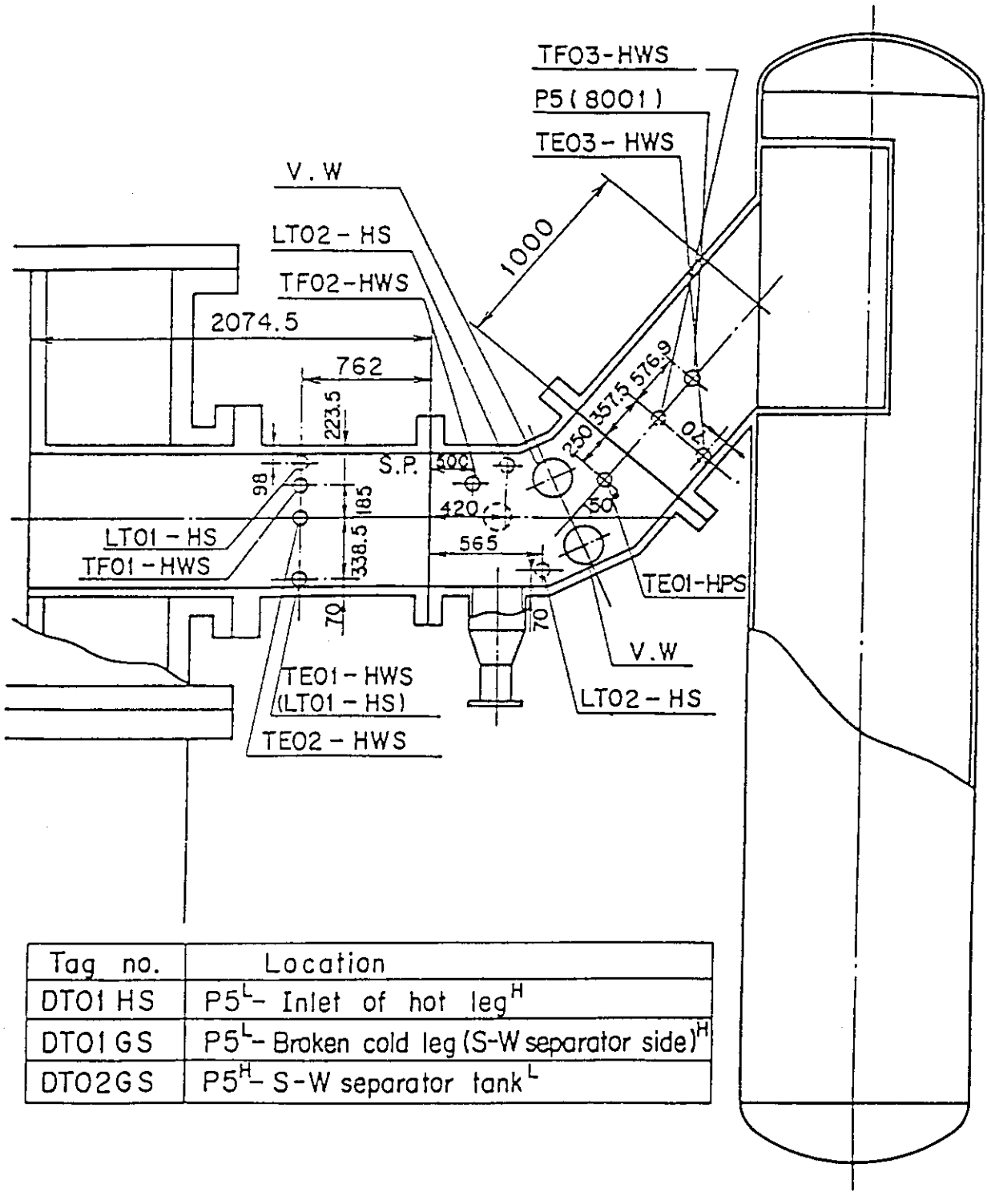

Tag no.	Location
DT01 HS	P5[L]- Inlet of hot leg[H]
DT01 GS	P5[L]- Broken cold leg (S-W separator side)[H]
DT02GS	P5[H]- S-W separator tank[L]

Fig. A-41 Locations of Hot Leg Instruments

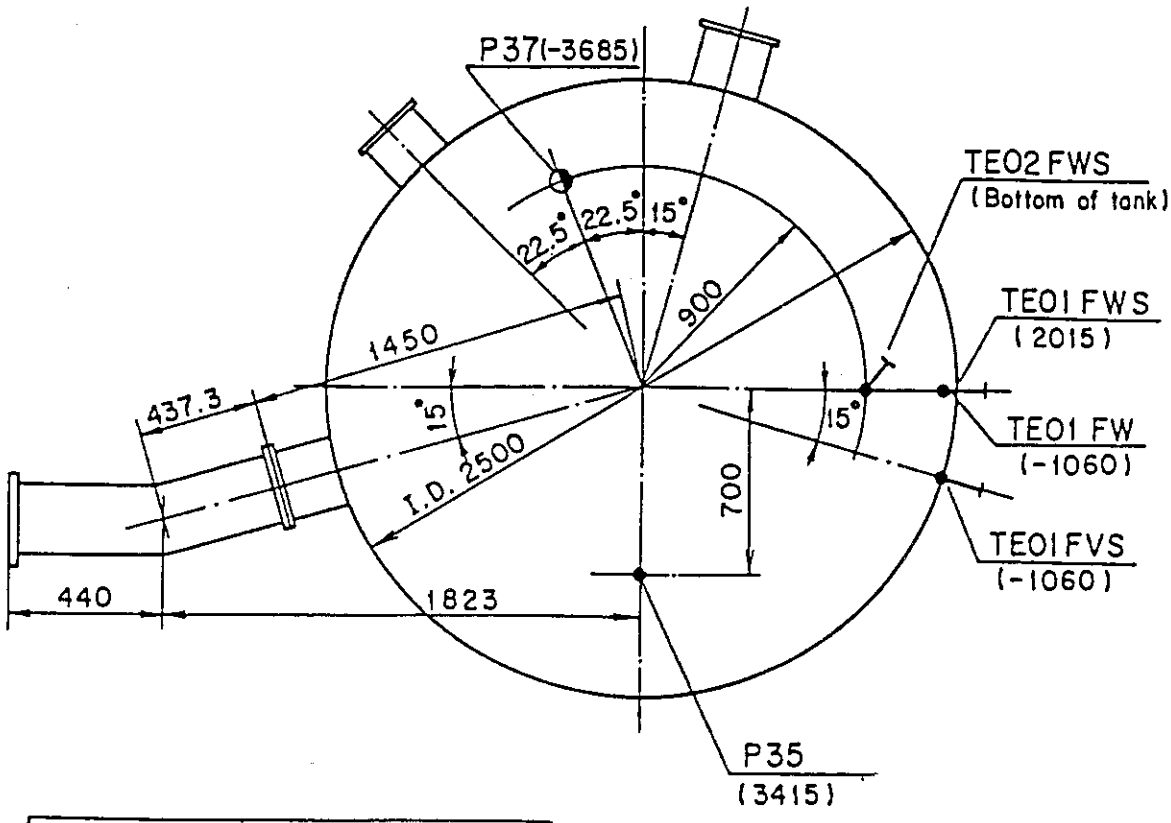

Tag. no.	Location
LT01 FS	$P35^{L}$ – $P37^{H}$
DT01 FS	$P35^{H}$ – $Downcomer^{L}$
DT01E	$P35^{L}$ – P36(C.T. II)^{H}
PT01F	P35

Fig. A-42 Locations of Containment Tank-I Instruments

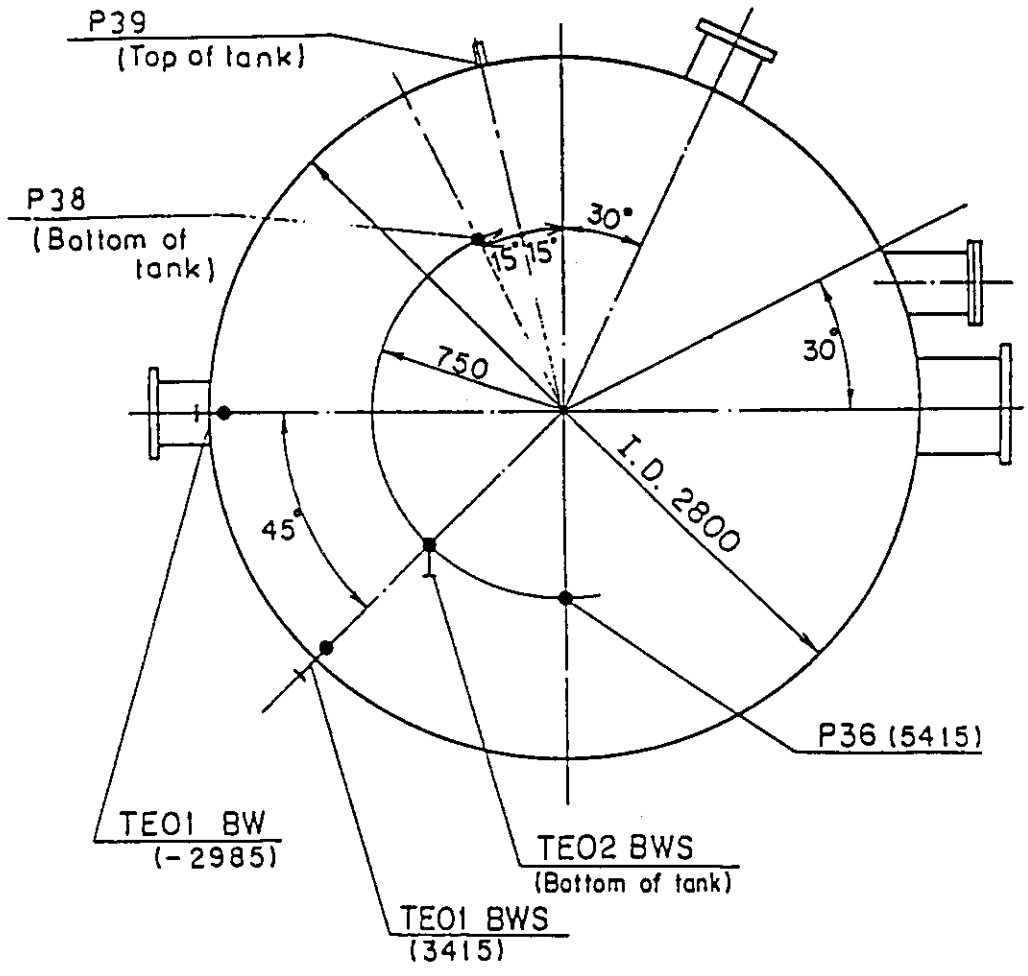

Tag no.	Location
DT01 BS	$P36^{H}$– Upper plenum^{L}
DT02 BS	$P36^{H}$– S-W Separator^{L}
DT01 E	$P36^{H}$– P35 (C.T.I)^{L}
PT01 B	P36
LT01 1B	$P38^{H}$– $P39^{L}$

Fig. A-43 Locations of Containment Tank-II Instruments

Appendix B

Selected Data from Test S3−20

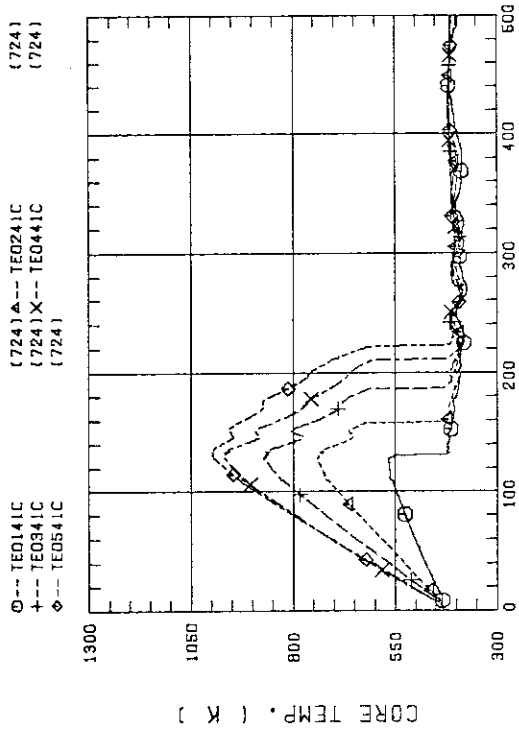

FIG. B-03 HEATER ROD TEMPERATURE
(BUNDLE 4-1C, LOWER HALF)

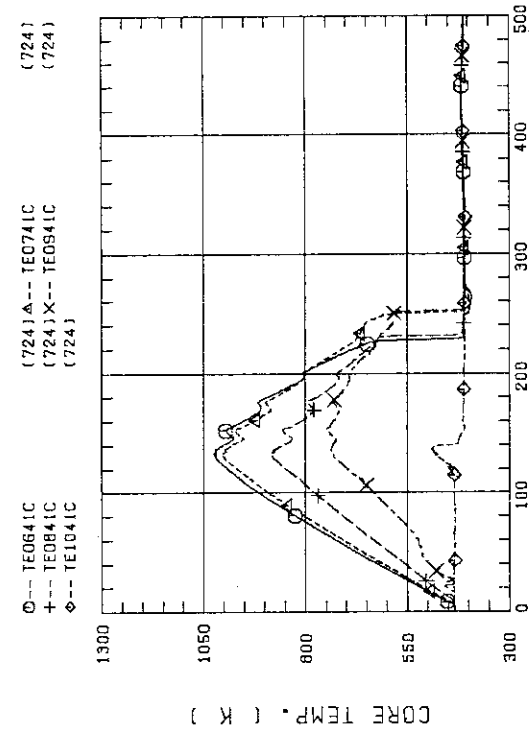

FIG. B-04 HEATER ROD TEMPERATURE
(BUNDLE 4-1C, UPPER HALF)

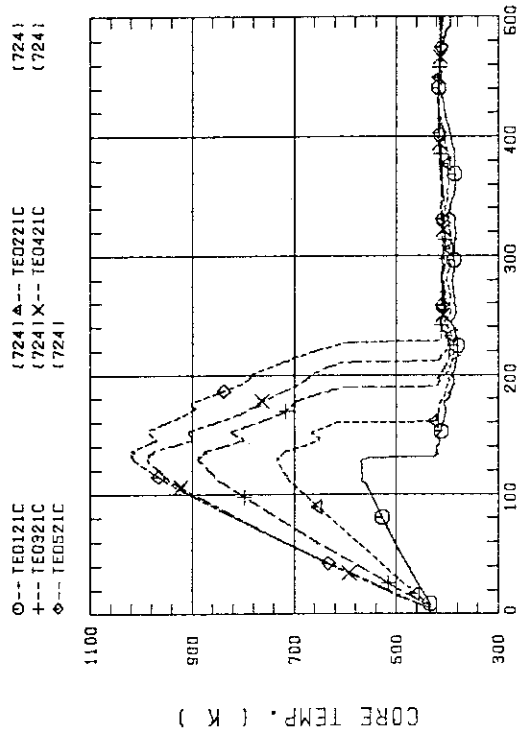

FIG. B-01 HEATER ROD TEMPERATURE
(BUNDLE 2-1C, LOWER HALF)

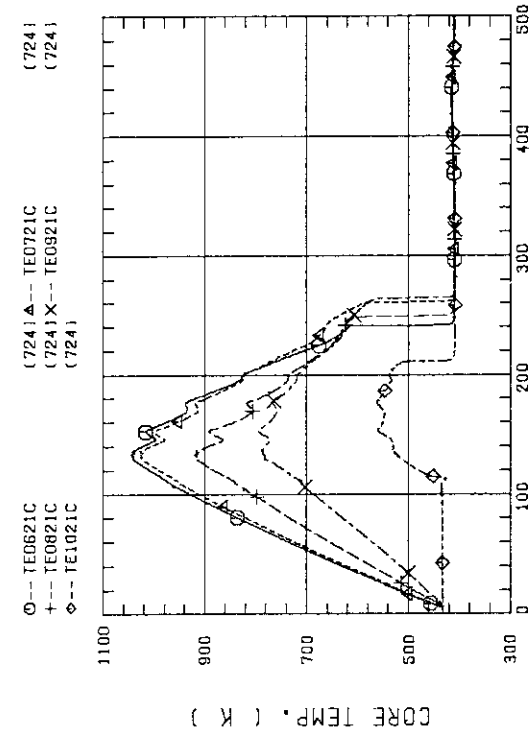

FIG. B-02 HEATER ROD TEMPERATURE
(BUNDLE 2-1C, UPPER HALF)

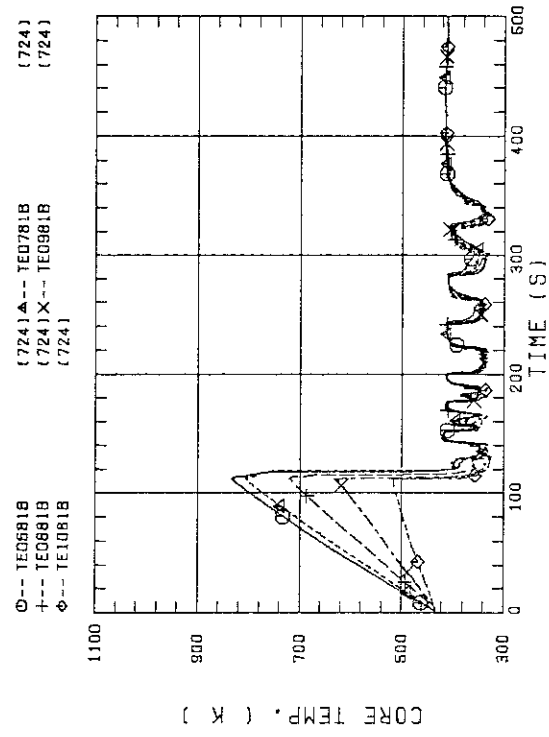

FIG. B-07 HEATER ROD TEMPERATURE (BUNDLE 8-1B, UPPER HALF)

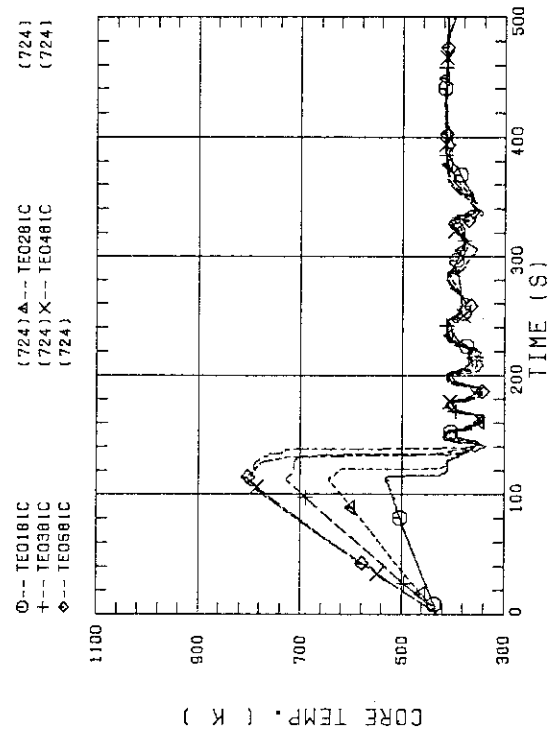

FIG. B-08 HEATER ROD TEMPERATURE (BUNDLE 8-1C, LOWER HALF)

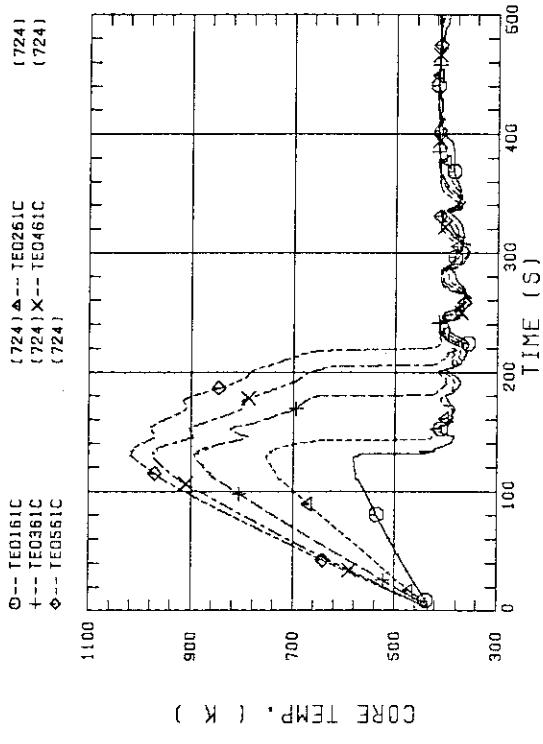

FIG. B-05 HEATER ROD TEMPERATURE (BUNDLE 6-1C, LOWER HALF)

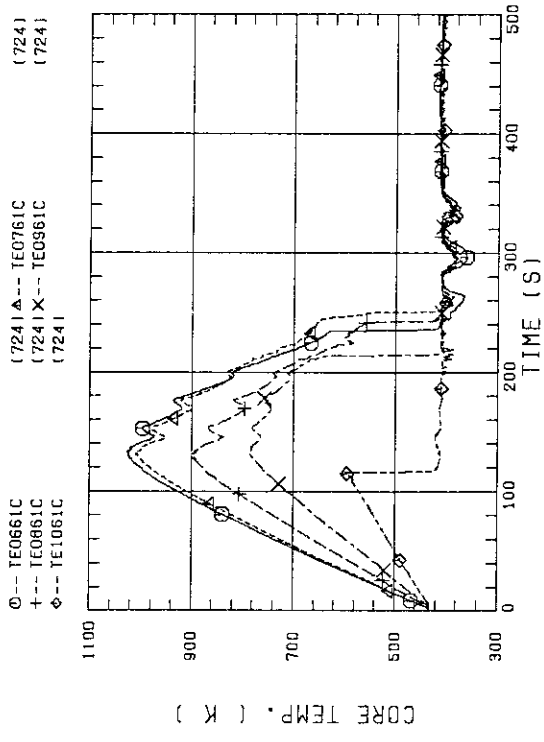

FIG. B-06 HEATER ROD TEMPERATURE (BUNDLE 6-1C, UPPER HALF)

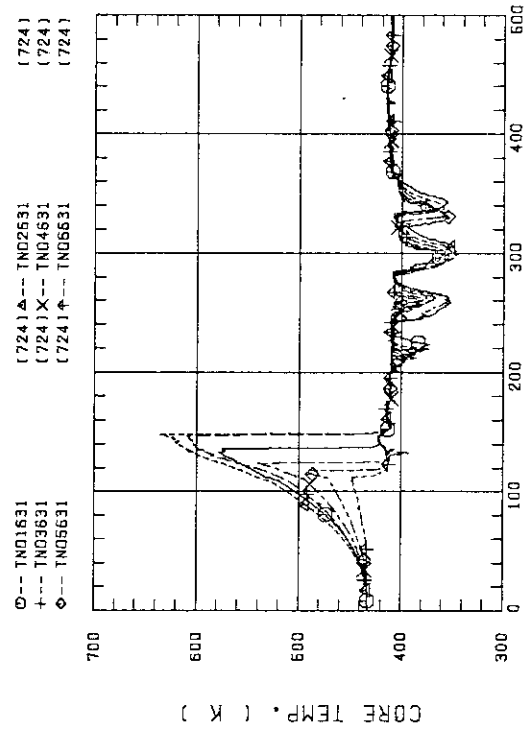

FIG. B-11 NON-HEATED ROD TEMPERATURE (BUNDLE 6-31)

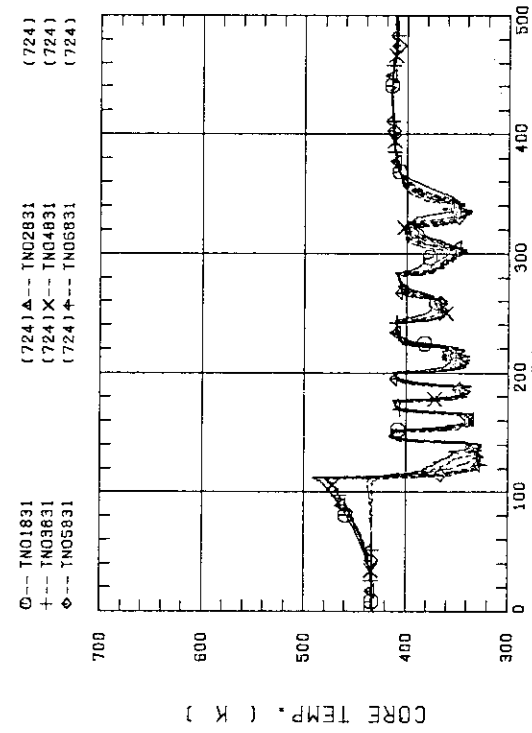

FIG. B-12 NON-HEATED ROD TEMPERATURE (BUNDLE 6-31)

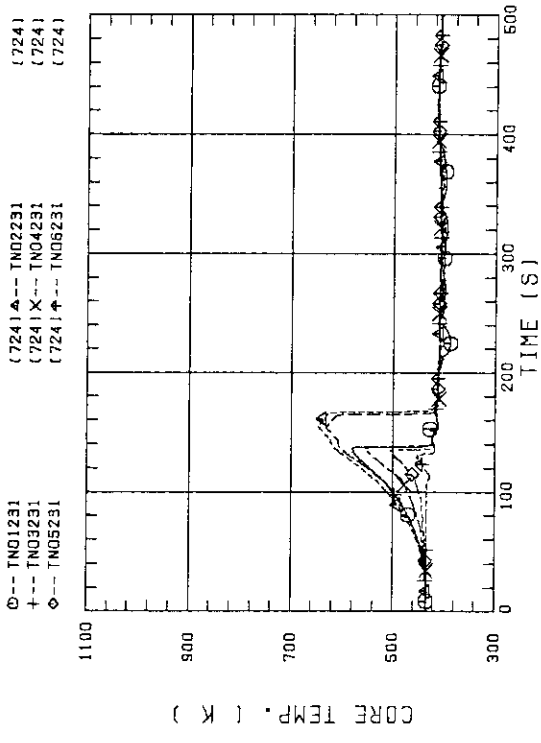

FIG. B-09 NON-HEATED ROD TEMPERATURE (BUNDLE 2-31)

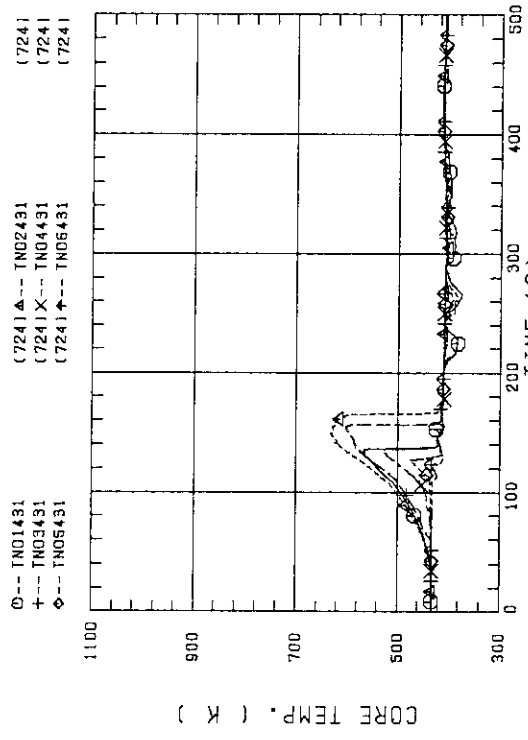

FIG. B-10 NON-HEATED ROD TEMPERATURE (BUNDLE 4-31)

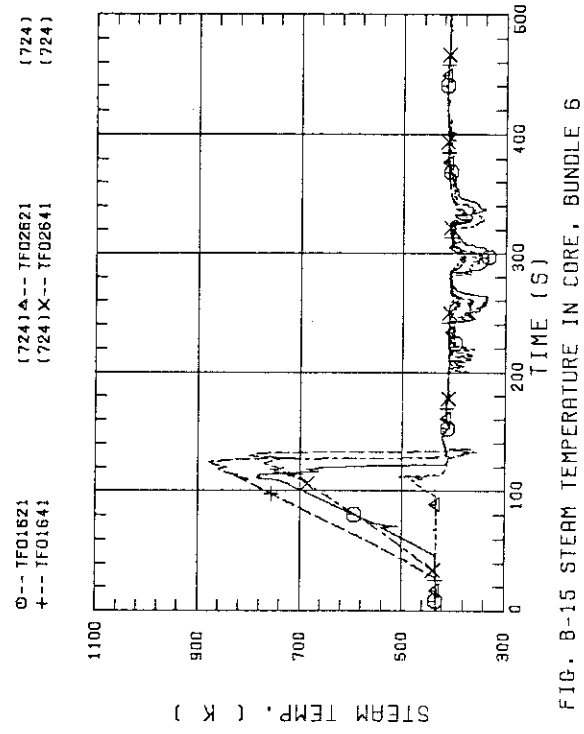

FIG. B-15 STEAM TEMPERATURE IN CORE, BUNDLE 6

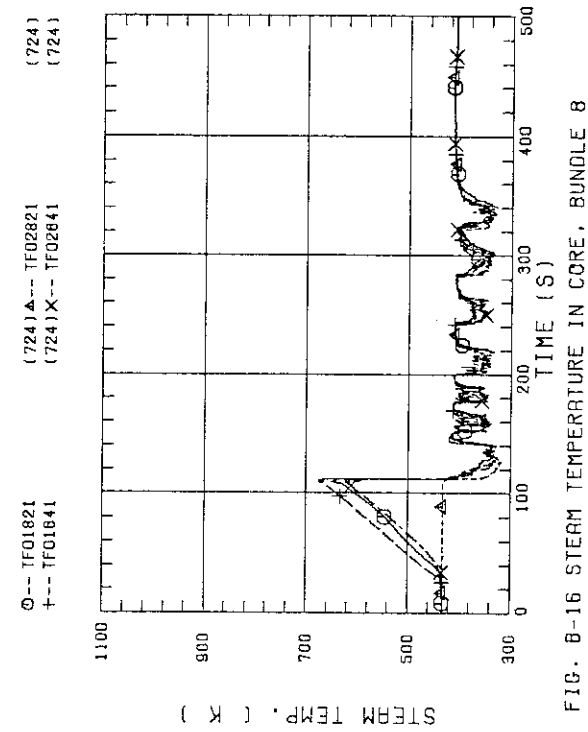

FIG. B-16 STEAM TEMPERATURE IN CORE, BUNDLE 8

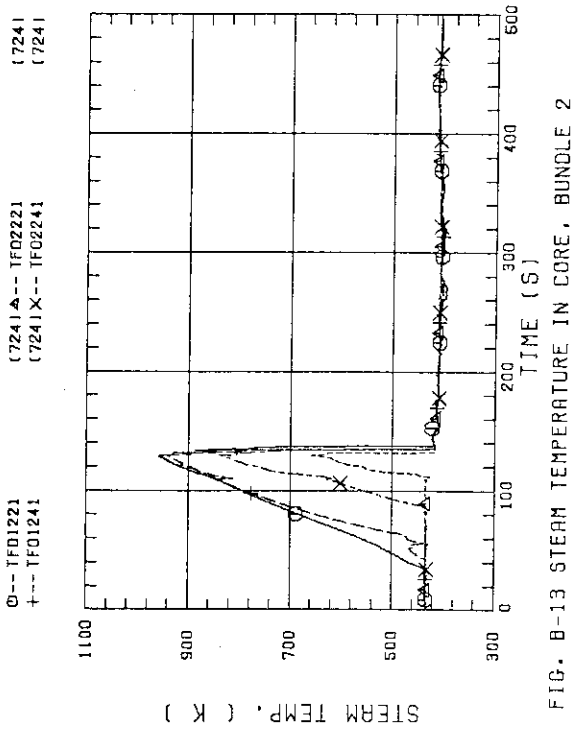

FIG. B-13 STEAM TEMPERATURE IN CORE, BUNDLE 2

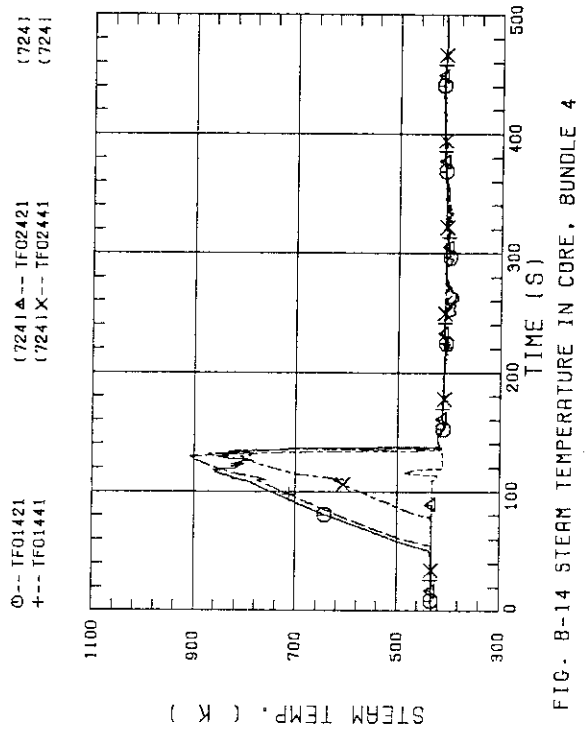

FIG. B-14 STEAM TEMPERATURE IN CORE, BUNDLE 4

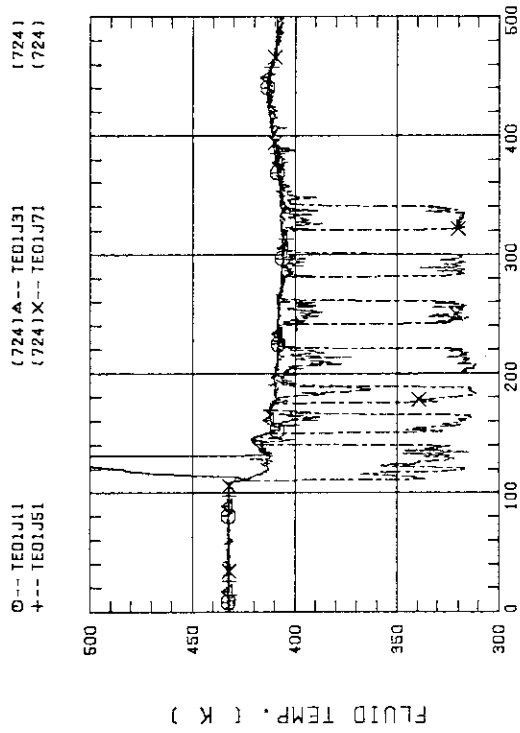

FIG. B-19 FLUID TEMPERATURE ABOVE UCSP
(BUNDLE 1,3,5,7 100MM ABOVE UCSP)

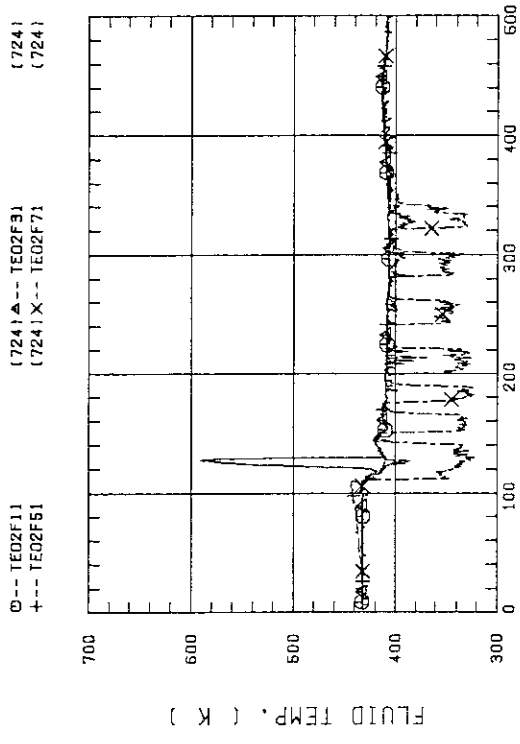

FIG. B-17 FLUID TEMPERATURE JUST ABOVE END BOX TIE PLATE
(BUNDLE 1,3,5,7 OPPOSITE SIDE OF COLD LEG, OUTER)

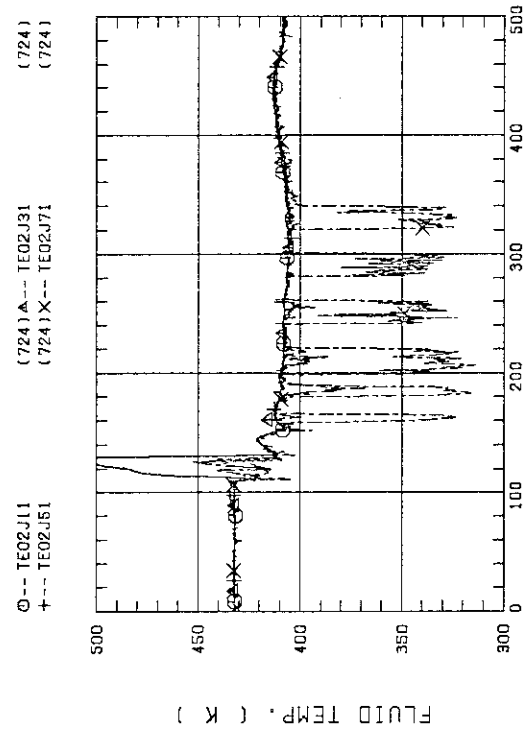

FIG. B-20 FLUID TEMPERATURE ABOVE UCSP
(BUNDLE 1,3,5,7 250MM ABOVE UCSP)

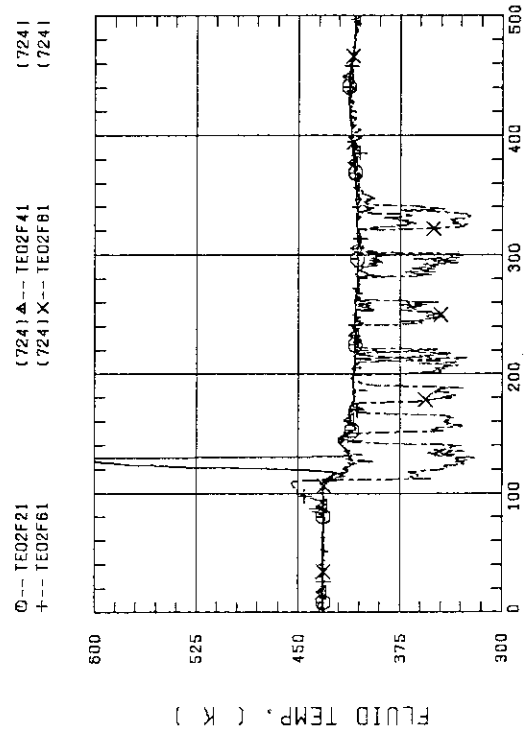

FIG. B-18 FLUID TEMPERATURE JUST ABOVE END BOX TIE PLATE
(BUNDLE 2,4,6,8 OPPOSITE SIDE OF COLD LEG, OUTER)

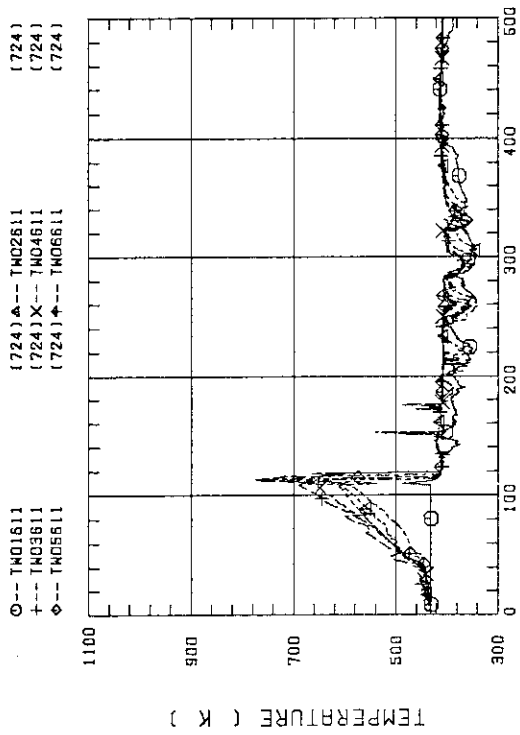

FIG. B-23 TEMPERATURE FOR SPUTTERING DETECTION BUNDLE 6 , REGION 1 , TYPE 3

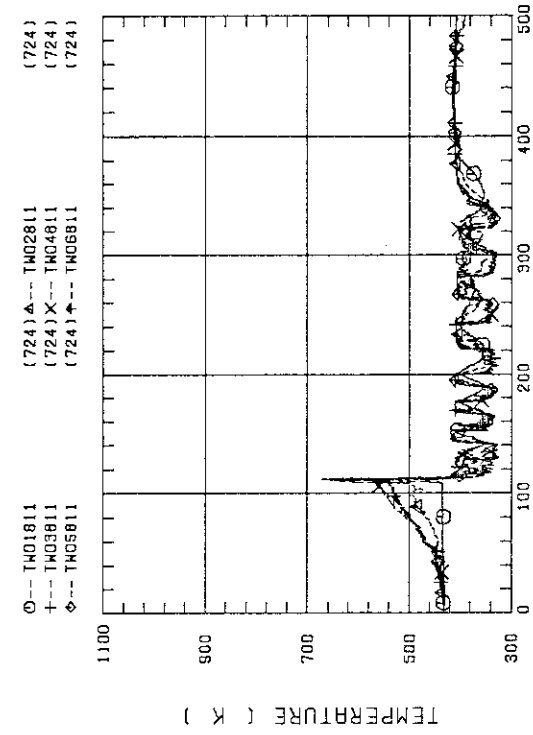

FIG. B-24 TEMPERATURE FOR SPUTTERING DETECTION BUNDLE 8 , REGION 1 , TYPE 3

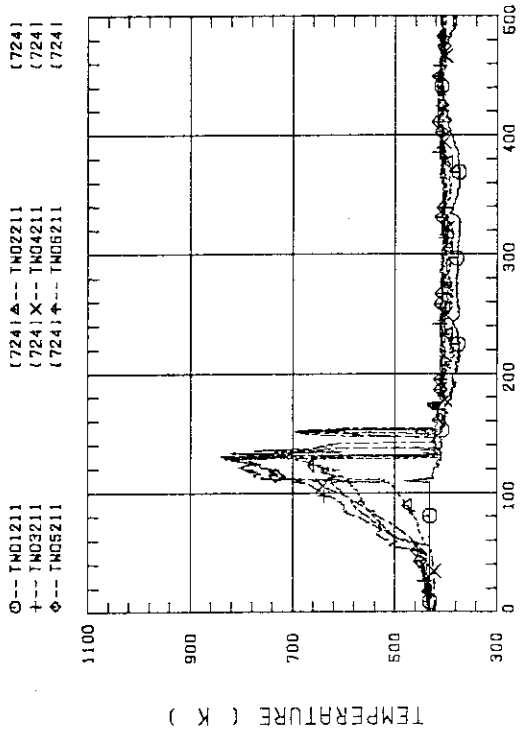

FIG. B-21 TEMPERATURE FOR SPUTTERING DETECTION BUNDLE 2 , REGION 1 , TYPE 3

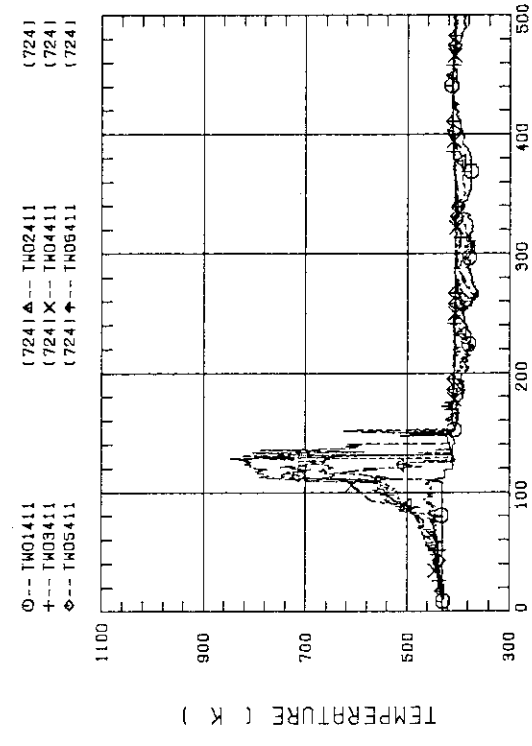

FIG. B-22 TEMPERATURE FOR SPUTTERING DETECTION BUNDLE 4 , REGION 1 , TYPE 3

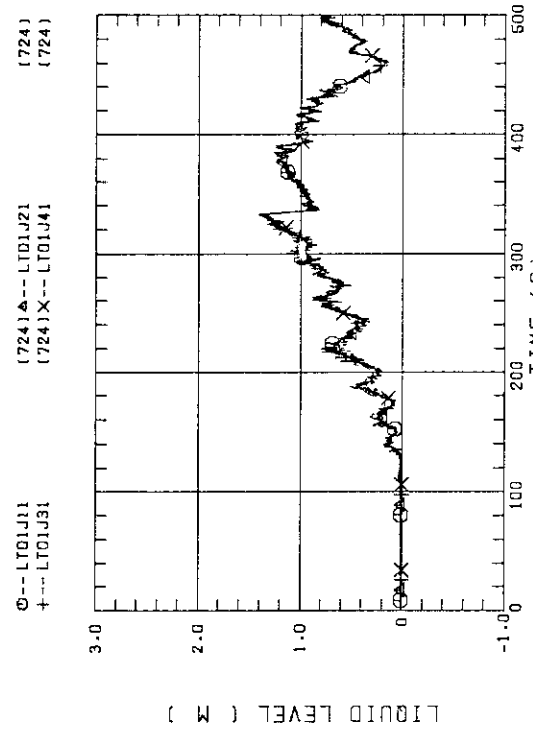

FIG. B-27 LIQUID LEVEL ABOVE UCSP
(BUNDLE 1,2,3,4)

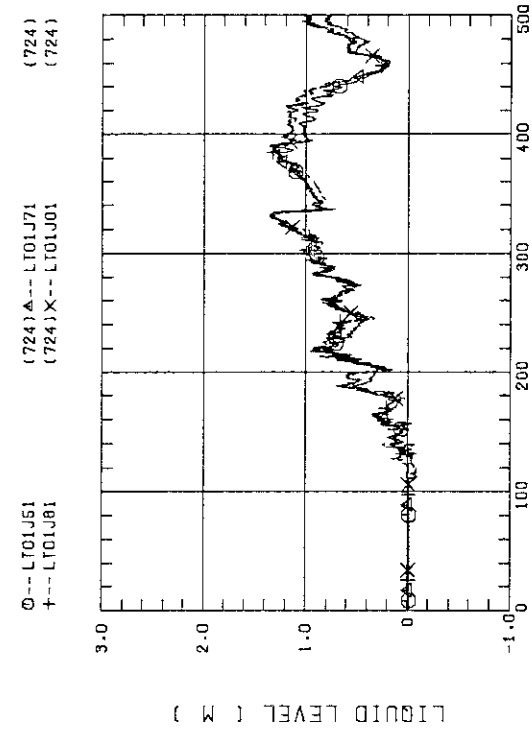

FIG. B-28 LIQUID LEVEL ABOVE UCSP
(BUNDLE 5,6,7,8 AND CORE BUFFLE)

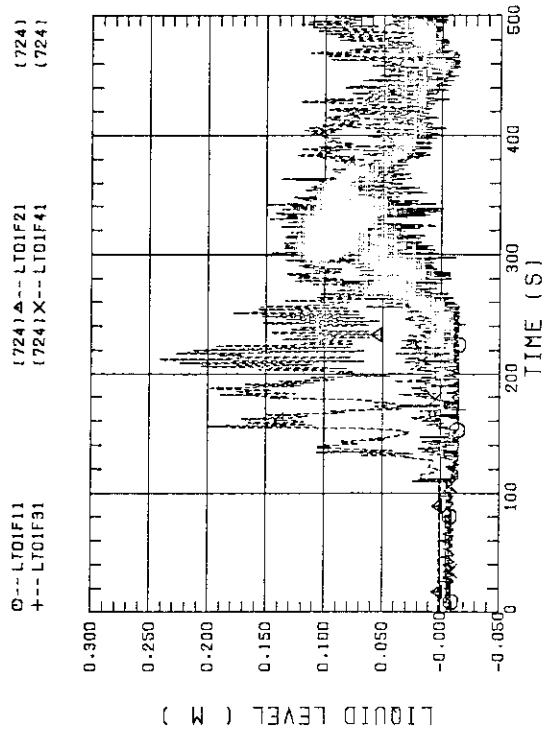

FIG. B-25 LIQUID LEVEL ABOVE END BOX TIE PLATE
(BUNDLE 1,2,3,4)

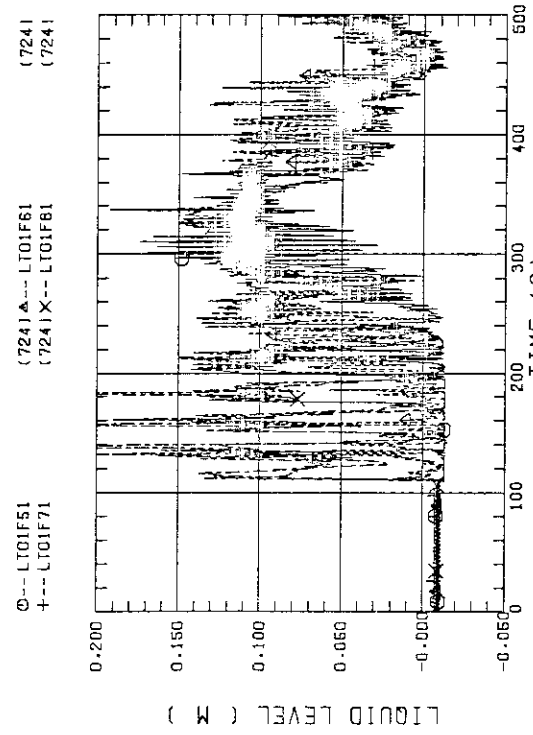

FIG. B-26 LIQUID LEVEL ABOVE END BOX TIE PLATE
(BUNDLE 5,6,7,8)

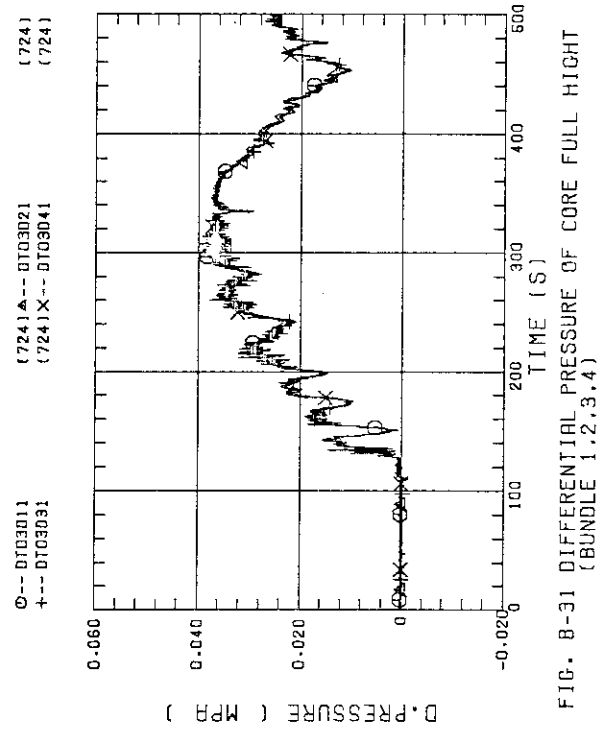

FIG. B-31 DIFFERENTIAL PRESSURE OF CORE FULL HIGHT (BUNDLE 1,2,3,4)

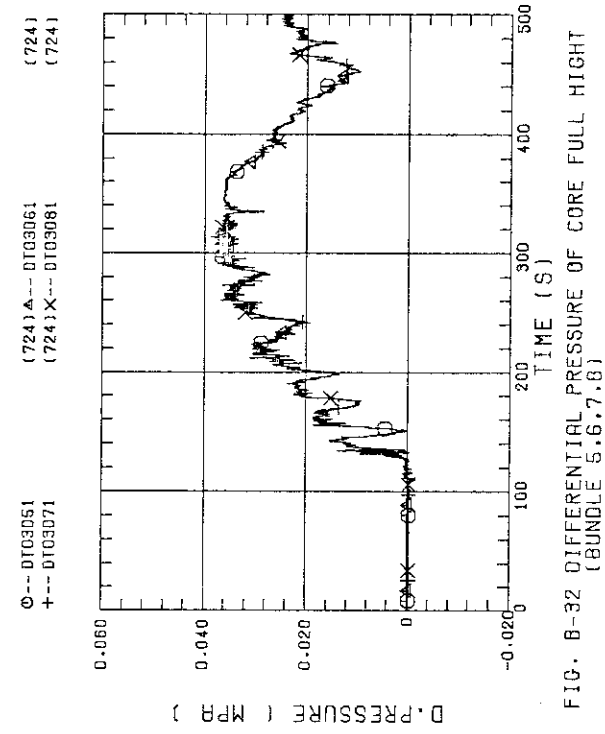

FIG. B-32 DIFFERENTIAL PRESSURE OF CORE FULL HIGHT (BUNDLE 5,6,7,8)

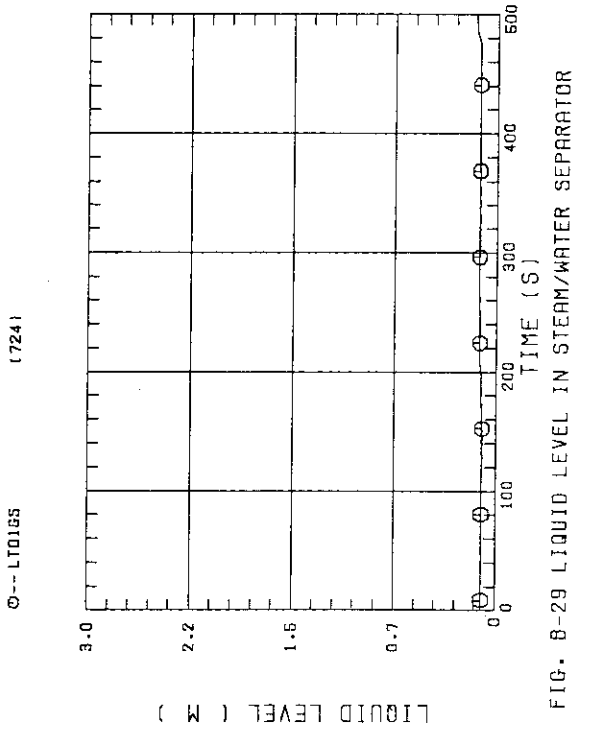

FIG. B-29 LIQUID LEVEL IN STEAM/WATER SEPARATOR

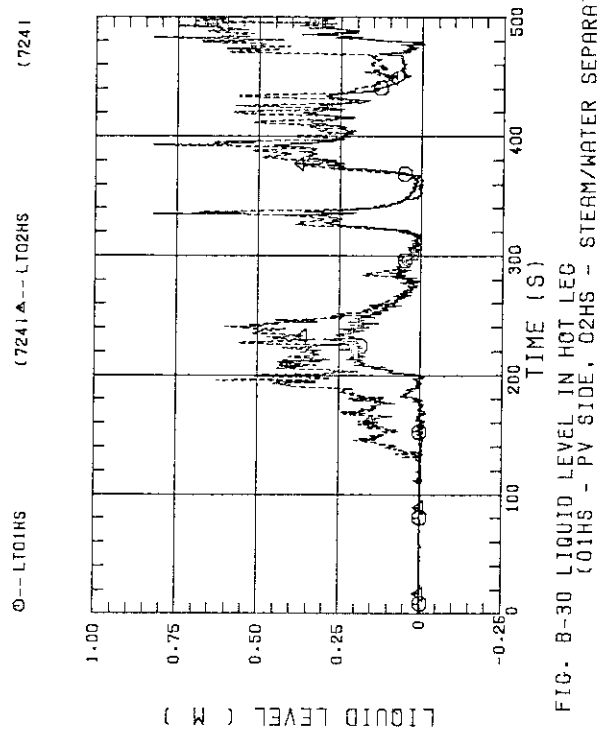

FIG. B-30 LIQUID LEVEL IN HOT LEG (O1HS - PV SIDE, O2HS - STEAM/WATER SEPARATOR SIDE)

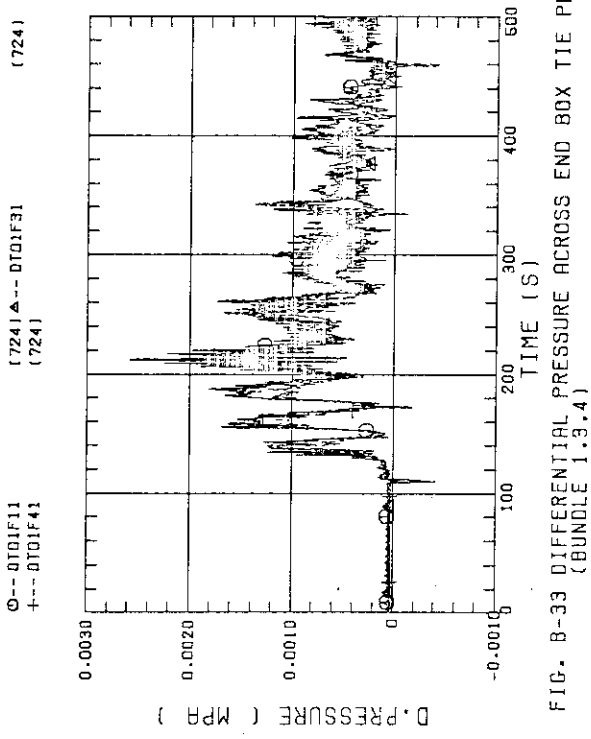

FIG. B-33 DIFFERENTIAL PRESSURE ACROSS END BOX TIE PLATE (BUNDLE 1.3.4)

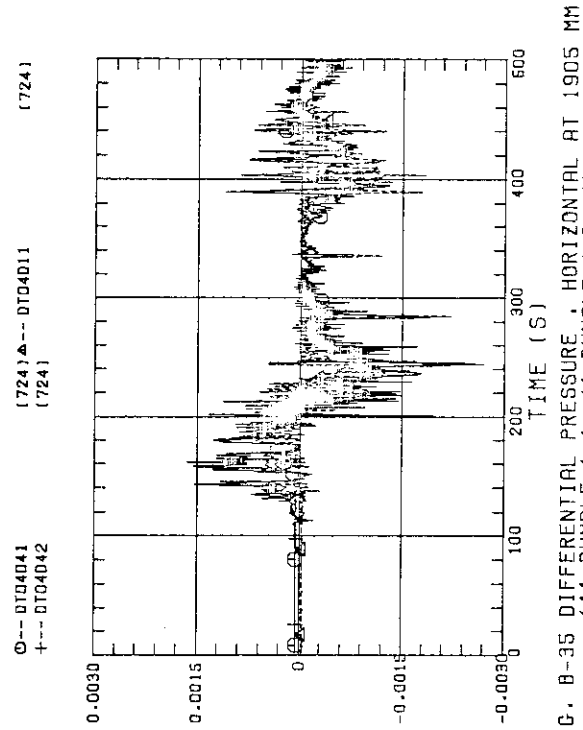

FIG. B-35 DIFFERENTIAL PRESSURE , HORIZONTAL AT 1905 MM (11-BUNDLE 1-4, 41-BUNDLE 4-8, 42-BUNDLE 4-6)

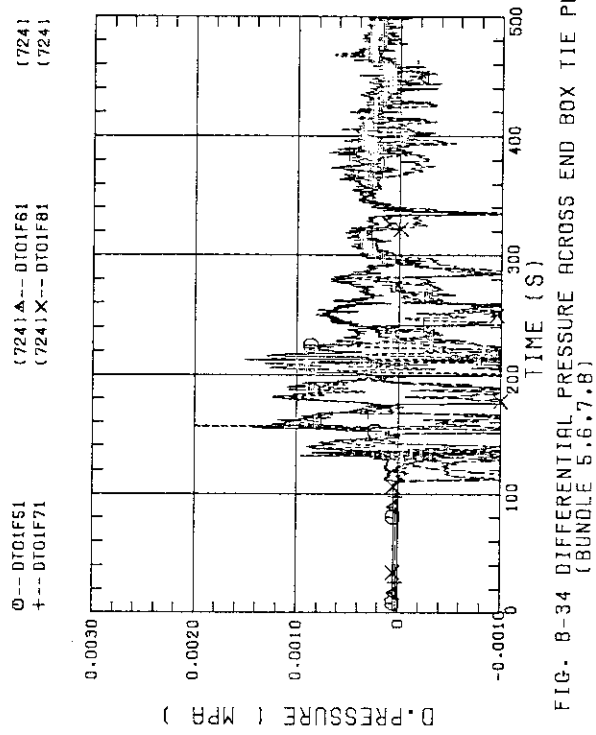

FIG. B-34 DIFFERENTIAL PRESSURE ACROSS END BOX TIE PLATE (BUNDLE 5.6.7.8)

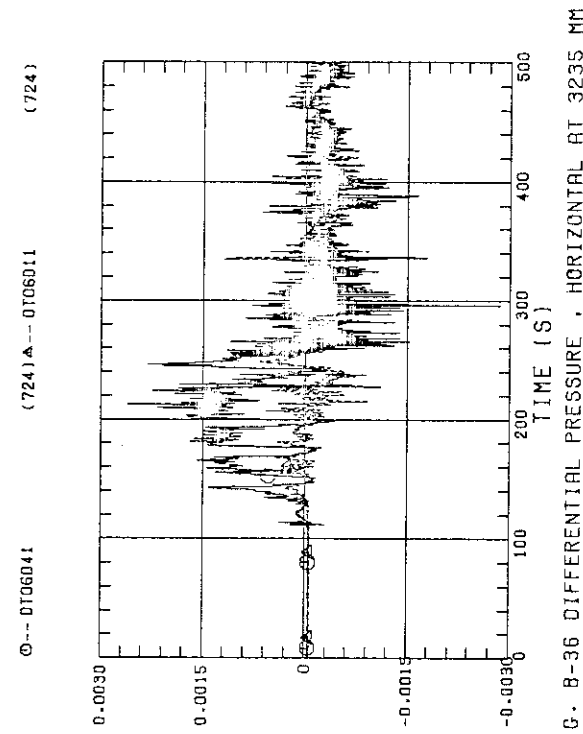

FIG. B-36 DIFFERENTIAL PRESSURE , HORIZONTAL AT 3235 MM (11-BUNDLE 1-4, 41-BUNDLE 4-8)

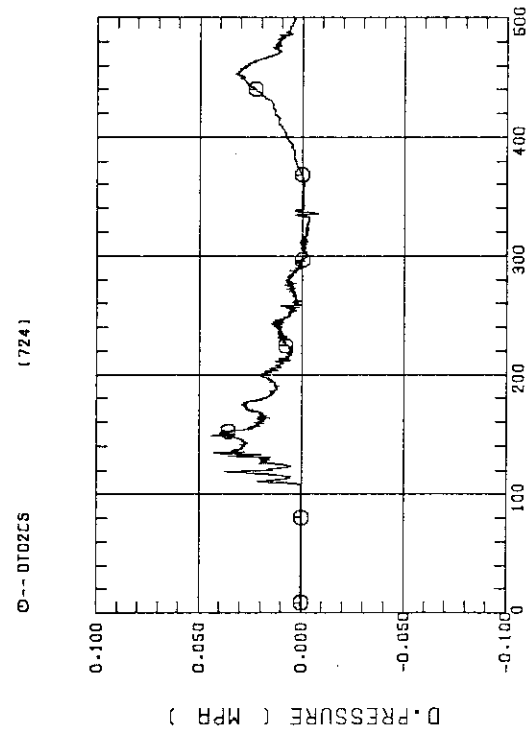

FIG. B-39 DIFFERENTIAL PRESSURE OF INTACT COLD LEG

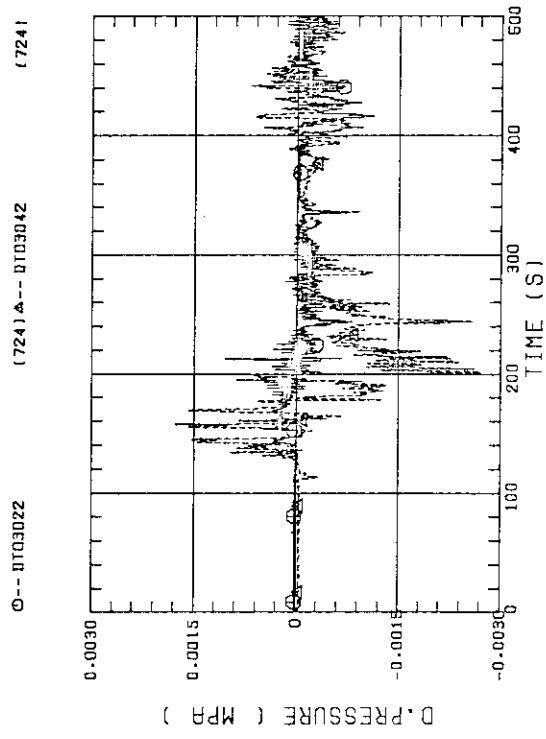

FIG. B-37 DIFFERENTIAL PRESSURE, HORIZONTAL AT 1365 MM (22-BUNDLE 2-4, 42-BUNDLE 4-8)

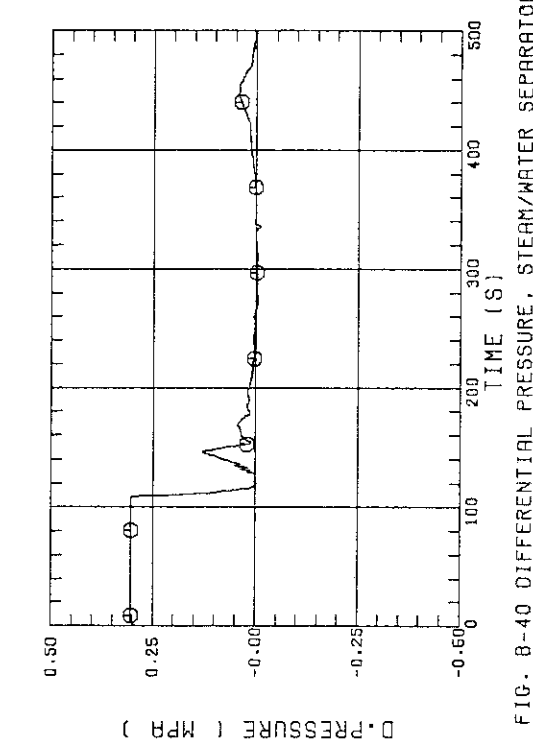

FIG. B-40 DIFFERENTIAL PRESSURE, STEAM/WATER SEPARATOR - CONTAINMENT TANK-II

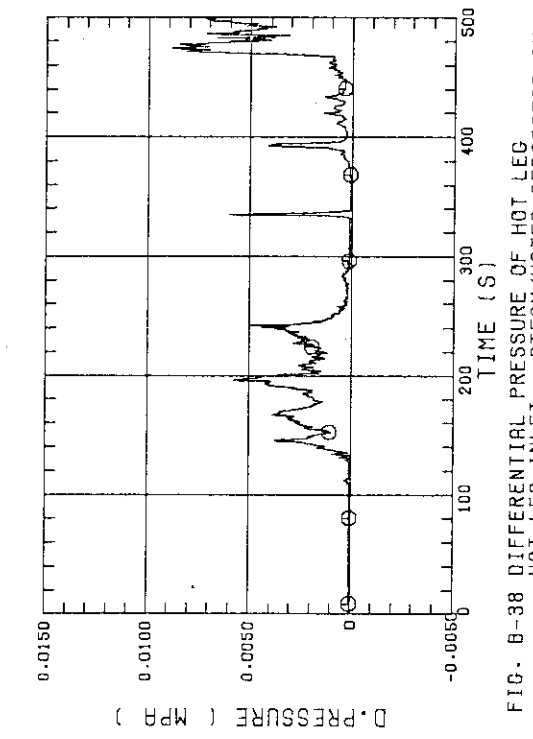

FIG. B-38 DIFFERENTIAL PRESSURE OF HOT LEG HOT LEG INLET - STEAM/WATER SEPARATOR INLET

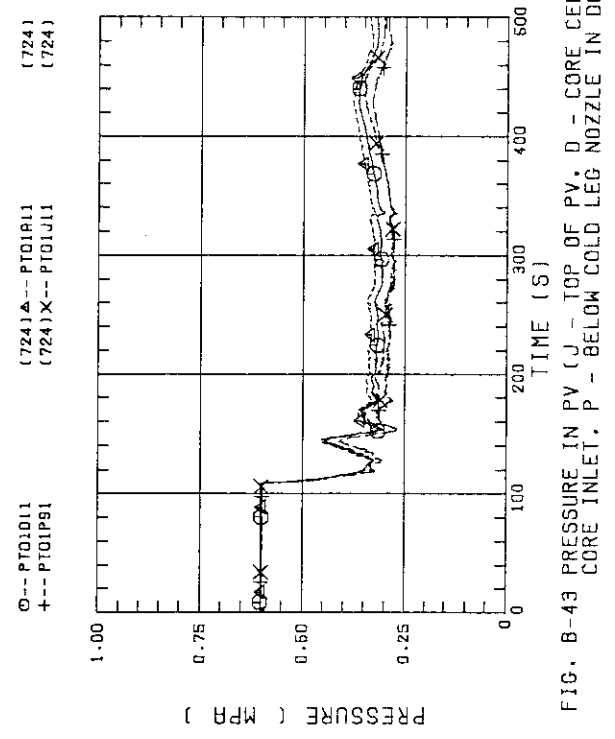

FIG. B-43 PRESSURE IN PV (J - TOP OF PV, D - CORE CENTER, A - CORE INLET, P - BELOW COLD LEG NOZZLE IN DOWNCOMER)

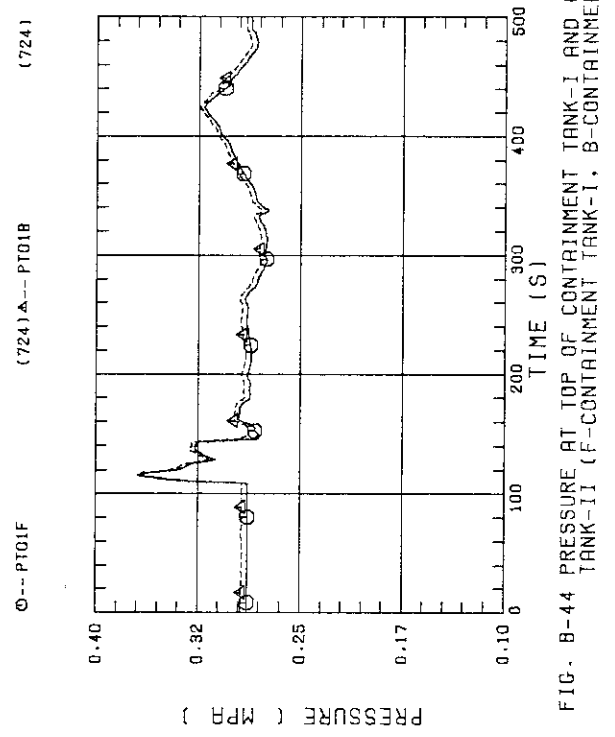

FIG. B-44 PRESSURE AT TOP OF CONTAINMENT TANK-I AND CONTAINMENT TANK-II (F-CONTAINMENT TANK-I, B-CONTAINMENT TANK-II)

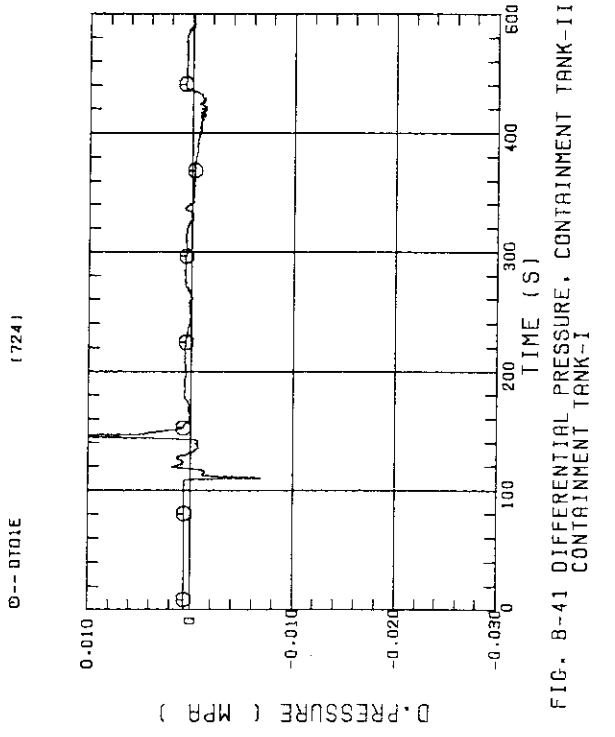

FIG. B-41 DIFFERENTIAL PRESSURE, CONTAINMENT TANK-II - CONTAINMENT TANK-I

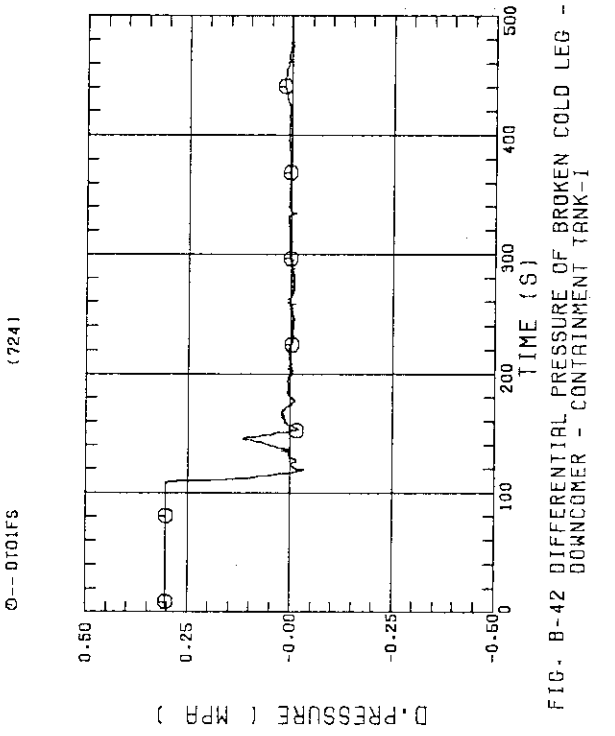

FIG. B-42 DIFFERENTIAL PRESSURE OF BROKEN COLD LEG - PV SIDE, DOWNCOMER - CONTAINMENT TANK-I

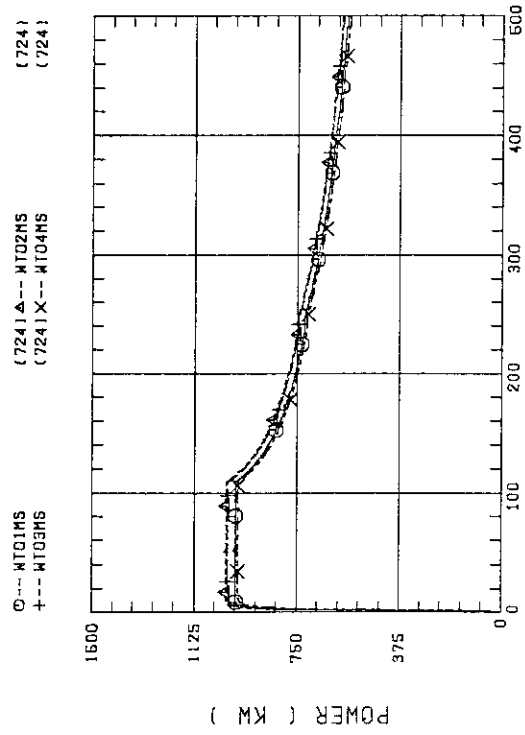

FIG. B-45 BUNDLE POWER
(BUNDLE 1.2.3.4)

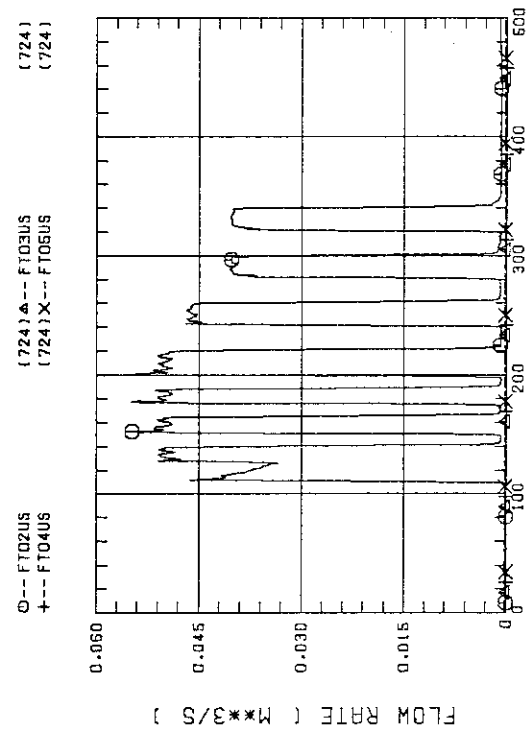

FIG. B-47 FLOW RATE OF UCSP INJECTION
LINE-1(BUNDLE7,8),LINE-2(5,6),LINE-3(3,4),
LINE-4(1,2)

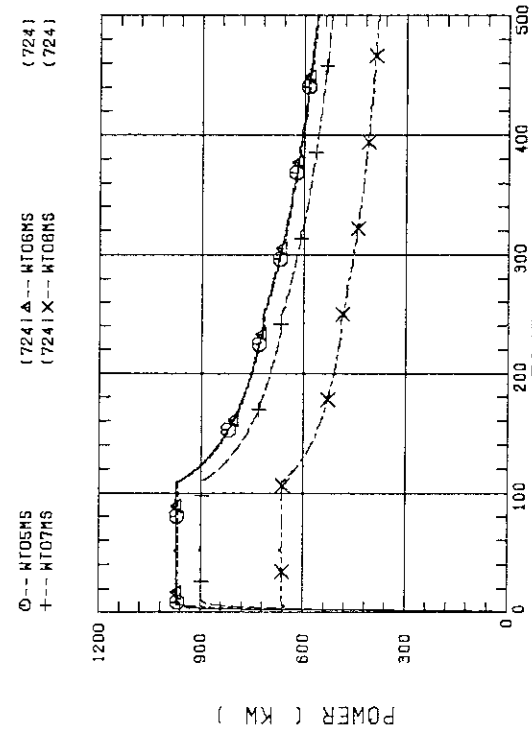

FIG. B-46 BUNDLE POWER
(BUNDLE 5.6.7.8)

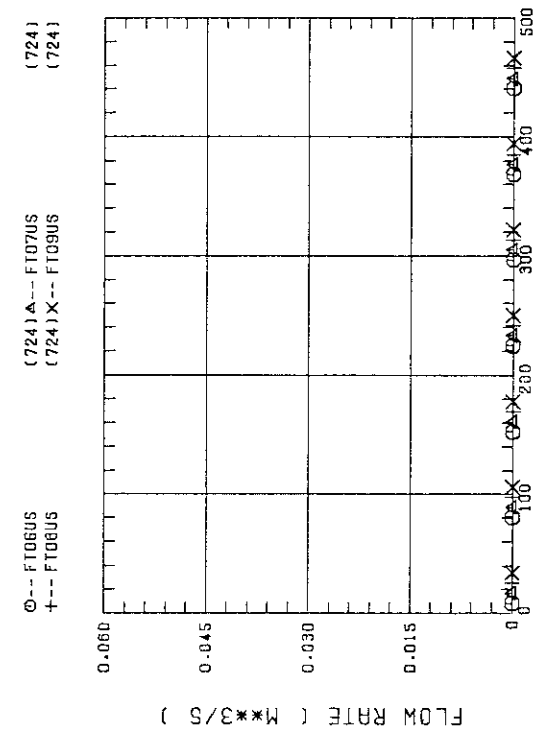

FIG. B-48 FLOW RATE OF UPPER HEAD INJECTION
LINE-4(BUNDLE1,2),LINE-3(3,4),LINE-2(5,6),
LINE-1(7,8)

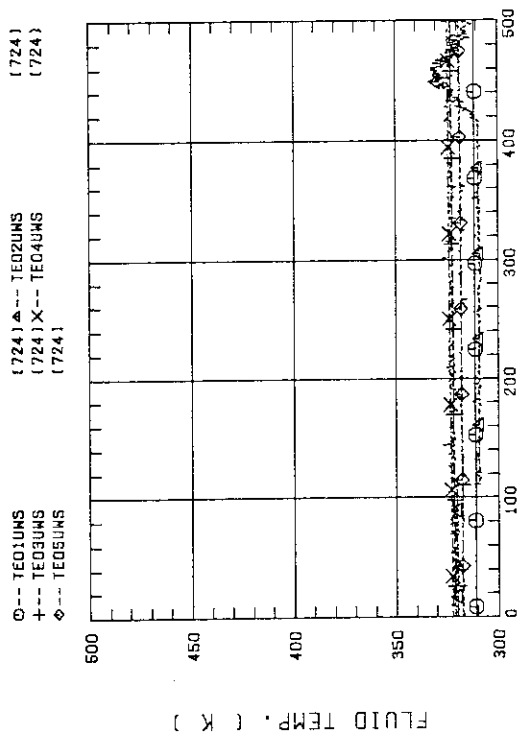

FIG. B-51 FLUID TEMPERATURE IN UCSP INJECTION LINE, O2(BUNDLE7,8),03(5,6),04(3,4),05(1,2), O1(LOWER PLENUM)

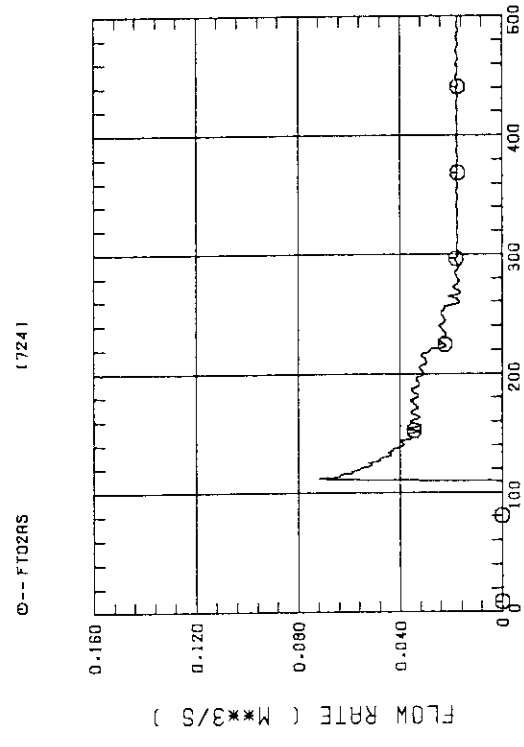

FIG. B-49 FLOW RATE OF ECC WATER (01-LOWER PLENUM, 02-INTACT COLD LEG, 03-BROKEN COLD LEG)

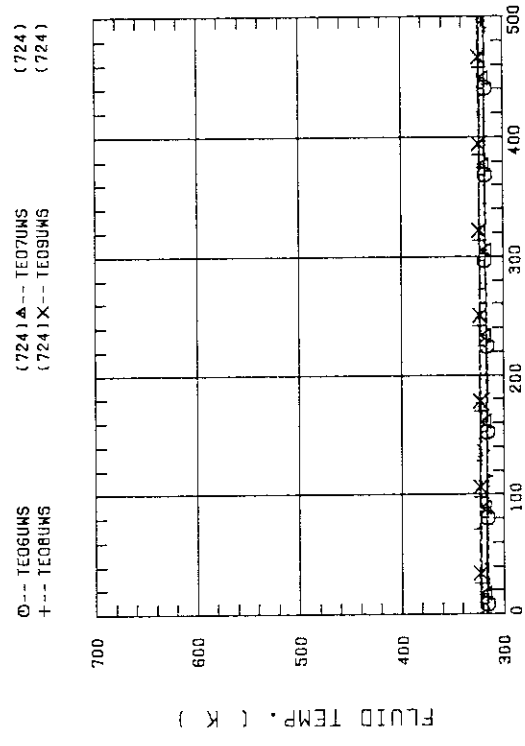

FIG. B-52 FLUID TEMPERATURE IN UCSP INJECTION LINE, LINE-4(BUNDLE1,2),LINE-3(3,4),LINE-2(5,6), LINE-1(7,8)

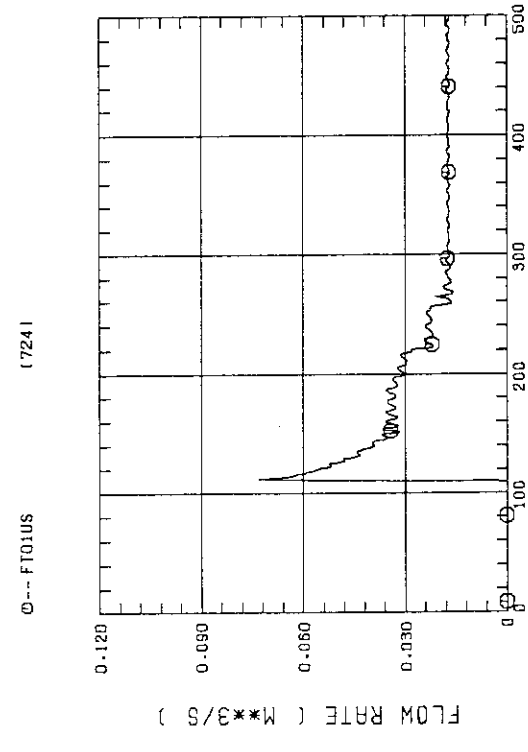

FIG. B-50 FLOW RATE OF LOWER PLENUM INJECTION WATER (ACC HEADER LINE)

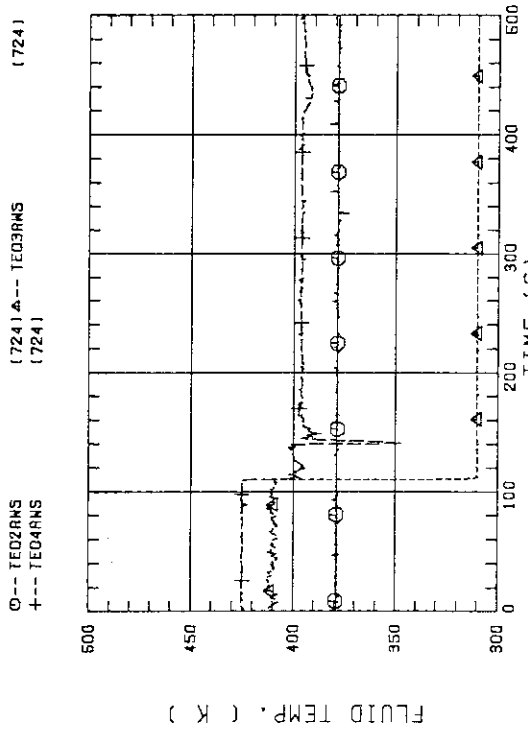

FIG. B-53 FLUID TEMPERATURE IN ECC INJECTION PORT HOT LEG, IC LEG, BC LEG